Towards a method for the simultaneous quantification of $G\alpha_q$ activation and β-arrestin2 recruitment

DISSERTATION

ZUR ERLANGUNG DES DOKTORGRADES DER NATURWISSENSCHAFTEN (DR. RER. NAT.)

AN DER FAKULTÄT FÜR CHEMIE UND PHARMAZIE

DER UNIVERSITÄT REGENSBURG

Vorgelegt von Timo Littmann

aus Wüsten

im Jahr 2018

Diese Arbeit entstand von Oktober 2014 bis November 2018 unter der Anleitung von Prof. Dr. Armin Buschauer, der leider viel zu früh verstorben ist, und Prof. Dr. Günther Bernhardt an der Fakultät für Chemie und Pharmazie der Universität Regensburg

Promotionsgesuch eingereicht am:	14.12.2018
Tag der mündlichen Prüfung:	29.04.2019
Vorsitzender des Prüfungsausschusses:	Prof. Dr. Jens Schlossmann
Erstgutachter:	Prof. Dr. Günther Bernhardt
Zweitgutachter:	Prof. Dr. Carsten Hoffmann
Drittprüfer:	Prof. Dr. Joachim Wegener

Acknowledgments

First and foremost, I would like to thank Prof. Dr. Armin Buschauer, who died far too early and could therefore not witness the finalisation of this thesis, for giving me the opportunity to work on this very interesting project and for his continuous scientific advice.

Another very important person for the realisation of this thesis was Prof. Dr. Günther Bernhardt. I would like to express my gratitude to him for his continuous scientific support and input, and especially for being always in the mood to give spontaneous ideas a try.

Furthermore, I would like to thank Prof. Dr. Takeaki Ozawa from the University of Tokyo for hosting my research stay abroad and his scientific support, not only during my time in Tokyo, but also during the entire course of this thesis. At this point, I would also like to thank Dr. Osamu Takenouchi for his help with all kinds of issues in the lab in Tokyo, his scientific input and for taking his time to show and explain the Japanese culture to me. Beyond that, I want to thank all lab members of the Ozawa group for the pleasant working atmosphere and scientific input.

Thanks are due to Prof. Dr. Carsten Hoffmann and the input he gave to this thesis, especially for chapter 3, and for being the second examiner of this thesis.

I would like to thank Prof. Dr. Joachim Wegener for inspiring scientific conversations on various occasions during my time at the University of Regensburg and for taking part in the evaluation committee of this thesis.

I would like to thank Prof. Dr. Jens Schlossmann, for being part of the evaluation committee of this thesis and for the fruitful collaboration in the proteinkinase G project. In this context, I also want to thank Dr. Andrea Schramm, Philip Müller-Thümen and the other co-authors.

For the productive collaboration on the comparison of the different label-free and label-dependent assays at the human histamine H_1 receptor, I want to thank Dr. Nicole Plank, Dr. Sebastian Lieb and the other co-authors.

I want to thank Maria Beer-Krön for help in many situations during my time in the lab, Elvira Schreiber for showing me how to operate ancient technologies (Ca^{2+} assay) and Denise Mönnich for excellent technical assistance with some of the experiments presented in chapters 5 and 6.

Beyond that, I thank all colleagues in the lab for the excellent working atmosphere and the members of the international doctoral programme “Receptor Dynamics – Emerging Paradigms of Novel Drugs” for many interesting conferences, symposia and workshops.

For their financial support I would like to thank the Elite Network of Bavaria for awarding me with a PhD-position within the international doctoral programme “Receptor Dynamics – Emerging Paradigms of Novel Drugs” and the Deutsche Forschungsgemeinschaft for the association to the research training group 1910 “Medicinal Chemistry of Selective GPCR Ligands”.

I want to express my gratitude to my parents for their continuous support during my education.

Zu guter Letzt möchte ich noch meiner geliebten Edith danken. Für ihre Liebe und den Rückhalt den sie mir tagtäglich gibt.

Publications, presentations and professional training

Peer-reviewed journal articles

(published prior to the submission of this thesis)

Littmann, T., Ozawa, T., Hoffmann, C., Buschauer, A. & Bernhardt, G. A split luciferase-based probe for quantitative proximal determination of $G\alpha_q$ signalling in live cells. *Sci Rep* **8**, 17179 (2018).

Schramm, A., Müller-Thümen, P., **Littmann, T.**, Harloff, M., Ozawa, T. & Schlossmann, J. Establishing a Split Luciferase Assay for Proteinkinase G (PKG) Interaction Studies. *Int J Mol Sci* **19** (2018).

Yang, Z., Han, S., Keller, M., Kaiser, A., Bender, B. J., Bosse, M., Burkert, K., Kögler, L. M., Wifling, D., Bernhardt, G., Plank, N., **Littmann, T.**, Schmidt, P., Yi, C., Li, B., Ye, S., Zhang, R., Xu, B., Larhammar, D., Stevens, R. C., Huster, D., Meiler, J., Zhao, Q., Beck-Sickinger, A. G., Buschauer, A. & Wu, B. Structural basis of ligand binding modes at the neuropeptide Y Y_1 receptor. *Nature* **556**, 520-524 (2018).

Kuhn, K. K., **Littmann, T.**, Dukorn, S., Tanaka, M., Keller, M., Ozawa, T., Bernhardt, G. & Buschauer, A. In Search of NPY Y_4R Antagonists: Incorporation of Carbamoylated Arginine, Aza-Amino Acids, or D-Amino Acids into Oligopeptides Derived from the C-Termini of the Endogenous Agonists. *ACS Omega* **2** (2017).

Dukorn, S., **Littmann, T.**, Keller, M., Kuhn, K., Cabrele, C., Baumeister, P., Bernhardt, G. & Buschauer, A. Fluorescence- and Radiolabeling of [Lys^4,$Nle^{17,30}$]hPP Yields Molecular Tools for the NPY Y_4 Receptor. *Bioconjug Chem* **28**, 1291-1304 (2017).

Lieb, S.*, **Littmann, T.***, Plank, N.*, Felixberger, J., Tanaka, M., Schäfer, T., Krief, S., Elz, S., Friedland, K., Bernhardt, G., Wegener, J., Ozawa, T. & Buschauer, A. Label-free versus conventional cellular assays: Functional investigations on the human histamine H_1 receptor. *Pharmacol Res* **114**, 13-26 (2016). (*equal contribution)

Oral presentations

Littmann, T., Ozawa, T., Hoffmann, C., Buschauer, A. & Bernhardt, G. Split-luciferase complementation enables visualization and quantification of $G\alpha_q$-dependent signaling. *Frontiers in Medicinal Chemistry* (2018, Jena, Germany)

Littmann, T., Ozawa, T., Hoffmann, C., Bernhardt, G. & Buschauer, A. Split-luciferase complementation enables quantification of $G\alpha_q$ activation and live cell imaging. *1st Joint Meeting of the European and Japanese Histamine Research Societies* (2017, Amsterdam, Netherlands)

Littmann, T., Ozawa, T., Hoffmann, C., Bernhardt, G. & Buschauer, A. Split-luciferase complementation enables quantification of the $G\alpha_q$/PLC-β3 interaction. *8th Summer School in Medicinal Chemistry* (2016, Regensburg, Germany)

Poster presentations

(only contributions as presenting author are listed)

Littmann, T., Ozawa, T., Hoffmann, C., Buschauer, A. & Bernhardt, G. Simultaneous quantification of $G\alpha_q$ activation and β-arrestin2 recruitment. *9th International Summer School in Medicinal Chemistry* (2018, Regensburg, Germany)

Littmann, T., Ozawa, T., Hoffmann, C., Buschauer, A. & Bernhardt, G. Split-luciferase complementation enables visualization and quantification of $G\alpha_q$-dependent signalling. *Frontiers in Medicinal Chemistry* (2018, Jena, Germany)

Littmann, T., Ozawa, T., Hoffmann, C., Bernhardt, G. & Buschauer, A. Split-luciferase complementation enables quantification of the $G\alpha_q$/PLC-β3 interaction. *8th International Summer School in Medicinal Chemistry* (2016, Regensburg, Germany)

Littmann, T., Ozawa, T., Hoffmann, C., Bernhardt, G. & Buschauer, A. Using split-luciferase complementation for quantification of $G\alpha_q$ signalling. *XXIV EFMC International Symposium on Medicinal Chemistry* (2016, Manchester, United Kingdom)

Littmann, T., Ozawa, T., Hoffmann, C., Bernhardt, G. & Buschauer, A. Quantification of $G\alpha_q$ protein activation by split-luciferase complementation. *COST CM1207: GLISTEN Meeting* (2016, Erlangen, Germany)

Professional training

Since October 2014 member of the international doctoral programme “Receptor Dynamics – Emerging Paradigms of Novel Drugs” funded by the Elite Network of Bavaria

Since December 2016 associated member of the research training group 1910 “Medicinal Chemistry of Selective GPCR Ligands” funded by the Deutsche Forschungsgemeinschaft

Index

1. Introduction

1.1 G protein-coupled receptors: a historical perspective

G protein-coupled receptors (GPCRs) are proteins responsible for transducing signals across plasma membranes[1]. Although, Paul Ehrlich was the first one describing the principle of a receptor/ligand interaction already at the end of the 19th century with the proposal of his side-chain theory[2], it was John Langley, who formally introduced the term "receptor", or "receptive substance"[3] a few years later. He investigated the effects of nicotine and curare on the neuromuscular junction of frogs and proposed the existence of "receptive substances" in muscles, which are activated through an endogenous agonist, secreted by neurons. We now know that muscle contraction is mainly regulated by ionotropic receptors, but the principle of the receptor/ligand interaction also applies to GPCRs.

1.1.1 G protein-dependent signalling

First work in context with GPCRs started in the 1950s and 1960s with Earl Sutherland and co-workers, who investigated the regulation of glycogenolysis in liver homogenates. They found out that a key regulator enzyme in this process, namely glycogen phosphorylase, was activated by administration of glucagon or epinephrine, not in a direct manner, but via the formation of an unknown "factor"[4]. Several years later, this factor was identified as 3',5'-cyclic adenosine monophosphate (cAMP), which is formed from adenosine-5'-triphosphate (ATP) by an enzyme designated adenylyl cyclase (AC)[5,6]. This finding led Sutherland to the proposal of the concept of "second messengers"[5], which are molecules such as cAMP. The formation of second messengers is a direct consequence of an extracellular stimulation of cells by, e.g. hormones[5]. Although at that time, it was unclear, if hormones act directly via an allosteric binding site on the AC itself, or if additional proteins are involved in the process[6,7].

In the following years, research could profit from developments made in the pharmaceutical industry[8]. In search of compounds to treat asthma and hay fever, for example, antagonists like propranolol[9] and mepyramine[10] were developed. Antagonists are ideal pharmacological tools to characterise the function of receptors by blocking the action of (endogenous) agonists.

Some twenty years later, evidences began to accumulate that guanosine-5'-triphosphate (GTP) and a "transducer" protein[11] are playing an important role in the AC signalling cascade[12-14]. The hypothesis arose that the so-called "β adrenoceptor-regulated adenylyl cyclase", which was the most widely used model system to study cAMP-dependent effects at that time, actually consists of three different proteins, composed of the AC, the "transducer" and the receptor itself. Rodbell et al., also working on ACs in liver lysates stimulated through glucagon, discovered that the formation of cAMP is drastically enhanced when GTP is added to the lysates together with glucagon, compared to the stimulation with glucagon alone[12]. Cassel and co-workers, investigating catecholamine effects on erythrocyte membranes, showed that the hydrolysis of [^{32}P]-GTP was drastically enhanced after addition of isoproterenol,

an epinephrine analogue[13]. At about the same time, radioligand competition binding experiments, also on erythrocyte membranes, using the tritiated β-blocker dihydroalprenolol, revealed substantially different characteristics of agonists and antagonist, when displacing the radioligand. Antagonists displaced the radioligand in a uniform manner[15,16]. By contrast, agonists showed biphasic displacement curves with two inflection points, reflecting a high and a low binding constant. The addition of GTP converted the biphasic character into a monophasic one, and the corresponding binding constant was then similar to the lower one of the biphasic curve[16]. These findings inspired De Lean and co-workers to propose the ternary complex model, providing an explanation for the two affinity states of the receptor[17]. The authors postulated in addition to receptor and ligand a third interaction partner, which is only present, when an agonist binds to the receptor and which can be uncoupled from the receptor/ligand complex by addition of GTP. The latter then leads to a reduced affinity between agonist and receptor[17].

Direct evidence for the existence of this interaction partner and the above-mentioned transducer protein, the G protein, was published in 1980, when it was purified from rabbit plasma membranes[18]. It was shown to directly stimulate cAMP formation when titrated to membranes containing ACs. The characterisation also revealed the heterotrimeric nature of the G protein[18], consisting of the α, the β and the γ subunit[11]. The α-subunit is the one binding GTP and the one causing the activation of the AC[19] (cf. Fig. 1.1A). Upon agonist binding, the GPCR/Gαβγ complex dissociates into the GPCR, the α subunit and the βγ complex[19]. Both components of the G protein are then capable of activating different downstream effector proteins[11,19,20].

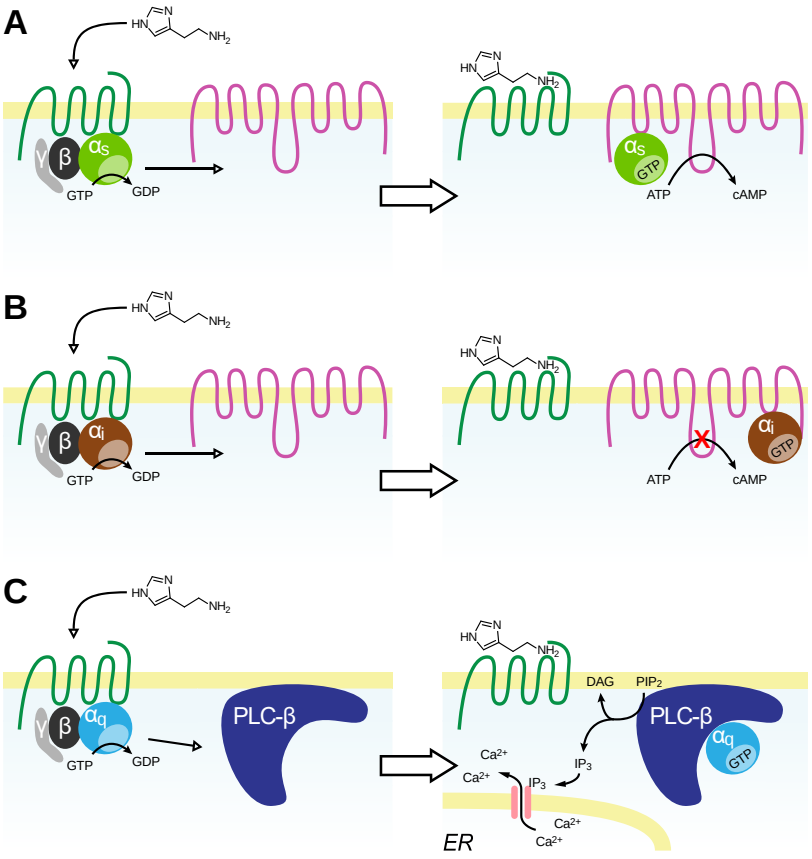

Fig. 1.1: Schematic illustration of the activation and effectuation of $G\alpha_s$, $G\alpha_i$ and $G\alpha_q$ proteins. Binding of an agonist to a GPCR results in a GDP/GTP exchange within the α subunit. The subsequent influence on effector proteins depends on the type of α subunit activated. GPCRs usually have a canonical G protein, to which they predominantly couple to. In case of the H_2 histamine receptor (hH_2R) (**A**), for example, it is the $G\alpha_s$ protein, which translocates to ACs and activates their enzymatic activity, leading to the formation of cAMP from ATP. Histamine H_3 and H_4 receptors ($hH_{3,4}R$) (**B**) couple to $G\alpha_i$ proteins, which also interact with ACs. By contrast, interaction with $G\alpha_i$ proteins leads to a decrease in AC activity. A third major Gα protein is the $G\alpha_q$ (**C**), which is activated, for example, through histamine H_1 receptors (hH_1R). Their effector proteins are from the PLC-β class and catalyse the formation of IP_3 and DAG from PIP_2. The second messenger IP_3 then promotes the release of Ca^{2+} into the cytosol, e.g. by opening ion channels located in the ER-membrane.

The G protein, purified by Northup et al, and the one responsible for the stimulation of ACs is what we now call the $G\alpha_s$ protein[11]. Its counterpart, the $G\alpha_i$ protein was discovered during investigations on the mode of action of the whooping cough-causing toxin secreted by *Bordetella pertussis*, the pertussis toxin[21]. Activation of $G\alpha_i$ leads to an inhibition of the enzymatic activity of the AC, as illustrated in Fig. 1.1B. Pertussis toxin inhibits these $G\alpha_i$ proteins, which is the reason that it is still widely used as a pharmacological tool, especially for investigations on the coupling specificity of a GPCR[22,23].

A third major Gα subtype, the $G\alpha_q$, was discovered during investigations on receptor-promoted Ca^{2+} ion influx into the cytosol. It was known that Ca^{2+} influx and the formation of inositol trisphosphate (IP_3) from phosphatidylinositol 4-phosphate (PIP_2) by phospholipases C-β (PLC-β) was interconnected, but it was not known, if the influx of Ca^{2+} caused IP_3 formation, or vice versa[24]. However, in 1983 Streb et al. showed that the addition of exogenous IP_3 to permeabilised cells caused a Ca^{2+} efflux from intracellular stores, which gave insight into the order of events within this signalling cascade[25]. Although it was already known that hormones can cause Ca^{2+} influx into the cytosol and that treatment of specific membrane preparations with the non-hydrolysable GTP analogue GTPγS leads to the production of IP_3[19], it took until the 1990s to identify and purify the regulator of PLC-βs[26,27]. By using affinity chromatography with immobilized βγ-subunits, novel Gα subtypes were purified[26] of which $G\alpha_q$ was identified as the regulator of PLC-β proteins[27] (cf. Fig. 1.1C). Both, IP_3 and Ca^{2+} are also referred to as second messengers and the other product formed by PLC-βs from PIP_2, diacylglycerol (DAG), is a third one involved in this signalling pathway. It was shown that DAG, which diffuses in the cellular membrane after formation, due to its lipophilic nature, directly stimulates the activity of, e.g. protein kinase C[24].

Also, βγ-subunits were identified as signal transducers. Several publications described them as modulators of PLCs[28], ACs[29], and different types of ion channels[30,31].

With the cloning of GPCRs, beginning with the β_2 adrenoceptor[32], and especially the human genome project, a new era in receptor research began. On one hand, recombinant expression of receptors in e.g. cancer cell lines became possible making research more convenient, but on the other hand the complexity increased tremendously[7]: multiple different receptors and their splice variants were identified, amounting to approx. 2000 different proteins[33]. Furthermore, differences in sequence of the same receptor between species became apparent, which, in some cases, also put the translational validity of animal models into question[34,35].

1.1.2 Discovery of mechanisms curbing signalling

Already in 1968, the existence of a regulatory mechanism of unknown function was described that causes a reduction of cAMP concentration after continuous incubation of rat cerebellar slices with norepinephrine to the basal level within several minutes[36]. But it took until the mid-1980s, when Mahan and

co-workers demonstrated by radioligand binding studies that receptors disappear from the cellular surface after stimulation with an agonist[37]. This was the first direct evidence that cells prevent themselves from an over-stimulation via down-regulation of receptors and not of the G proteins or effector proteins[38]. In addition, it was demonstrated that phosphorylation of the activated receptors, e.g. by GPCR kinases (GRKs)[39], is linked to the internalisation of the receptors[14,40] and that it also impairs their ability to activate G proteins[41]. However, GPCR desensitisation by GRKs was only observable with crude kinase preparations. The purer the preparation was, the less efficacious was the desensitisation, which led to the assumption that an additional protein had to be involved in the process[42].

This protein was found to be β-arrestin[43], which binds to phosphorylated receptors with high affinity[39]. Therefore, it is the key protein responsible for receptor desensitisation (cf. Fig. 1.2). On one hand, it provokes a steric hindrance when bound to the receptor, making G protein activation impossible[38]. On the other hand, it functions as an adaptor for clathrins, facilitating the formation of pits at the membrane[44]. From these so-called clathrin-coated pits vesicles are formed that internalise together with the receptors[45]. After internalisation, the receptors undergo different ways of processing. They can be rapidly recycled back to the plasma membrane, or degradation[46], mediated by ubiquitinilation[47], can occur[48]. The receptors that get recycled back to the plasma membrane to the most part, such as e.g. the β_2 adrenoceptor[45], are categorised as class A GPCRs[49]. Receptors are considered class B receptors, such as e.g. the neurotensin NTS_1 receptor ($hNTS_1R$)[46], when they are preferentially degraded in lysosomes after internalisation[49].

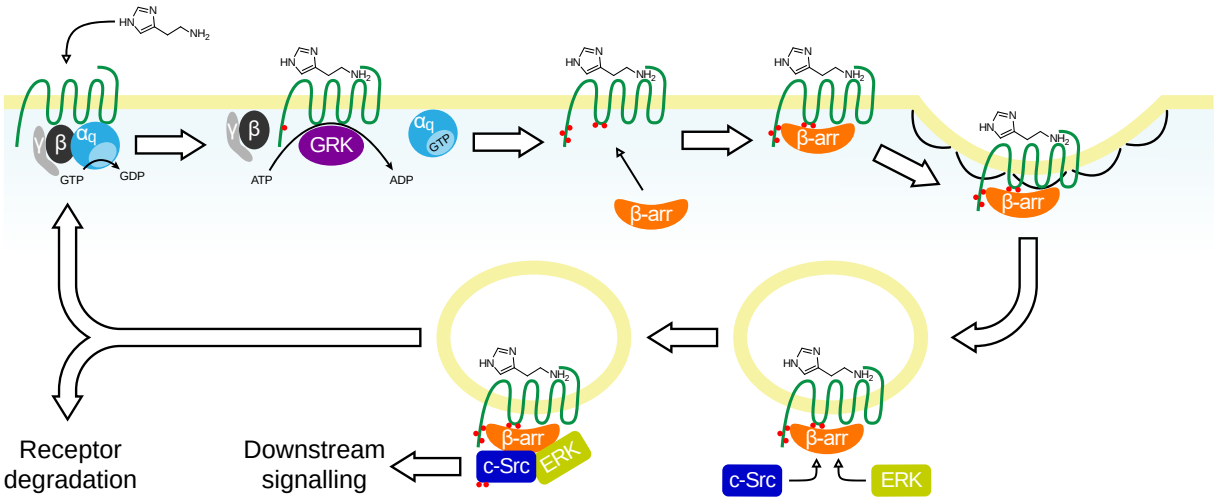

Fig. 1.2: Schematic illustration of β-arrestin-mediated internalisation of receptors and G protein-independent signalling. Upon agonist binding, a GDP/GTP exchange occurs within the α subunit, leading to the dissociation of the receptor/G protein complex. The agonist-bound receptor is now accessible for phosphorylation through, e.g. GRKs at its C-terminus and intracellular loop regions. This process results in an increased affinity of the receptor for β-arrestins, which bind the receptor and mediate its internalisation through clathrin-coated pits. Before and during the internalisation process, arrestin acts as a scaffolding protein. It brings proteins, which are part of a common signalling cascade, in close proximity, so that they can activate each other. After internalisation and gathering in vesicles, the receptors can undergo two different pathways. On one hand, recycling, back to the plasma membrane, can occur, or the receptors can be degraded by the ubiquitin/proteasome machinery.

Two different isoforms of β-arrestin are known, namely β-arrestin1 and β-arrestin2. Both isoforms are ubiquitously expressed in the human body[38,50,51]. Studies with knock-out mice suggest that both isoforms serve a similar function[33], since mice lacking only one variant, appear normal, provided that they are not pharmacologically challenged[52-54]. The latter might be explained by reports on higher affinities of class A receptors for β-arrestin2 than for β-arrestin1[46]. A double knock-out, however, is prenatally lethal[33].

1.1.3 β-Arrestin-dependent signalling

Besides blocking the interaction site of G proteins and mediating the internalisation of receptors, β-arrestins are involved in intracellular signalling[33]. They act as scaffolding proteins within signalling cascades[38,55]. For example, kinases, which activate the enzymatic function of other proteins by phosphorylation, directly bind to β-arrestin. Prominent representatives are the extracellularly-regulated kinases 1 and 2 (ERK1/2), which are mitogen-activated protein (MAP) kinases[56,57]. Both bind to β-arrestins, and their downstream signalling partners do the same. In this way ERK1/2 and e.g. c-Src[58] are brought into close proximity, leading to phosphorylation and therefore, to the activation of the latter[33]. In addition to ERK1/2 and c-Src, there are numerous interaction partners[33] such as p38 MAP-[59] or Akt kinases[60] and signalling pathways[61] described that are activated through β-arrestins. By contrast, through the binding of E3 ubiquitin ligases, β-arrestins convey the degradation of receptors[46,47,62], whereas phosphodiesterases as interaction partners are responsible for the cleavage of cAMP[63].

1.1.4 Three-dimensional structure of GPCRs

Although at that time scientists were oblivious to that[64], structural investigations on GPCRs began independently with the work of two research groups, determining the amino acid sequence of rhodopsin by Edman degradation[65,66]. Direct evidence that rhodopsin and GPCRs share the same overall structure was reported, when the first GPCR, the β_2 adrenoceptor, was cloned[32]. It became obvious that both proteins consist of seven transmembrane helices with their N-terminus facing the extracellular space and their C-terminus the inside[32,65,66].

The first three-dimensional structure was reported in 2000, again of rhodopsin[67], with the up to now most commonly used technique, i.e. X-ray diffraction analysis of proteins crystals[68]. Seven years later, the first crystal structure of a ligand-activated GPCR was reported by the Kobilka and Stevens groups. The authors were able to crystallise the β_2 adrenoceptor in complex with the β-blocker carazolol[69].

These reports demonstrated that crystallisation of a GPCR is challenging, requiring specialised procedures, which must be individually optimised for each receptor[70]: for reconstitution, some kind of synthetic membrane environment is needed, e.g. lipid bicelles, or the so-called lipidic cubic phase. To enhance crystal packing, a fusion protein of the receptor together with a well-crystallising protein, such as lysozyme, is generated. Furthermore, crystallisation of the receptor alone is not possible, a stabilisation

of the inactive conformation is needed and achieved by adding an antagonist. Finally, since the formation of crystals can take a long time, the receptor´s primary structure must be mutated, to increase its long-term stability.

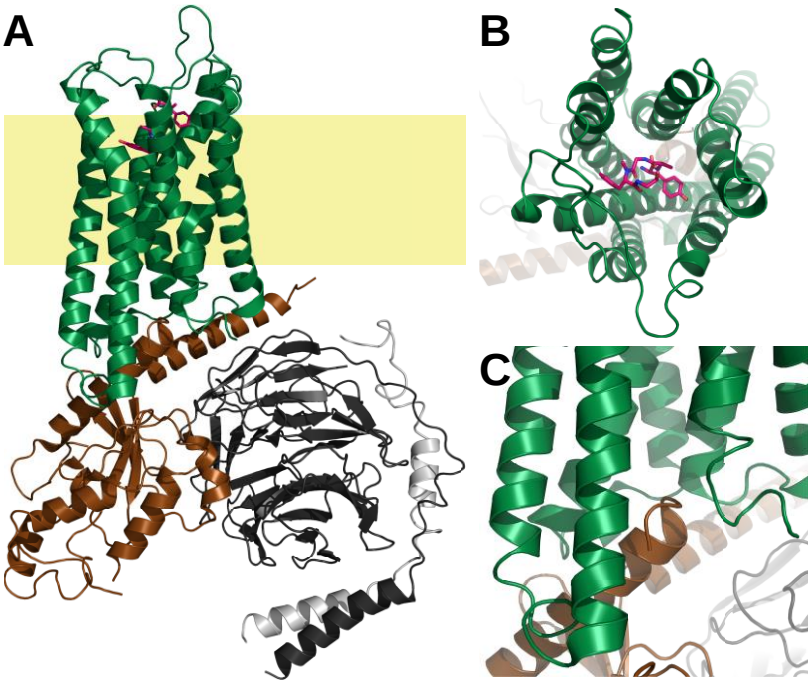

Fig. 1.3: Cartoon representation of the three-dimensional structure of the μ-opioid receptor in complex with $G\alpha_i\beta\gamma$ as a general example the structure of a GPCR. The coordinates of the μ-opioid receptor/Gi-complex[77] were obtained from pdb (6ddf) and processed using PyMOL. The receptor is represented in green, the $G\alpha_i$ is brown, the Gβ is black and the Gγ is depicted in light-grey. The putative localisation of the membrane is represented in light-yellow. **A** is a full-size representation of the entire complex. **B** is a close-up on the ligand, bound in the middle of the seven-helix bundle. The interaction site between GPCR and $G\alpha_i$ is shown in **C**, where the C-terminus of $G\alpha_i$ points inside the helix bundle after an outward movement of helix 6.

These findings paved the way for the crystallisation of a plethora of different receptors, such as the histamine H_1 receptor (hH_1R)[71], the dopamine D_3 receptor[72], the chemokine receptor CXCR4[73], or the neuropeptide Y Y_1 receptor[74]. Another milestone was reached soon with the description of the first structure of a GPCR in complex with its canonical G protein, the β_2 adrenoceptor/G_s complex[75]. Until now, over 200 structures of approx. 30 different GPCRs have been solved[68], which help not only pharmacologists to understand the activation of such receptors, but also medicinal chemists to design compounds with enhanced binding and functional properties. In addition to X-ray diffraction, advances in the field of cryo-electron microscopy (EM) begin to influence receptor structure determination more and more[68]. Although the size of a GPCR alone is insufficient for structure determination using cryo-EM[76], a receptor in complex with intracellular signalling partners, such as G proteins or arrestins, is. The structure of the μ-opioid receptor in complex with $G\alpha_i\beta\gamma$ and the ligand DAMGO, obtained by Koehl et al. through cryo-EM[77], is shown in Fig. 1.3.

The GPCR consists of seven bundled α-helices within the plasma membrane. The ligand binds on the extracellular side, in a cave formed by the helix bundle, to the receptor (Fig. 1.3B). Through the types of amino acids, their localisation and their orientation inside the binding cleft, the unique ligand specificity of each GPCR is determined. From several studies, a general activation mechanism, which starts with an outward movement of the sixth α-helix of the receptor (the foremost helix in Fig. 1.3A and C) upon agonist binding, became clear[1]. This movement generates space for the C-terminal helix of the Gα subunit, which then points from the intracellular side to the helix bundle (Fig. 1.3C). Structural investigations on

GPCR/G protein complexes suggest that this intracellular binding pocket functions analogously to the extracellular one. The amino acids interacting with the C-terminal α5-helix of the Gα subunit determine to which Gα subtype the GPCR couples[1,77]. This intracellular interface is also one of the key interaction sides of arrestins with GPCRs, and by occupying the very same space as the C-terminus of Gα does, it directly prevents the receptor from activating the latter[1,78,79].

1.1.5 Functional selectivity

The classical ternary complex model of receptor activation takes only one intracellular binding partner of the GPCR, the G protein, into account[17]. However, as mentioned under 1.1.2, there are at least GRKs and β-arrestins also interacting with GPCRs[39,51], and it was shown that certain ligands preferentially activate (or are biased towards the activation of) Gα proteins over the recruitment of β-arrestins[80], or vice versa[81]. Furthermore, agonists were reported that led to the selective activation of one Gα subtype over another[82], which shows that GPCRs not always signal exclusively through their primarily-attributed G protein subtype. Taken together, these findings imply that each agonist can stabilise its own distinct receptor conformation, each of which can differ in its ability to activate downstream signalling partners[83]. Evidence for these agonist-dependent receptor conformations was found using X-ray crystallography[84] and was demonstrated multiple times with different ligands at different receptors[84-87]. Therefore, the classical ternary complex model of receptor activation is inadequate, suggesting that a GPCR is more than a simple on/off-switch[88]. Rather than having an inactive and only one active conformation, a receptor has multiple active conformations differing in their ability to signal downstream[89]. To further increase complexity, allosteric modulators of receptor activation, which unveil their effects only in the presence of an orthosteric ligand[90-92], have been described. Moreover, multiple receptors were reported to exist as homo-[93] or heterodimers[94] within the cellular membrane, capable of e.g. transactivating each other[94]. To conclude, a reductionist approach in functional ligand characterisation can be misleading and sensitive techniques for the characterisation of multiple pathways, ideally in a simultaneous manner, are needed, because important effects might otherwise be overlooked.

1.1.6 GPCRs as drug targets

GPCRs have been a drug target long before their existence was even known[9,10,95]. First compounds addressing GPCRs with a therapeutic purpose were antihistamines and β-blockers, which were the first so-called blockbuster medications. As mentioned above, these compounds helped researchers to elucidate the function of GPCRs[8]. To date, approx. 27% of the global market share are drugs that target GPCRs[96] with a multitude of different indications, such as asthma, diabetes type 2 or various autoimmune diseases[96]. The mode of action of the drugs or drug candidates varies from classical agonists and antagonists[96] to more recently identified compounds, which are allosteric modulators[96].

Especially certain biased agonists are considered to be promising drug candidates, because side-effects are seen in connection with the activation of unwanted signalling pathways at several receptors[97,98]. An example is the μ-opioid receptor, at which the induction of β-arrestin recruitment is presumably responsible for the severe side-effects[99,100] associated with opioid analgesics and for which recently a G protein-biased agonist (PZM21) was reported[80]. However, it should be mentioned that in a very recent study G protein bias of PZM21 and lacking respiratory depression were not confirmed[101]. Hill et al. [101] point out the difficulty to quantify bias, in particular of low efficacy agonists, and to compare bias between different cell types and assays, a problem, which is increasingly being acknowledged[102-104]. These contradictory studies demonstrate that there is a need for techniques enabling a reliable quantification of agonist bias.

1.2 Functional characterisation of GPCR ligands

As mentioned in the beginning, functional investigations on GPCRs began with pharmacology in living animals[95] or isolated organs[3], which is an approach that has been used until to date[105]. Due to structural differences between the receptor orthologues, data obtained by organ pharmacology from, e.g. guinea-pigs, might not always apply in the exact same way to the corresponding human tissue[34,106,107]. Hence, cancer cell lines of human origin with endogenous expression of a certain receptor[108], or recombinant expression of the receptor under study in immortal(-ised) cell lines have become the most prominent systems for investigations on GPCRs[109,110].

First in vitro experiments were focused on the formation of second messengers, such as cAMP[6], IP species[111,112], or Ca^{2+} ions[113,114] and these are still the most often assessed effects provoked by receptor activation, because they can be determined using assays with moderate to high throughput. By determining the activity of the GTPase of the Gα subunit, receptor activation can be probed more proximally. This is beneficial for precise determinations of agonist efficacies, or agonist bias, since substantial amplification occurs the more distally the activation of the signalling cascade is probed. The latter can result in an over-interpretation of agonistic effects[101,115]. Classical assays for a proximal determination of GPCR activation are the steady-state GTPase assay[13], in which the hydrolysis of a [^{32,33}P]-labelled γ-phosphate of GTP is determined, or the [^{35}S]GTPγS assay[116,117], which utilises a non-hydrolysable GTP analogue. The readouts of these two assays are both based on the radioactive decay of phosphorus or sulfate isotopes.

There are several major drawbacks of the aforementioned techniques: most of them are lysis-based or require the preparation of membranes, and, if this is not the case, throughput is often limited. Thus, sensitive assays for the proximal quantification of GPCR-mediated activation of various pathways in live cells are needed[118]. Most promising techniques that should meet the demands are resonance energy transfer techniques (RET), or split luciferase complementation (SLC), employed to probe protein/protein interactions (PPIs) within signalling cascades activated through GPCRs.

1.2.1 Resonance energy transfer-based techniques

Förster, or “fluorescence” resonance energy transfer (FRET) was initially described by Theodor Förster[119] and describes a phenomenon that applies to two fluorophores, the excitation and emission spectra of which overlap. If the first fluorophore (donor) with the shorter excitation and emission maxima is excited by an external light source, it can transfer its energy (a radiationless process) to the other (acceptor) fluorophore, provided that both are in close proximity (≤ 10 nm) and in correct orientation[120]. Therefore, resonance energy transfer can be used for investigations on PPIs. It was successfully applied using proteins labelled with organic fluorophores[121], but with the discovery and cloning of the green-fluorescent

protein (GFP)[122,123] and the subsequent engineering of its colour variants[124], it became possible between fluorescent proteins and also in intact cells[125].

In addition, RET can also occur between luciferases, which are enzymes capable of emitting light when their substrates are provided, and appropriate fluorescent proteins[126,127]. This variant of RET is called bioluminescence resonance energy transfer (BRET) and is, although rarely, occurring in nature. The jellyfish *Aequorea victoria*, for example, from which GFP originates, uses its blue light-emitting luciferase aequorin as donor to excite GFP[122]. In modern molecular biology the most prominent luciferases used for BRET studies are the renilla luciferase (RLuc) from the sea pansy *Renilla reniformis*[128], the firefly luciferase from the firefly *Photinus pyralis*[129] and more recently, genetically optimised luciferases such as the NanoLuc (NLuc)[130,131], derived from a luciferase excreted by the deep-sea shrimp *Oplophorus gracilirostris*.

On one hand, FRET has the advantage that the overall light-intensities are high, which means that only very short integration times of the detectors are needed, enabling a high temporal resolution during measurements[120]. On the other hand, since no external excitation light is needed, BRET often has better signal-to-noise ratios.

With respect to the functional characterisation of GPCRs, FRET and BRET have been successfully applied multiple times to probe, e.g. second messenger formation[125,132-134], dissociation and rearrangements of G protein subunits[135-138], β-arrestin recruitment[139,140] and even conformational changes of the GPCR itself[141-144]. The high temporal resolution that can be achieved using FRET[141,145], helped to unravel the temporal order of the events taking place after agonist binding to the receptor[120,141], some of which happening on the µs time-scale.

However, a major shortcoming of FRET- and BRET-based assays is the fact that multiparametric measurements of the activation of two or more signalling pathways at once are very challenging. A large fraction of the visible part of the light spectrum is already covered by the excitation light and the emitted light of the two luminescent proteins used, which would make meticulous spectral unmixing necessary[146-148].

1.2.2 Split luciferase complementation

A better option for probing multiple pathways simultaneously is SLC, belonging to the overall group of split-reporter assays. The underlying principle is the “dissection” of a protein into two complementing fragments, which can restore the catalytic function of the original protein when brought into close proximity[149,150]. By means of molecular biology techniques, fusion proteins, consisting of the proteins for which a specific interaction is expected and reporter protein fragments, must be generated[150-152]. The

induction of the interaction of the two host proteins brings the reporter fragments in close proximity, leading to the restoration of the enzymatic function (Fig. 1.4).

The first described approach, using split-reporter complementation, involved ubiquitin. Upon interaction of the two host proteins, a reporter enzyme becomes cleaved off the complex by a ubiquitin-specific protease, which can be detected by SDS-PAGE[153]. The first assays that did not depend on cell lysis were based on split β-galactosidase or split β-lactamase. Both make use of synthetic substrates, which change their optical properties (e.g. formation of a fluorescent dye) after processing by the enzymes[154,155].

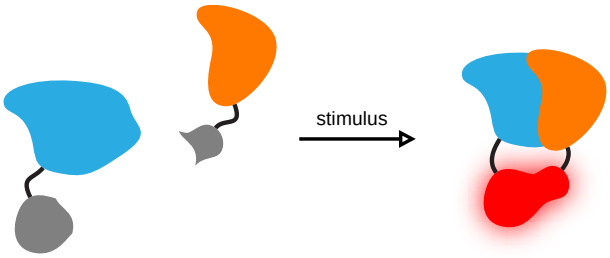

Fig. 1.4: Schematic illustration of the split-reporter principle. A reporter protein is split into two catalytically-inactive fragments, which are capable of restoring the enzymatic function, when brought into close proximity. These two fragments are then fused to two proteins through flexible linkers, from which a specific interaction is expected. When applying a stimulus, which induces the interaction of the host proteins, the enzymatic activity of the reporter is restored and can be detected.

Imaging was already possible using the split β-galactosidase assay, due to the formation of the fluorescent dye. The localisation of the fluorophore, however, did not resemble the exact site of the probed PPI within the cell. Precise localisation became possible when Ozawa et al. and Ghosh et al. reported independently that also GFP can be used in a split reporter assay[156-158]. Shortly after, this was also achieved in a multiplexed manner using colour variants of GFP[159]. However, a major disadvantage of the split GFP technique are the long maturation times, which are needed for GFP to fully refold and rebuilt its fluorophore[158]. This makes kinetic analyses nearly impossible. Furthermore, the interaction of the two fragments is not reversible once the full-size GFP has been restored[151,156].

Therefore, a very attractive option are luciferases as reporter proteins. Although first approaches used intein-assisted luciferase complementation, causing an irreversible reaction[160], newer assays are not dependent on inteins anymore, which provides a dynamic, fully reversible, system[161]. The relatively short maturation time periods, compared to split GFP, enable kinetic analyses of the probed PPI, and the independence of excitation light results in a low background and therefore, higher sensitivities[161,162].

In the context of GPCR research, SLC has been applied multiple times e.g. for the detection of second messenger formation[163,164], or β-arrestin recruitment[152,165-167].

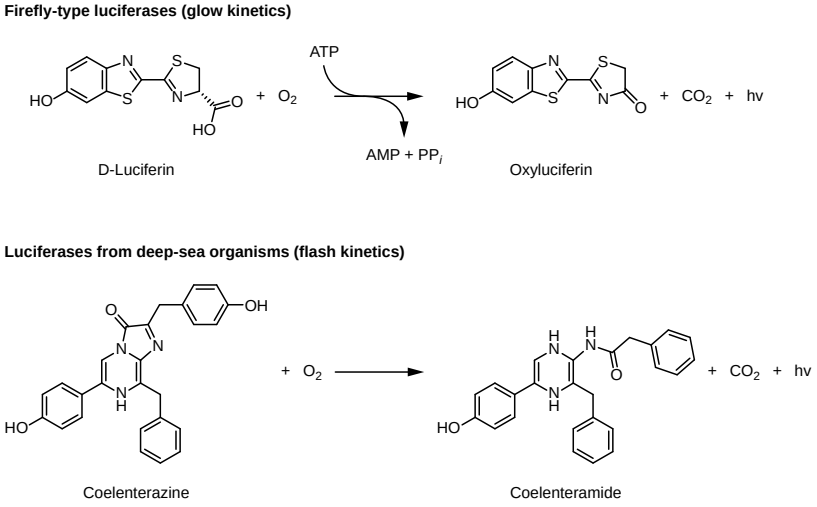

Scheme 1.1: Reactions catalysed by luciferases, which are most-commonly used in molecular biology. Both luciferase types catalyse an oxidative decarboxylation under consumption of molecular oxygen. In addition, firefly-type luciferases utilize ATP as reactant, which is dephosphorylated into AMP and pyrophosphate.

Luciferases used in these assays are mainly the same as mentioned under 1.2.1. On one hand, glow-type luciferases, such as the firefly luciferase, or luciferases cloned from click-beetles, which utilise D-luciferin, ATP and O_2 as substrate (Scheme 1.1), have the advantage that longer time periods can be analysed, due to the continuous light emission[152,163,164]. On the other hand, flash-type luciferases, like RLuc or NLuc, which consume coelenterazine and O_2 (Scheme 1.1) have the advantage that their initial brightness is very high[130,168].

NLuc, when split into two fragments, has a short maturation time, and the two fragments have a very low auto-affinity, making the measurement of faster kinetics possible[165]. However, the duration of the measurements is limited by the flash kinetics of the luminescence reaction, which causes a rapid decline in light output, reaching the lower detection limit of most devices, already after a few hours and makes a precise baseline correction necessary to unveil the true kinetics of the PPI.

Another advantage of luciferases is the availability of enzymes, emitting light of different wavelengths[169], enabling the application of different luciferases in the same assay to probe two or more PPIs simultaneously[170,171]. On one hand, the emission spectrum depends on the amino acids surrounding the catalytic site of the protein[172-174]. On the other hand, derivatives of the native substrates can shift the emission peak[175,176]. Most flash-type luciferases emit light of shorter wavelength, with peaks in the blue range of the visible spectrum[128,130]. The glow-type luciferases are available in "different colours"[169]. For example, the firefly luciferase emits light with an intensity peak in the orange range[173,177], whereas luciferases from click-beetles, and genetically-engineered variants thereof, emit green, or red light[169,174]. Therefore, SLC harbours the highest potential with respect to easy and reliable multiparametric measurements of PPIs at a proximal stage within signalling cascades activated by GPCRs with high throughput.

1.3 References

1 Hilger, D., Masureel, M. & Kobilka, B. K. Structure and dynamics of GPCR signaling complexes. *Nat Struct Mol Biol* **25**, 4-12, doi:10.1038/s41594-017-0011-7 (2018).

2 Ehrlich, P. Address in Pathology, On Chemotherapy: Scientific principles, methods and results. *Br Med J* **2**, 353-359 (1913).

3 Langley, J. N. On the contraction of muscle, chiefly in relation to the presence of 'receptive' substances: Part IV. The effect of curari and of some other substances on the nicotine response of the sartorius and gastrocnemius muscles of the frog. *J Physiol* **39**, 235-295 (1909).

4 Berthet, J., Rall, T. W. & Sutherland, E. W. The relationship of epinephrine and glucagon to liver phosphorylase. IV. Effect of epinephrine and glucagon on the reactivation of phosphorylase in liver homogenates. *J Biol Chem* **224**, 463-475 (1957).

5 Sutherland, E. W., Oye, I. & Butcher, R. W. The Action of Epinephrine and the Role of the Adenyl Cyclase System in Hormone Action. *Recent Prog Horm Res* **21**, 623-646 (1965).

6 Robison, G. A., Butcher, R. W. & Sutherland, E. W. Adenyl cyclase as an adrenergic receptor. *Ann N Y Acad Sci* **139**, 703-723 (1967).

7 Lefkowitz, R. J. The superfamily of heptahelical receptors. *Nat Cell Biol* **2**, E133-136, doi:10.1038/35017152 (2000).

8 Hill, S. J. G-protein-coupled receptors: past, present and future. *Br J Pharmacol* **147 Suppl 1**, S27-37, doi:10.1038/sj.bjp.0706455 (2006).

9 Black, J. W., Duncan, W. A. & Shanks, R. G. Comparison of some properties of pronethalol and propranolol. *Br J Pharmacol Chemother* **25**, 577-591 (1965).

10 Bain, W. A., Broadbent, J. L. & Warin, R. P. Comparison of anthisan (mepyramine maleate) and phenergan as histamine antagonists. *Lancet* **2**, 47-52 (1949).

11 Hepler, J. R. & Gilman, A. G. G proteins. *Trends Biochem Sci* **17**, 383-387 (1992).

12 Rodbell, M., Birnbaumer, L., Pohl, S. L. & Krans, H. M. The glucagon-sensitive adenyl cyclase system in plasma membranes of rat liver. V. An obligatory role of guanylnucleotides in glucagon action. *J Biol Chem* **246**, 1877-1882 (1971).

13 Cassel, D. & Selinger, Z. Catecholamine-stimulated GTPase activity in turkey erythrocyte membranes. *Biochim Biophys Acta* **452**, 538-551 (1976).

14 Harden, T. K. Agonist-induced desensitization of the β-adrenergic receptor-linked adenylate cyclase. *Pharmacol Rev* **35**, 5-32 (1983).

15 Stadel, J. M., DeLean, A. & Lefkowitz, R. J. A high affinity agonist-β-adrenergic receptor complex is an intermediate for catecholamine stimulation of adenylate cyclase in turkey and frog erythrocyte membranes. *J Biol Chem* **255**, 1436-1441 (1980).

16 Kent, R. S., De Lean, A. & Lefkowitz, R. J. A quantitative analysis of beta-adrenergic receptor interactions: resolution of high and low affinity states of the receptor by computer modeling of ligand binding data. *Mol Pharmacol* **17**, 14-23 (1980).

17 De Lean, A., Stadel, J. M. & Lefkowitz, R. J. A ternary complex model explains the agonist-specific binding properties of the adenylate cyclase-coupled β-adrenergic receptor. *J Biol Chem* **255**, 7108-7117 (1980).

18 Northup, J. K., Sternweis, P. C., Smigel, M. D., Schleifer, L. S., Ross, E. M. & Gilman, A. G. Purification of the regulatory component of adenylate cyclase. *Proc Natl Acad Sci U S A* **77**, 6516-6520 (1980).

19 Gilman, A. G. G proteins: transducers of receptor-generated signals. *Annu Rev Biochem* **56**, 615-649, doi:10.1146/annurev.bi.56.070187.003151 (1987).

20 Birnbaumer, L. Expansion of signal transduction by G proteins. The second 15 years or so: from 3 to 16 α subunits plus βγ dimers. *Biochim Biophys Acta* **1768**, 772-793, doi:10.1016/j.bbamem.2006.12.002 (2007).

21 Bokoch, G. M., Katada, T., Northup, J. K., Ui, M. & Gilman, A. G. Purification and properties of the inhibitory guanine nucleotide-binding regulatory component of adenylate cyclase. *J Biol Chem* **259**, 3560-3567 (1984).

22 Schröder, R., Janssen, N., Schmidt, J., Kebig, A., Merten, N., Hennen, S., Müller, A., Blättermann, S., Mohr-Andrä, M., Zahn, S., Wenzel, J., Smith, N. J., Gomeza, J., Drewke, C., Milligan, G., Mohr, K. & Kostenis, E. Deconvolution of complex G protein-coupled receptor signaling in live cells using dynamic mass redistribution measurements. *Nat Biotechnol* **28**, 943-949, doi:10.1038/nbt.1671 (2010).

23 Lieb, S., Littmann, T., Plank, N., Felixberger, J., Tanaka, M., Schäfer, T., Krief, S., Elz, S., Friedland, K., Bernhardt, G., Wegener, J., Ozawa, T. & Buschauer, A. Label-free versus conventional cellular assays: Functional investigations on the human histamine H_1 receptor. *Pharmacol Res* **114**, 13-26, doi:10.1016/j.phrs.2016.10.010 (2016).

24 Michell, R. H. Inositol lipids in cellular signalling mechanisms. *Trends Biochem Sci* **17**, 274-276 (1992).

25 Streb, H., Irvine, R. F., Berridge, M. J. & Schulz, I. Release of Ca^{2+} from a nonmitochondrial intracellular store in pancreatic acinar cells by inositol-1,4,5-trisphosphate. *Nature* **306**, 67-69 (1983).

26 Pang, I. H. & Sternweis, P. C. Purification of unique α subunits of GTP-binding regulatory proteins (G proteins) by affinity chromatography with immobilized βγ subunits. *J Biol Chem* **265**, 18707-18712 (1990).

27 Smrcka, A. V., Hepler, J. R., Brown, K. O. & Sternweis, P. C. Regulation of polyphosphoinositide-specific phospholipase C activity by purified G_q. *Science* **251**, 804-807 (1991).

28 Boyer, J. L., Waldo, G. L., Evans, T., Northup, J. K., Downes, C. P. & Harden, T. K. Modification of AlF_4^-- and receptor-stimulated phospholipase C activity by G-protein βγ subunits. *J Biol Chem* **264**, 13917-13922 (1989).

29 Taussig, R., Tang, W. J., Hepler, J. R. & Gilman, A. G. Distinct patterns of bidirectional regulation of mammalian adenylyl cyclases. *J Biol Chem* **269**, 6093-6100 (1994).

30 Herlitze, S., Garcia, D. E., Mackie, K., Hille, B., Scheuer, T. & Catterall, W. A. Modulation of Ca^{2+} channels by G-protein βγ subunits. *Nature* **380**, 258-262, doi:10.1038/380258a0 (1996).

31 Ikeda, S. R. Voltage-dependent modulation of N-type calcium channels by G-protein βγ subunits. *Nature* **380**, 255-258, doi:10.1038/380255a0 (1996).

32 Dixon, R. A., Kobilka, B. K., Strader, D. J., Benovic, J. L., Dohlman, H. G., Frielle, T., Bolanowski, M. A., Bennett, C. D., Rands, E., Diehl, R. E., Mumford, R. A., Slater, E. E., Sigal, I. S., Caron, M. G., Lefkowitz, R. J. & Strader, C. D. Cloning of the gene and cDNA for mammalian β-adrenergic receptor and homology with rhodopsin. *Nature* **321**, 75-79, doi:10.1038/321075a0 (1986).

33 Luttrell, L. M. & Gesty-Palmer, D. Beyond desensitization: physiological relevance of arrestin-dependent signaling. *Pharmacol Rev* **62**, 305-330, doi:10.1124/pr.109.002436 (2010).

34 Xie, S. X., Schalkhausser, F., Ye, Q. Z., Seifert, R. & Buschauer, A. Effects of impromidine- and arpromidine-derived guanidines on recombinant human and guinea pig histamine H_1 and H_2 receptors. *Arch Pharm (Weinheim)* **340**, 9-16, doi:10.1002/ardp.200600140 (2007).

35 Strasser, A., Wittmann, H. J., Buschauer, A., Schneider, E. H. & Seifert, R. Species-dependent activities of G-protein-coupled receptor ligands: lessons from histamine receptor orthologs. *Trends Pharmacol Sci* **34**, 13-32, doi:10.1016/j.tips.2012.10.004 (2013).

36 Kakiuchi, S. & Rall, T. W. The influence of chemical agents on the accumulation of adenosine 3',5'-Phosphate in slices of rabbit cerebellum. *Mol Pharmacol* **4**, 367-378 (1968).

37 Mahan, L. C., Koachman, A. M. & Insel, P. A. Genetic analysis of β-adrenergic receptor internalization and down-regulation. *Proc Natl Acad Sci U S A* **82**, 129-133 (1985).

38 Ferguson, S. S. Evolving concepts in G protein-coupled receptor endocytosis: the role in receptor desensitization and signaling. *Pharmacol Rev* **53**, 1-24 (2001).

39 Gurevich, E. V., Tesmer, J. J., Mushegian, A. & Gurevich, V. V. G protein-coupled receptor kinases: more than just kinases and not only for GPCRs. *Pharmacol Ther* **133**, 40-69, doi:10.1016/j.pharmthera.2011.08.001 (2012).

40 Benovic, J. L., Strasser, R. H., Caron, M. G. & Lefkowitz, R. J. β-adrenergic receptor kinase: identification of a novel protein kinase that phosphorylates the agonist-occupied form of the receptor. *Proc Natl Acad Sci U S A* **83**, 2797-2801 (1986).

41 Benovic, J. L., Kühn, H., Weyand, I., Codina, J., Caron, M. G. & Lefkowitz, R. J. Functional desensitization of the isolated β-adrenergic receptor by the β-adrenergic receptor kinase: potential role of an analog of the retinal protein arrestin (48-kDa protein). *Proc Natl Acad Sci U S A* **84**, 8879-8882 (1987).

42 DeWire, S. M., Ahn, S., Lefkowitz, R. J. & Shenoy, S. K. β-Arrestins and Cell Signaling. *Annual Review of Physiology* **69**, 483-510, doi:10.1146/annurev.physiol.69.022405.154749 (2007).

43 Lohse, M. J., Benovic, J. L., Codina, J., Caron, M. G. & Lefkowitz, R. J. β-Arrestin: a protein that regulates β-adrenergic receptor function. *Science* **248**, 1547-1550 (1990).

44 Goodman, O. B., Jr., Krupnick, J. G., Santini, F., Gurevich, V. V., Penn, R. B., Gagnon, A. W., Keen, J. H. & Benovic, J. L. β-Arrestin acts as a clathrin adaptor in endocytosis of the β_2-adrenergic receptor. *Nature* **383**, 447-450, doi:10.1038/383447a0 (1996).

45 Oakley, R. H., Laporte, S. A., Holt, J. A., Barak, L. S. & Caron, M. G. Association of β-arrestin with G protein-coupled receptors during clathrin-mediated endocytosis dictates the profile of receptor resensitization. *J Biol Chem* **274**, 32248-32257 (1999).

46 Oakley, R. H., Laporte, S. A., Holt, J. A., Caron, M. G. & Barak, L. S. Differential affinities of visual arrestin, β-arrestin1, and β-arrestin2 for G protein-coupled receptors delineate two major classes of receptors. *J Biol Chem* **275**, 17201-17210, doi:10.1074/jbc.M910348199 (2000).

47 Martin, N. P., Lefkowitz, R. J. & Shenoy, S. K. Regulation of V2 vasopressin receptor degradation by agonist-promoted ubiquitination. *J Biol Chem* **278**, 45954-45959, doi:10.1074/jbc.M308285200 (2003).

48 Oakley, R. H., Laporte, S. A., Holt, J. A., Barak, L. S. & Caron, M. G. Molecular determinants underlying the formation of stable intracellular G protein-coupled receptor-β-arrestin complexes after receptor endocytosis. *J Biol Chem* **276**, 19452-19460, doi:10.1074/jbc.M101450200 (2001).

49 Kendall, R. T. & Luttrell, L. M. Diversity in arrestin function. *Cell Mol Life Sci* **66**, 2953-2973, doi:10.1007/s00018-009-0088-1 (2009).

50 Sterne-Marr, R., Gurevich, V. V., Goldsmith, P., Bodine, R. C., Sanders, C., Donoso, L. A. & Benovic, J. L. Polypeptide variants of β-arrestin and arrestin3. *J Biol Chem* **268**, 15640-15648 (1993).

51 Lohse, M. J. & Hoffmann, C. Arrestin interactions with G protein-coupled receptors. *Handb Exp Pharmacol* **219**, 15-56, doi:10.1007/978-3-642-41199-1_2 (2014).

52 Conner, D. A., Mathier, M. A., Mortensen, R. M., Christe, M., Vatner, S. F., Seidman, C. E. & Seidman, J. G. β-Arrestin1 knockout mice appear normal but demonstrate altered cardiac responses to β-adrenergic stimulation. *Circ Res* **81**, 1021-1026 (1997).

53 Bohn, L. M., Lefkowitz, R. J. & Caron, M. G. Differential mechanisms of morphine antinociceptive tolerance revealed in β-arrestin-2 knock-out mice. *J Neurosci* **22**, 10494-10500 (2002).

54 Bohn, L. M., Lefkowitz, R. J., Gainetdinov, R. R., Peppel, K., Caron, M. G. & Lin, F. T. Enhanced morphine analgesia in mice lacking β-arrestin 2. *Science* **286**, 2495-2498 (1999).

55 Witzel, F., Maddison, L. & Blüthgen, N. How scaffolds shape MAPK signaling: what we know and opportunities for systems approaches. *Front Physiol* **3**, 475, doi:10.3389/fphys.2012.00475 (2012).

56 Khoury, E., Nikolajev, L., Simaan, M., Namkung, Y. & Laporte, S. A. Differential regulation of endosomal GPCR/β-arrestin complexes and trafficking by MAPK. *J Biol Chem* **289**, 23302-23317, doi:10.1074/jbc.M114.568147 (2014).

57 Shenoy, S. K., Drake, M. T., Nelson, C. D., Houtz, D. A., Xiao, K., Madabushi, S., Reiter, E., Premont, R. T., Lichtarge, O. & Lefkowitz, R. J. β-Arrestin-dependent, G protein-independent ERK1/2 activation by the β_2 adrenergic receptor. *J Biol Chem* **281**, 1261-1273, doi:10.1074/jbc.M506576200 (2006).

58 Luttrell, L. M., Ferguson, S. S. G., Daaka, Y., Miller, W. E., Maudsley, S., Della Rocca, G. J., Lin, F. T., Kawakatsu, H., Owada, K., Luttrell, D. K., Caron, M. G. & Lefkowitz, R. J. β-Arrestin-Dependent Formation of β_2-Adrenergic Receptor-Src Protein Kinase Complexes. *Science* **283**, 655-661, doi:10.1126/science.283.5402.655 (1999).

59 Gong, K., Li, Z., Xu, M., Du, J., Lv, Z. & Zhang, Y. A novel protein kinase A-independent, β-arrestin-1-dependent signaling pathway for p38 mitogen-activated protein kinase activation by β_2-adrenergic receptors. *J Biol Chem* **283**, 29028-29036, doi:10.1074/jbc.M801313200 (2008).

60 Beaulieu, J. M., Sotnikova, T. D., Marion, S., Lefkowitz, R. J., Gainetdinov, R. R. & Caron, M. G. An Akt/β-arrestin 2/PP2A signaling complex mediates dopaminergic neurotransmission and behavior. *Cell* **122**, 261-273, doi:10.1016/j.cell.2005.05.012 (2005).

61 Shukla, A. K., Xiao, K. & Lefkowitz, R. J. Emerging paradigms of β-arrestin-dependent seven transmembrane receptor signaling. *Trends Biochem Sci* **36**, 457-469, doi:10.1016/j.tibs.2011.06.003 (2011).

62 Shenoy, S. K., McDonald, P. H., Kohout, T. A. & Lefkowitz, R. J. Regulation of receptor fate by ubiquitination of activated β_2-adrenergic receptor and β-arrestin. *Science* **294**, 1307-1313, doi:10.1126/science.1063866 (2001).

63 Perry, S. J., Baillie, G. S., Kohout, T. A., McPhee, I., Magiera, M. M., Ang, K. L., Miller, W. E., McLean, A. J., Conti, M., Houslay, M. D. & Lefkowitz, R. J. Targeting of cyclic AMP degradation to β_2-adrenergic receptors by β-arrestins. *Science* **298**, 834-836, doi:10.1126/science.1074683 (2002).

64 Costanzi, S., Siegel, J., Tikhonova, I. G. & Jacobson, K. A. Rhodopsin and the others: a historical perspective on structural studies of G protein-coupled receptors. *Curr Pharm Des* **15**, 3994-4002 (2009).

65 Ovchinnikov Iu, A., Abdulaev, N. G., Feigina, M., Artamonov, I. D. & Bogachuk, A. S. Visual rhodopsin. III. Complete amino acid sequence and topography in a membrane. *Bioorg Khim* **9**, 1331-1340 (1983).

66 Hargrave, P. A., McDowell, J. H., Curtis, D. R., Wang, J. K., Juszczak, E., Fong, S. L., Rao, J. K. & Argos, P. The structure of bovine rhodopsin. *Biophys Struct Mech* **9**, 235-244 (1983).

67 Palczewski, K., Kumasaka, T., Hori, T., Behnke, C. A., Motoshima, H., Fox, B. A., Le Trong, I., Teller, D. C., Okada, T., Stenkamp, R. E., Yamamoto, M. & Miyano, M. Crystal structure of rhodopsin: A G protein-coupled receptor. *Science* **289**, 739-745 (2000).

68 Thal, D. M., Vuckovic, Z., Draper-Joyce, C. J., Liang, Y. L., Glukhova, A., Christopoulos, A. & Sexton, P. M. Recent advances in the determination of G protein-coupled receptor structures. *Curr Opin Struct Biol* **51**, 28-34, doi:10.1016/j.sbi.2018.03.002 (2018).

69 Cherezov, V., Rosenbaum, D. M., Hanson, M. A., Rasmussen, S. G., Thian, F. S., Kobilka, T. S., Choi, H. J., Kuhn, P., Weis, W. I., Kobilka, B. K. & Stevens, R. C. High-resolution crystal structure of an engineered human β_2-adrenergic G protein-coupled receptor. *Science* **318**, 1258-1265, doi:10.1126/science.1150577 (2007).

70 Ghosh, E., Kumari, P., Jaiman, D. & Shukla, A. K. Methodological advances: the unsung heroes of the GPCR structural revolution. *Nat Rev Mol Cell Biol* **16**, 69-81, doi:10.1038/nrm3933 (2015).

71 Shimamura, T., Shiroishi, M., Weyand, S., Tsujimoto, H., Winter, G., Katritch, V., Abagyan, R., Cherezov, V., Liu, W., Han, G. W., Kobayashi, T., Stevens, R. C. & Iwata, S. Structure of the human histamine H_1 receptor complex with doxepin. *Nature* **475**, 65-70, doi:10.1038/nature10236 (2011).

72 Chien, E. Y., Liu, W., Zhao, Q., Katritch, V., Han, G. W., Hanson, M. A., Shi, L., Newman, A. H., Javitch, J. A., Cherezov, V. & Stevens, R. C. Structure of the human dopamine D3 receptor in complex with a D2/D3 selective antagonist. *Science* **330**, 1091-1095, doi:10.1126/science.1197410 (2010).

73 Wu, B., Chien, E. Y., Mol, C. D., Fenalti, G., Liu, W., Katritch, V., Abagyan, R., Brooun, A., Wells, P., Bi, F. C., Hamel, D. J., Kuhn, P., Handel, T. M., Cherezov, V. & Stevens, R. C. Structures of the CXCR4 chemokine GPCR with small-molecule and cyclic peptide antagonists. *Science* **330**, 1066-1071, doi:10.1126/science.1194396 (2010).

74 Yang, Z., Han, S., Keller, M., Kaiser, A., Bender, B. J., Bosse, M., Burkert, K., Kögler, L. M., Wifling, D., Bernhardt, G., Plank, N., Littmann, T., Schmidt, P., Yi, C., Li, B., Ye, S., Zhang, R., Xu, B., Larhammar, D., Stevens, R. C., Huster, D., Meiler, J., Zhao, Q., Beck-Sickinger, A. G., Buschauer, A. & Wu, B. Structural basis of ligand binding modes at the neuropeptide Y Y_1 receptor. *Nature* **556**, 520-524, doi:10.1038/s41586-018-0046-x (2018).

75 Rasmussen, S. G., DeVree, B. T., Zou, Y., Kruse, A. C., Chung, K. Y., Kobilka, T. S., Thian, F. S., Chae, P. S., Pardon, E., Calinski, D., Mathiesen, J. M., Shah, S. T., Lyons, J. A., Caffrey, M., Gellman, S. H., Steyaert, J., Skiniotis, G., Weis, W. I., Sunahara, R. K. & Kobilka, B. K. Crystal structure of the β_2 adrenergic receptor-G_s protein complex. *Nature* **477**, 549-555, doi:10.1038/nature10361 (2011).

76 Baidya, M., Dwivedi, H. & Shukla, A. K. Frozen in action: cryo-EM structure of a GPCR-G-protein complex. *Nat Struct Mol Biol* **24**, 500-502, doi:10.1038/nsmb.3418 (2017).

77 Koehl, A., Hu, H., Maeda, S., Zhang, Y., Qu, Q., Paggi, J. M., Latorraca, N. R., Hilger, D., Dawson, R., Matile, H., Schertler, G. F. X., Granier, S., Weis, W. I., Dror, R. O., Manglik, A., Skiniotis, G. & Kobilka, B. K. Structure of the μ-opioid receptor-G_i protein complex. *Nature* **558**, 547-552, doi:10.1038/s41586-018-0219-7 (2018).

78 Kang, Y., Zhou, X. E., Gao, X., He, Y., Liu, W., Ishchenko, A., Barty, A., White, T. A., Yefanov, O., Han, G. W., Xu, Q., de Waal, P. W., Ke, J., Tan, M. H., Zhang, C., Moeller, A., West, G. M., Pascal, B. D., Van Eps, N., Caro, L. N., Vishnivetskiy, S. A., Lee, R. J., Suino-Powell, K. M., Gu, X., Pal, K., Ma, J., Zhi, X., Boutet, S., Williams, G. J., Messerschmidt, M., Gati, C., Zatsepin, N. A., Wang, D., James, D., Basu, S., Roy-Chowdhury, S., Conrad, C. E., Coe, J., Liu, H., Lisova, S., Kupitz, C., Grotjohann, I., Fromme, R., Jiang, Y., Tan, M., Yang, H., Li, J., Wang, M., Zheng, Z., Li, D., Howe, N., Zhao, Y., Standfuss, J., Diederichs, K., Dong, Y., Potter, C. S., Carragher, B., Caffrey, M., Jiang, H., Chapman, H. N., Spence, J. C., Fromme, P., Weierstall, U., Ernst, O. P., Katritch, V., Gurevich, V. V., Griffin, P. R., Hubbell, W. L., Stevens, R. C., Cherezov, V., Melcher, K. & Xu, H. E. Crystal structure of rhodopsin bound to arrestin by femtosecond X-ray laser. *Nature* **523**, 561-567, doi:10.1038/nature14656 (2015).

79 Zhou, X. E., He, Y., de Waal, P. W., Gao, X., Kang, Y., Van Eps, N., Yin, Y., Pal, K., Goswami, D., White, T. A., Barty, A., Latorraca, N. R., Chapman, H. N., Hubbell, W. L., Dror, R. O., Stevens, R. C., Cherezov, V., Gurevich, V. V.,

Griffin, P. R., Ernst, O. P., Melcher, K. & Xu, H. E. Identification of Phosphorylation Codes for Arrestin Recruitment by G Protein-Coupled Receptors. *Cell* **170**, 457-469 e413, doi:10.1016/j.cell.2017.07.002 (2017).

80 Manglik, A., Lin, H., Aryal, D. K., McCorvy, J. D., Dengler, D., Corder, G., Levit, A., Kling, R. C., Bernat, V., Hübner, H., Huang, X. P., Sassano, M. F., Giguere, P. M., Löber, S., Da, D., Scherrer, G., Kobilka, B. K., Gmeiner, P., Roth, B. L. & Shoichet, B. K. Structure-based discovery of opioid analgesics with reduced side effects. *Nature* **537**, 185-190, doi:10.1038/nature19112 (2016).

81 Drake, M. T., Violin, J. D., Whalen, E. J., Wisler, J. W., Shenoy, S. K. & Lefkowitz, R. J. β-Arrestin-biased agonism at the β_2-adrenergic receptor. *J Biol Chem* **283**, 5669-5676, doi:10.1074/jbc.M708118200 (2008).

82 Heldman, E., Barg, J., Fisher, A., Levy, R., Pittel, Z., Zimlichman, R., Kushnir, M. & Vogel, Z. Pharmacological basis for functional selectivity of partial muscarinic receptor agonists. *Eur J Pharmacol* **297**, 283-291 (1996).

83 Latorraca, N. R., Venkatakrishnan, A. J. & Dror, R. O. GPCR Dynamics: Structures in Motion. *Chem Rev* **117**, 139-155, doi:10.1021/acs.chemrev.6b00177 (2017).

84 Wacker, D., Wang, C., Katritch, V., Han, G. W., Huang, X. P., Vardy, E., McCorvy, J. D., Jiang, Y., Chu, M., Siu, F. Y., Liu, W., Xu, H. E., Cherezov, V., Roth, B. L. & Stevens, R. C. Structural features for functional selectivity at serotonin receptors. *Science* **340**, 615-619, doi:10.1126/science.1232808 (2013).

85 Kahsai, A. W., Xiao, K., Rajagopal, S., Ahn, S., Shukla, A. K., Sun, J., Oas, T. G. & Lefkowitz, R. J. Multiple ligand-specific conformations of the β_2-adrenergic receptor. *Nat Chem Biol* **7**, 692-700, doi:10.1038/nchembio.634 (2011).

86 Reinartz, M. T., Kälble, S., Littmann, T., Ozawa, T., Dove, S., Kaever, V., Wainer, I. W. & Seifert, R. Structure-bias relationships for fenoterol stereoisomers in six molecular and cellular assays at the β_2-adrenoceptor. *Naunyn Schmiedebergs Arch Pharmacol* **388**, 51-65, doi:10.1007/s00210-014-1054-5 (2015).

87 Rosethorne, E. M. & Charlton, S. J. Agonist-biased signaling at the histamine H_4 receptor: JNJ7777120 recruits β-arrestin without activating G proteins. *Mol Pharmacol* **79**, 749-757, doi:10.1124/mol.110.068395 (2011).

88 Correll, C. C. & McKittrick, B. A. Biased ligand modulation of seven transmembrane receptors (7TMRs): functional implications for drug discovery. *J Med Chem* **57**, 6887-6896, doi:10.1021/jm401677g (2014).

89 Seifert, R. Functional selectivity of G-protein-coupled receptors: from recombinant systems to native human cells. *Biochem Pharmacol* **86**, 853-861, doi:10.1016/j.bcp.2013.07.029 (2013).

90 Kruse, A. C., Ring, A. M., Manglik, A., Hu, J., Hu, K., Eitel, K., Hübner, H., Pardon, E., Valant, C., Sexton, P. M., Christopoulos, A., Felder, C. C., Gmeiner, P., Steyaert, J., Weis, W. I., Garcia, K. C., Wess, J. & Kobilka, B. K. Activation and allosteric modulation of a muscarinic acetylcholine receptor. *Nature* **504**, 101-106, doi:10.1038/nature12735 (2013).

91 Wold, E. A., Chen, J., Cunningham, K. A. & Zhou, J. Allosteric Modulation of Class A GPCRs: Targets, Agents, and Emerging Concepts. *J Med Chem*, doi:10.1021/acs.jmedchem.8b00875 (2018).

92 Schubert, M., Stichel, J., Du, Y., Tough, I. R., Sliwoski, G., Meiler, J., Cox, H. M., Weaver, C. D. & Beck-Sickinger, A. G. Identification and Characterization of the First Selective Y_4 Receptor Positive Allosteric Modulator. *J Med Chem* **60**, 7605-7612, doi:10.1021/acs.jmedchem.7b00976 (2017).

93 Tateyama, M., Abe, H., Nakata, H., Saito, O. & Kubo, Y. Ligand-induced rearrangement of the dimeric metabotropic glutamate receptor 1α. *Nat Struct Mol Biol* **11**, 637-642, doi:10.1038/nsmb770 (2004).

94 Hübner, H., Schellhorn, T., Gienger, M., Schaab, C., Kaindl, J., Leeb, L., Clark, T., Möller, D. & Gmeiner, P. Structure-guided development of heterodimer-selective GPCR ligands. *Nat Commun* **7**, 12298, doi:10.1038/ncomms12298 (2016).

95 Powell, C. E. & Slater, I. H. Blocking of inhibitory adrenergic receptors by a dichloro analog of isoproterenol. *J Pharmacol Exp Ther* **122**, 480-488 (1958).

96 Hauser, A. S., Attwood, M. M., Rask-Andersen, M., Schiöth, H. B. & Gloriam, D. E. Trends in GPCR drug discovery: new agents, targets and indications. *Nat Rev Drug Discov* **16**, 829-842, doi:10.1038/nrd.2017.178 (2017).

97 Violin, J. D., DeWire, S. M., Yamashita, D., Rominger, D. H., Nguyen, L., Schiller, K., Whalen, E. J., Gowen, M. & Lark, M. W. Selectively engaging β-arrestins at the angiotensin II type 1 receptor reduces blood pressure and increases cardiac performance. *J Pharmacol Exp Ther* **335**, 572-579, doi:10.1124/jpet.110.173005 (2010).

98 Walker, J. K., Penn, R. B., Hanania, N. A., Dickey, B. F. & Bond, R. A. New perspectives regarding β_2-adrenoceptor ligands in the treatment of asthma. *Br J Pharmacol* **163**, 18-28, doi:10.1111/j.1476-5381.2010.01178.x (2011).

99 Raehal, K. M., Walker, J. K. & Bohn, L. M. Morphine side effects in β-arrestin 2 knockout mice. *J Pharmacol Exp Ther* **314**, 1195-1201, doi:10.1124/jpet.105.087254 (2005).

100 DeWire, S. M., Yamashita, D. S., Rominger, D. H., Liu, G., Cowan, C. L., Graczyk, T. M., Chen, X. T., Pitis, P. M., Gotchev, D., Yuan, C., Koblish, M., Lark, M. W. & Violin, J. D. A G protein-biased ligand at the μ-opioid receptor is potently analgesic with reduced gastrointestinal and respiratory dysfunction compared with morphine. *J Pharmacol Exp Ther* **344**, 708-717, doi:10.1124/jpet.112.201616 (2013).

101 Hill, R., Disney, A., Conibear, A., Sutcliffe, K., Dewey, W., Husbands, S., Bailey, C., Kelly, E. & Henderson, G. The novel μ-opioid receptor agonist PZM21 depresses respiration and induces tolerance to antinociception. *Br J Pharmacol* **175**, 2653-2661, doi:10.1111/bph.14224 (2018).

102 Thompson, G. L., Kelly, E., Christopoulos, A. & Canals, M. Novel GPCR paradigms at the μ-opioid receptor. *Br J Pharmacol* **172**, 287-296, doi:10.1111/bph.12600 (2015).

103 Winpenny, D., Clark, M. & Cawkill, D. Biased ligand quantification in drug discovery: from theory to high throughput screening to identify new biased μ opioid receptor agonists. *Br J Pharmacol* **173**, 1393-1403, doi:10.1111/bph.13441 (2016).

104 Michel, M. C. & Charlton, S. J. Biased agonism in drug discovery - is it too soon to choose a path? *Mol Pharmacol* **93**, 259-265, doi:10.1124/mol.117.110890 (2018).

105 Pockes, S., Wifling, D., Keller, M., Buschauer, A. & Elz, S. Highly Potent, Stable, and Selective Dimeric Hetarylpropylguanidine-Type Histamine H_2 Receptor Agonists. *ACS Omega* **3**, 2865-2882, doi:10.1021/acsomega.8b00128 (2018).

106 Seifert, R., Wenzel-Seifert, K., Bürckstümmer, T., Pertz, H. H., Schunack, W., Dove, S., Buschauer, A. & Elz, S. Multiple differences in agonist and antagonist pharmacology between human and guinea pig histamine H_1-receptor. *J Pharmacol Exp Ther* **305**, 1104-1115, doi:10.1124/jpet.103.049619 (2003).

107 Thurmond, R. L., Venable, J., Savall, B., La, D., Snook, S., Dunford, P. J. & Edwards, J. P. Clinical Development of Histamine H_4 Receptor Antagonists. *Handb Exp Pharmacol* **241**, 301-320, doi:10.1007/164_2016_130 (2017).

108 Amlal, H., Faroqui, S., Balasubramaniam, A. & Sheriff, S. Estrogen up-regulates neuropeptide Y Y1 receptor expression in a human breast cancer cell line. *Cancer Res* **66**, 3706-3714, doi:10.1158/0008-5472.CAN-05-2744 (2006).

109 Thomsen, W., Frazer, J. & Unett, D. Functional assays for screening GPCR targets. *Curr Opin Biotechnol* **16**, 655-665, doi:10.1016/j.copbio.2005.10.008 (2005).

110 Miyano, K., Sudo, Y., Yokoyama, A., Hisaoka-Nakashima, K., Morioka, N., Takebayashi, M., Nakata, Y., Higami, Y. & Uezono, Y. History of the G protein-coupled receptor (GPCR) assays from traditional to a state-of-the-art biosensor assay. *J Pharmacol Sci* **126**, 302-309, doi:10.1254/jphs.14R13CP (2014).

111 Berridge, M. J., Dawson, R. M., Downes, C. P., Heslop, J. P. & Irvine, R. F. Changes in the levels of inositol phosphates after agonist-dependent hydrolysis of membrane phosphoinositides. *Biochem J* **212**, 473-482 (1983).

112 Benjamin, E. R., Haftl, S. L., Xanthos, D. N., Crumley, G., Hachicha, M. & Valenzano, K. J. A miniaturized column chromatography method for measuring receptor-mediated inositol phosphate accumulation. *J Biomol Screen* **9**, 343-353, doi:10.1177/1087057103262841 (2004).

113 Grynkiewicz, G., Poenie, M. & Tsien, R. Y. A new generation of Ca^{2+} indicators with greatly improved fluorescence properties. *J Biol Chem* **260**, 3440-3450 (1985).

114 Gee, K. R., Brown, K. A., Chen, W. N., Bishop-Stewart, J., Gray, D. & Johnson, I. Chemical and physiological characterization of fluo-4 Ca^{2+}-indicator dyes. *Cell Calcium* **27**, 97-106, doi:10.1054/ceca.1999.0095 (2000).

115 Nordemann, U., Wifling, D., Schnell, D., Bernhardt, G., Stark, H., Seifert, R. & Buschauer, A. Luciferase reporter gene assay on human, murine and rat histamine H_4 receptor orthologs: correlations and discrepancies between distal and proximal readouts. *PLoS One* **8**, e73961, doi:10.1371/journal.pone.0073961 (2013).

116 Harrison, C. & Traynor, J. R. The [^{35}S]GTPγS binding assay: approaches and applications in pharmacology. *Life Sciences* **74**, 489-508, doi:10.1016/j.lfs.2003.07.005 (2003).

117 Hilf, G., Gierschik, P. & Jakobs, K. H. Muscarinic acetylcholine receptor-stimulated binding of guanosine 5'-O-(3-thiotriphosphate) to guanine-nucleotide-binding proteins in cardiac membranes. *Eur J Biochem* **186**, 725-731 (1989).

118 Schrage, R., De Min, A., Hochheiser, K., Kostenis, E. & Mohr, K. Superagonism at G protein-coupled receptors and beyond. *Br J Pharmacol* **173**, 3018-3027, doi:10.1111/bph.13278 (2016).

119 Förster, T. Zwischenmolekulare Energiewanderung und Fluoreszenz. *Annalen der Physik* **437**, 55-75, doi:10.1002/andp.19484370105 (1948).

120 Lohse, M. J., Nuber, S. & Hoffmann, C. Fluorescence/bioluminescence resonance energy transfer techniques to study G-protein-coupled receptor activation and signaling. *Pharmacol Rev* **64**, 299-336, doi:10.1124/pr.110.004309 (2012).

121 Uster, P. S. & Pagano, R. E. Resonance energy transfer microscopy: observations of membrane-bound fluorescent probes in model membranes and in living cells. *J Cell Biol* **103**, 1221-1234 (1986).

122 Shimomura, O., Johnson, F. H. & Saiga, Y. Extraction, purification and properties of aequorin, a bioluminescent protein from the luminous hydromedusan, *Aequorea*. *J Cell Comp Physiol* **59**, 223-239 (1962).

123 Prasher, D. C., Eckenrode, V. K., Ward, W. W., Prendergast, F. G. & Cormier, M. J. Primary structure of the *Aequorea victoria* green-fluorescent protein. *Gene* **111**, 229-233 (1992).

124 Shaner, N. C., Steinbach, P. A. & Tsien, R. Y. A guide to choosing fluorescent proteins. *Nat Methods* **2**, 905-909, doi:10.1038/nmeth819 (2005).

125 Adams, S. R., Harootunian, A. T., Buechler, Y. J., Taylor, S. S. & Tsien, R. Y. Fluorescence ratio imaging of cyclic AMP in single cells. *Nature* **349**, 694-697, doi:10.1038/349694a0 (1991).

126 Xu, Y., Piston, D. W. & Johnson, C. H. A bioluminescence resonance energy transfer (BRET) system: application to interacting circadian clock proteins. *Proc Natl Acad Sci U S A* **96**, 151-156 (1999).

127 Pfleger, K. D. & Eidne, K. A. Illuminating insights into protein-protein interactions using bioluminescence resonance energy transfer (BRET). *Nat Methods* **3**, 165-174, doi:10.1038/nmeth841 (2006).

128 Lorenz, W. W., McCann, R. O., Longiaru, M. & Cormier, M. J. Isolation and expression of a cDNA encoding *Renilla reniformis* luciferase. *Proc Natl Acad Sci U S A* **88**, 4438-4442 (1991).

129 de Wet, J. R., Wood, K. V., Helinski, D. R. & DeLuca, M. Cloning of firefly luciferase cDNA and the expression of active luciferase in *Escherichia coli*. *Proc Natl Acad Sci U S A* **82**, 7870-7873 (1985).

130 Hall, M. P., Unch, J., Binkowski, B. F., Valley, M. P., Butler, B. L., Wood, M. G., Otto, P., Zimmerman, K., Vidugiris, G., Machleidt, T., Robers, M. B., Benink, H. A., Eggers, C. T., Slater, M. R., Meisenheimer, P. L., Klaubert, D. H., Fan, F., Encell, L. P. & Wood, K. V. Engineered luciferase reporter from a deep sea shrimp utilizing a novel imidazopyrazinone substrate. *ACS Chem Biol* **7**, 1848-1857, doi:10.1021/cb3002478 (2012).

131 Machleidt, T., Woodroofe, C. C., Schwinn, M. K., Méndez, J., Robers, M. B., Zimmerman, K., Otto, P., Daniels, D. L., Kirkland, T. A. & Wood, K. V. NanoBRET-A Novel BRET Platform for the Analysis of Protein-Protein Interactions. *ACS Chem Biol* **10**, 1797-1804, doi:10.1021/acschembio.5b00143 (2015).

132 Nikolaev, V. O., Bünemann, M., Hein, L., Hannawacker, A. & Lohse, M. J. Novel single chain cAMP sensors for receptor-induced signal propagation. *J Biol Chem* **279**, 37215-37218, doi:10.1074/jbc.C400302200 (2004).

133 Gulyás, G., Tóth, J. T., Tóth, D. J., Kurucz, I., Hunyady, L., Balla, T. & Várnai, P. Measurement of inositol 1,4,5-trisphosphate in living cells using an improved set of resonance energy transfer-based biosensors. *PLoS One* **10**, e0125601, doi:10.1371/journal.pone.0125601 (2015).

134 Miyawaki, A., Llopis, J., Heim, R., McCaffery, J. M., Adams, J. A., Ikura, M. & Tsien, R. Y. Fluorescent indicators for Ca^{2+} based on green fluorescent proteins and calmodulin. *Nature* **388**, 882-887, doi:10.1038/42264 (1997).

135 Janetopoulos, C., Jin, T. & Devreotes, P. Receptor-mediated activation of heterotrimeric G-proteins in living cells. *Science* **291**, 2408-2411, doi:10.1126/science.1055835 (2001).

136 Galés, C., Van Durm, J. J., Schaak, S., Pontier, S., Percherancier, Y., Audet, M., Paris, H. & Bouvier, M. Probing the activation-promoted structural rearrangements in preassembled receptor-G protein complexes. *Nat Struct Mol Biol* **13**, 778-786, doi:10.1038/nsmb1134 (2006).

137 Bünemann, M., Frank, M. & Lohse, M. J. Gi protein activation in intact cells involves subunit rearrangement rather than dissociation. *Proc Natl Acad Sci U S A* **100**, 16077-16082, doi:10.1073/pnas.2536719100 (2003).

138 Goedhart, J., van Weeren, L., Adjobo-Hermans, M. J., Elzenaar, I., Hink, M. A. & Gadella, T. W., Jr. Quantitative co-expression of proteins at the single cell level - application to a multimeric FRET sensor. *PLoS One* **6**, e27321, doi:10.1371/journal.pone.0027321 (2011).

139 Angers, S., Salahpour, A., Joly, E., Hilairet, S., Chelsky, D., Dennis, M. & Bouvier, M. Detection of β_2-adrenergic receptor dimerization in living cells using bioluminescence resonance energy transfer (BRET). *Proc Natl Acad Sci U S A* **97**, 3684-3689, doi:10.1073/pnas.060590697 (2000).

140 Bosma, R., Moritani, R., Leurs, R. & Vischer, H. F. BRET-based β-arrestin2 recruitment to the histamine H_1 receptor for investigating antihistamine binding kinetics. *Pharmacol Res* **111**, 679-687, doi:10.1016/j.phrs.2016.07.034 (2016).

141 Vilardaga, J. P., Bünemann, M., Krasel, C., Castro, M. & Lohse, M. J. Measurement of the millisecond activation switch of G protein-coupled receptors in living cells. *Nat Biotechnol* **21**, 807-812, doi:10.1038/nbt838 (2003).

142 Hoffmann, C., Gaietta, G., Bünemann, M., Adams, S. R., Oberdorff-Maass, S., Behr, B., Vilardaga, J. P., Tsien, R. Y., Ellisman, M. H. & Lohse, M. J. A FlAsH-based FRET approach to determine G protein-coupled receptor activation in living cells. *Nat Methods* **2**, 171-176, doi:10.1038/nmeth742 (2005).

143 Ziegler, N., Batz, J., Zabel, U., Lohse, M. J. & Hoffmann, C. FRET-based sensors for the human M_1-, M_3-, and M_5-acetylcholine receptors. *Bioorg Med Chem* **19**, 1048-1054, doi:10.1016/j.bmc.2010.07.060 (2011).

144 Schihada, H., Vandenabeele, S., Zabel, U., Frank, M., Lohse, M. J. & Maiellaro, I. A universal bioluminescence resonance energy transfer sensor design enables high-sensitivity screening of GPCR activation dynamics. *Communications Biology* **1**, doi:10.1038/s42003-018-0072-0 (2018).

145 Milde, M., Rinne, A., Wunder, F., Engelhardt, S. & Bünemann, M. Dynamics of $G\alpha_{i1}$ interaction with type 5 adenylate cyclase reveal the molecular basis for high sensitivity of G_i-mediated inhibition of cAMP production. *Biochem J* **454**, 515-523, doi:10.1042/BJ20130554 (2013).

146 Hoppe, A. D., Scott, B. L., Welliver, T. P., Straight, S. W. & Swanson, J. A. N-way FRET microscopy of multiple protein-protein interactions in live cells. *PLoS One* **8**, e64760, doi:10.1371/journal.pone.0064760 (2013).

147 Woehler, A. Simultaneous quantitative live cell imaging of multiple FRET-based biosensors. *PLoS One* **8**, e61096, doi:10.1371/journal.pone.0061096 (2013).

148 Breton, B., Sauvageau, E., Zhou, J., Bonin, H., Le Gouill, C. & Bouvier, M. Multiplexing of multicolor bioluminescence resonance energy transfer. *Biophys J* **99**, 4037-4046, doi:10.1016/j.bpj.2010.10.025 (2010).

149 Piehler, J. New methodologies for measuring protein interactions in vivo and in vitro. *Curr Opin Struct Biol* **15**, 4-14, doi:10.1016/j.sbi.2005.01.008 (2005).

150 Yoshimura, H. & Ozawa, T. Methods of split reporter reconstitution for the analysis of biomolecules. *Chem Rec* **14**, 492-501, doi:10.1002/tcr.201402001 (2014).

151 Ozawa, T. Protein reconstitution methods for visualizing biomolecular function in living cells. *Yakugaku Zasshi* **129**, 289-295 (2009).

152 Misawa, N., Kafi, A. K., Hattori, M., Miura, K., Masuda, K. & Ozawa, T. Rapid and high-sensitivity cell-based assays of protein-protein interactions using split click beetle luciferase complementation: an approach to the study of G-protein-coupled receptors. *Anal Chem* **82**, 2552-2560, doi:10.1021/ac100104q (2010).

153 Johnsson, N. & Varshavsky, A. Split ubiquitin as a sensor of protein interactions in vivo. *Proc Natl Acad Sci U S A* **91**, 10340-10344 (1994).

154 Galarneau, A., Primeau, M., Trudeau, L. E. & Michnick, S. W. β-Lactamase protein fragment complementation assays as in vivo and in vitro sensors of protein protein interactions. *Nat Biotechnol* **20**, 619-622, doi:10.1038/nbt0602-619 (2002).

155 Rossi, F., Charlton, C. A. & Blau, H. M. Monitoring protein-protein interactions in intact eukaryotic cells by β-galactosidase complementation. *Proc Natl Acad Sci U S A* **94**, 8405-8410 (1997).

156 Ghosh, I., Hamilton, A. D. & Regan, L. Antiparallel leucine zipper-directed protein reassembly: Application to the green fluorescent protein. *J Am Chem Soc* **122**, 5658-5659, doi:DOI 10.1021/ja994421w (2000).

157 Ozawa, T., Takeuchi, T. M., Kaihara, A., Sato, M. & Umezawa, Y. Protein splicing-based reconstitution of split green fluorescent protein for monitoring protein-protein interactions in bacteria: improved sensitivity and reduced screening time. *Anal Chem* **73**, 5866-5874 (2001).

158 Hu, C. D., Chinenov, Y. & Kerppola, T. K. Visualization of interactions among bZIP and Rel family proteins in living cells using bimolecular fluorescence complementation. *Mol Cell* **9**, 789-798 (2002).

159 Hu, C. D. & Kerppola, T. K. Simultaneous visualization of multiple protein interactions in living cells using multicolor fluorescence complementation analysis. *Nat Biotechnol* **21**, 539-545, doi:10.1038/nbt816 (2003).

160 Ozawa, T., Kaihara, A., Sato, M., Tachihara, K. & Umezawa, Y. Split luciferase as an optical probe for detecting protein-protein interactions in mammalian cells based on protein splicing. *Anal Chem* **73**, 2516-2521 (2001).

161 Hattori, M. & Ozawa, T. Split luciferase complementation for analysis of intracellular signaling. *Anal Sci* **30**, 539-544 (2014).

162 Eglen, R. M. Assessing GPCR activation using protein complementation: a novel technique for HTS. *Biochem Soc Trans* **35**, 746-748, doi:10.1042/BST0350746 (2007).

163 Ataei, F., Torkzadeh-Mahani, M. & Hosseinkhani, S. A novel luminescent biosensor for rapid monitoring of IP_3 by split-luciferase complementary assay. *Biosens Bioelectron* **41**, 642-648, doi:10.1016/j.bios.2012.09.037 (2013).

164 Takeuchi, M., Nagaoka, Y., Yamada, T., Takakura, H. & Ozawa, T. Ratiometric bioluminescence indicators for monitoring cyclic adenosine 3',5'-monophosphate in live cells based on luciferase-fragment complementation. *Anal Chem* **82**, 9306-9313, doi:10.1021/ac102692u (2010).

165 Dixon, A. S., Schwinn, M. K., Hall, M. P., Zimmerman, K., Otto, P., Lubben, T. H., Butler, B. L., Binkowski, B. F., Machleidt, T., Kirkland, T. A., Wood, M. G., Eggers, C. T., Encell, L. P. & Wood, K. V. NanoLuc Complementation Reporter Optimized for Accurate Measurement of Protein Interactions in Cells. *ACS Chem Biol* **11**, 400-408, doi:10.1021/acschembio.5b00753 (2016).

166 Hattori, M., Tanaka, M., Takakura, H., Aoki, K., Miura, K., Anzai, T. & Ozawa, T. Analysis of temporal patterns of GPCR-β-arrestin interactions using split luciferase-fragment complementation. *Mol Biosyst* **9**, 957-964, doi:10.1039/c2mb25443c (2013).

167 Littmann, T., Göttle, M., Reinartz, M. T., Kälble, S., Wainer, I. W., Ozawa, T. & Seifert, R. Recruitment of β-arrestin 1 and 2 to the β_2-adrenoceptor: analysis of 65 ligands. *J Pharmacol Exp Ther* **355**, 183-190, doi:10.1124/jpet.115.227959 (2015).

168 Paulmurugan, R., Umezawa, Y. & Gambhir, S. S. Noninvasive imaging of protein-protein interactions in living subjects by using reporter protein complementation and reconstitution strategies. *Proc Natl Acad Sci U S A* **99**, 15608-15613, doi:10.1073/pnas.242594299 (2002).

169 Viviani, V. R., Prado, R. A., Neves, D. R., Kato, D. & Barbosa, J. A. A route from darkness to light: emergence and evolution of luciferase activity in AMP-CoA-ligases inferred from a mealworm luciferase-like enzyme. *Biochemistry* **52**, 3963-3973, doi:10.1021/bi400141u (2013).

170 Hida, N., Awais, M., Takeuchi, M., Ueno, N., Tashiro, M., Takagi, C., Singh, T., Hayashi, M., Ohmiya, Y. & Ozawa, T. High-sensitivity real-time imaging of dual protein-protein interactions in living subjects using multicolor luciferases. *PLoS One* **4**, e5868, doi:10.1371/journal.pone.0005868 (2009).

171 Villalobos, V., Naik, S., Bruinsma, M., Dothager, R. S., Pan, M. H., Samrakandi, M., Moss, B., Elhammali, A. & Piwnica-Worms, D. Dual-color click beetle luciferase heteroprotein fragment complementation assays. *Chem Biol* **17**, 1018-1029, doi:10.1016/j.chembiol.2010.06.018 (2010).

172 Branchini, B. R., Southworth, T. L., Khattak, N. F., Michelini, E. & Roda, A. Red- and green-emitting firefly luciferase mutants for bioluminescent reporter applications. *Anal Biochem* **345**, 140-148, doi:10.1016/j.ab.2005.07.015 (2005).

173 Branchini, B. R., Ablamsky, D. M., Murtiashaw, M. H., Uzasci, L., Fraga, H. & Southworth, T. L. Thermostable red and green light-producing firefly luciferase mutants for bioluminescent reporter applications. *Anal Biochem* **361**, 253-262, doi:10.1016/j.ab.2006.10.043 (2007).

174 Nishiguchi, T., Yamada, T., Nasu, Y., Ito, M., Yoshimura, H. & Ozawa, T. Development of red-shifted mutants derived from luciferase of Brazilian click beetle Pyrearinus termitilluminans. *J Biomed Opt* **20**, 101205, doi:10.1117/1.JBO.20.10.101205 (2015).

175 Sun, Y. Q., Liu, J., Wang, P., Zhang, J. & Guo, W. D-luciferin analogues: a multicolor toolbox for bioluminescence imaging. *Angew Chem Int Ed Engl* **51**, 8428-8430, doi:10.1002/anie.201203565 (2012).

176 Shakhmin, A., Hall, M. P., Machleidt, T., Walker, J. R., Wood, K. V. & Kirkland, T. A. Coelenterazine analogues emit red-shifted bioluminescence with NanoLuc. *Org Biomol Chem* **15**, 8559-8567, doi:10.1039/c7ob01985h (2017).

177 Branchini, B. R., Ablamsky, D. M., Davis, A. L., Southworth, T. L., Butler, B., Fan, F., Jathoul, A. P. & Pule, M. A. Red-emitting luciferases for bioluminescence reporter and imaging applications. *Anal Biochem* **396**, 290-297, doi:10.1016/j.ab.2009.09.009 (2010).

2. Objective and aim

In GPCR research, there is an increasing interest in the development of biased agonists as pharmacological tools and ultimately also as drugs[1,2], since adverse effects of certain pharmaceuticals are supposed to be associated with the activation of unfavourable signalling pathways[2-5]. Additionally, for several receptors, bias of endogenous agonists has been discovered[6,7]. Currently, the most common approach to determine biased agonism implies the application of two separate assays for detecting G protein-dependent and β-arrestin-dependent signalling (cf. Fig. 2.1), respectively. Apart from the additional time needed to perform two assays instead of one, major shortcomings are associated with this approach.

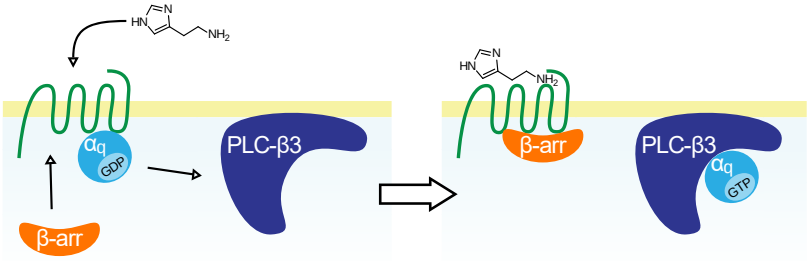

Fig. 2.1: Schematic illustration of the protein/protein interactions of interest. In view of a multiparametric determination of $G\alpha_q$ activation and β-arrestin recruitment, two protein/protein interactions were analysed. On one hand, the interaction between $G\alpha_q$ with its effector, the PLC-β3, was probed as a representative for activation of the $G\alpha_q$ pathway. On the other hand, the recruitment of β-arrestin to the GPCR was analysed.

Usually, two separate assay systems involve two receptor sources, which can substantially differ in the extent of receptor and effector protein expression[8], potentially leading to vast differences in the agonistic effects measured[4,9-11]. Often not even intact cells are used to quantify the activation of a pathway. A prominent example is the [^{35}S]-GTPγS-incorporation assay[12], which is frequently applied for the proximal determination of G protein activation. Another disadvantage is its dependency on the availability of appropriate (pure) radiolabelled compounds, which is becoming increasingly problematic. Other assays used for the proximal determination of G protein activation, e.g. FRET-based assays, which measure the rearrangement of the G protein subunits, are often limited in throughput. Such assays often rely on special microscopes, equipped with a perfusion system.

Since assays (e.g. [^{35}S]-GTPγS binding), delivering proximal information on G protein activation are scarce and compromised by several drawbacks, the most commonly used techniques to determine the activation of the G protein pathway rely on the quantification of second messengers[13]. This is unfavourable, when results from these assays are quantitatively compared with results obtained from β-arrestin recruitment assays, since the latter are usually not influenced by signal amplification[14], whereas second messenger data is[15]. As a consequence, agonists may erroneously be interpreted as G protein-biased.

This demonstrates that there is a need for sensitive non-radioactive methods, allowing a proximal determination of G protein activation, which can be performed in live cells rather than with membrane preparations. Moreover, such a method should harbour the potential to be easily combined with other functional assays (e.g. β-arrestin recruitment) to reliably quantify functional bias.

Therefore, the aim of this thesis was the development of two techniques, applicable to live cells with high throughput. Firstly, for proximal determination of $G\alpha_q$ protein activation and secondly, for β-arrestin recruitment. The two probes were designed to be potentially compatible with a multiparametric assay format, affording information on both signalling pathways at the same time (cf. Fig. 2.1).

Methodologically, this was achieved by split-luciferase complementation, using two luciferases of different evolutionary origin to avoid unspecific cross-complementation, which emit light with substantially different emission maxima. A red light-emitting luciferase from the click-beetle *Pyrophorus plagiophthalamus* (click-beetle red; CBR) was chosen to probe the interaction of $G\alpha_q$ with its effector, the PLC-β3. To probe β-arrestin recruitment, the genetically-engineered blue light-emitting NLuc, which stems from the deep-sea shrimp *Oplophorus gracilirostris*, was used. The performance of both assays was analysed separately in combination with different receptors. The focus was laid on the determination of signal-to-noise ratios and the pharmacological analysis of reference agonists. In a final step, both developed probes were co-expressed in a single engineered HEK293T cell population. By applying appropriate optical filters, the light emitted by each of the two probes could be discriminated, which led to the first assay enabling the simultaneous proximal determination of G protein activation and β-arrestin recruitment.

2.1 References

1 Whalen, E. J., Rajagopal, S. & Lefkowitz, R. J. Therapeutic potential of β-arrestin- and G protein-biased agonists. *Trends Mol Med* **17**, 126-139, doi:10.1016/j.molmed.2010.11.004 (2011).

2 Correll, C. C. & McKittrick, B. A. Biased ligand modulation of seven transmembrane receptors (7TMRs): functional implications for drug discovery. *J Med Chem* **57**, 6887-6896, doi:10.1021/jm401677g (2014).

3 Manglik, A., Lin, H., Aryal, D. K., McCorvy, J. D., Dengler, D., Corder, G., Levit, A., Kling, R. C., Bernat, V., Hübner, H., Huang, X. P., Sassano, M. F., Giguere, P. M., Löber, S., Da, D., Scherrer, G., Kobilka, B. K., Gmeiner, P., Roth, B. L. & Shoichet, B. K. Structure-based discovery of opioid analgesics with reduced side effects. *Nature* **537**, 185-190, doi:10.1038/nature19112 (2016).

4 Michel, M. C. & Charlton, S. J. Biased agonism in drug discovery - is it too soon to choose a path? *Mol Pharmacol* **93**, 259-265, doi:10.1124/mol.117.110890 (2018).

5 Seifert, R. Functional selectivity of G-protein-coupled receptors: from recombinant systems to native human cells. *Biochem Pharmacol* **86**, 853-861, doi:10.1016/j.bcp.2013.07.029 (2013).

6 Reyes-Alcaraz, A., Lee, Y. N., Yun, S., Hwang, J. I. & Seong, J. Y. Conformational signatures in β-arrestin2 reveal natural biased agonism at a G-protein-coupled receptor. *Commun Biol* **1**, 128, doi:10.1038/s42003-018-0134-3 (2018).

7 Zidar, D. A. Endogenous ligand bias by chemokines: implications at the front lines of infection and leukocyte trafficking. *Endocr Metab Immune Disord Drug Targets* **11**, 120-131 (2011).

8 Atwood, B. K., Lopez, J., Wager-Miller, J., Mackie, K. & Straiker, A. Expression of G protein-coupled receptors and related proteins in HEK293, AtT20, BV2, and N18 cell lines as revealed by microarray analysis. *BMC Genomics* **12**, 14, doi:10.1186/1471-2164-12-14 (2011).

9 Bräuner-Osborne, H., Ebert, B., Brann, M. R., Falch, E. & Krogsgaard-Larsen, P. Functional partial agonism at cloned human muscarinic acetylcholine receptors. *Eur J Pharmacol* **313**, 145-150 (1996).

10 Thompson, G. L., Kelly, E., Christopoulos, A. & Canals, M. Novel GPCR paradigms at the μ-opioid receptor. *Br J Pharmacol* **172**, 287-296, doi:10.1111/bph.12600 (2015).

11 Winpenny, D., Clark, M. & Cawkill, D. Biased ligand quantification in drug discovery: from theory to high throughput screening to identify new biased μ opioid receptor agonists. *Br J Pharmacol* **173**, 1393-1403, doi:10.1111/bph.13441 (2016).

12 Hilf, G., Gierschik, P. & Jakobs, K. H. Muscarinic acetylcholine receptor-stimulated binding of guanosine 5'-O-(3-thiotriphosphate) to guanine-nucleotide-binding proteins in cardiac membranes. *Eur J Biochem* **186**, 725-731 (1989).

13 Miyano, K., Sudo, Y., Yokoyama, A., Hisaoka-Nakashima, K., Morioka, N., Takebayashi, M., Nakata, Y., Higami, Y. & Uezono, Y. History of the G protein-coupled receptor (GPCR) assays from traditional to a state-of-the-art biosensor assay. *J Pharmacol Sci* **126**, 302-309, doi:10.1254/jphs.14R13CP (2014).

14 Littmann, T., Göttle, M., Reinartz, M. T., Kälble, S., Wainer, I. W., Ozawa, T. & Seifert, R. Recruitment of β-arrestin 1 and 2 to the β_2-adrenoceptor: analysis of 65 ligands. *J Pharmacol Exp Ther* **355**, 183-190, doi:10.1124/jpet.115.227959 (2015).

15 Nordemann, U., Wifling, D., Schnell, D., Bernhardt, G., Stark, H., Seifert, R. & Buschauer, A. Luciferase reporter gene assay on human, murine and rat histamine H_4 receptor orthologs: correlations and discrepancies between distal and proximal readouts. *PLoS One* **8**, e73961, doi:10.1371/journal.pone.0073961 (2013).

3. A split luciferase-based probe for quantitative proximal determination of $G\alpha_q$ signalling in live cells

Prior to the submission of this thesis, parts of this chapter have been published:

Littmann, T., Ozawa, T., Hoffmann, C., Buschauer, A. & Bernhardt, G. A split luciferase-based probe for quantitative proximal determination of $G\alpha_q$ signalling in live cells. *Sci Rep* **8**, 17179, doi:10.1038/s41598-018-35615-w (2018).

Author contributions: T.L. conceived the project with input from T.O., C.H., A.B. and G.B.. T.L. performed experiments and data analysis with continuous supervision by T.O., C.H., A.B. and G.B.. T.O. provided important plasmids and microscopy equipment. T.L. and G.B. wrote the manuscript with input from T.O. and C.H..

3.1 Introduction

GPCRs consist of seven transmembrane helices and are responsible for transducing stimuli, e.g. by hormones or neurotransmitters, across the cellular membrane. They represent the largest of all protein superfamilies in the human genome comprising more than 1000 different receptors[1], and are the most important drug targets with approximately 34% of all drugs addressing GPCRs[2]. Agonist binding to a GPCR leads to the activation of heterotrimeric G proteins comprising an α, β and γ subunit. Binding of an agonist to a GPCR leads to a structural rearrangement resulting in an exchange of GDP for GTP within the α subunit.

There are four major subfamilies of Gα proteins of which we focussed on the α_q type that upon activation of the receptor, interacts with effector proteins of the PLC-β class and triggers their enzymatic activity. PLCs catalyse the formation of IP_3 and DAG from PIP_2. DAG diffuses in the cell membrane, whereas IP_3 activates Ca^{2+} channels within the membrane of the endoplasmic reticulum and/or the cellular membrane, both leading to a transient increase in the concentration of Ca^{2+} in the cytosol. The latter is involved in a plethora of physiological processes such as rearrangements of the cytoskeleton and regulation of gene transcription[3].

In case of the second messengers IP_3 and Ca^{2+}, changes in intracellular levels are usually measured by liquid-scintillation counting or luminometry. When cells are incubated with tritiated *myo*-inositol, radioactive IP_3 (IP_1, IP_2) levels can be determined[4], whereas FRET[5]- and SLC-based[5,6] assays make use of specific interactions of IP_1 or IP_3 with various optical probes. Most often intracellular Ca^{2+} levels are measured either with fluorescent chelators, changing their optical properties upon complexation of Ca^{2+} ions[7-9] or a calcium-dependent luciferase (aequorin)[7,10].

However, substantial amplification, taking place with every step in the signalling cascade, potentially masking effects at earlier stages[11] can lead to misinterpretation, e.g. partial agonists appear as a full agonists in assays with a distal readout[3,12]. Furthermore, since there is an increasing interest in the discrimination of biased agonism with respect to G protein-dependent and β-arrestin-dependent pathways[13], techniques are needed, allowing a proximal quantification of signalling events[14]. Such methods comprise [^{35}S]GTPγS-incorporation[15] and steady-state [^{32,33}P]-based GTPase assays[16] or FRET[17]- and BRET-based techniques[17,18].

Most of the aforementioned approaches are compromised e.g. by requiring cell lysis, the preparation of membranes, the availability of radiolabelled chemicals or by low throughput. To overcome these limitations, we decided to use SLC to quantify the interaction of $G\alpha_q$ with PLC-β3. This technology is based on two catalytically inactive complementary fragments of a luciferase, reconstituting a functional enzyme, catalysing the oxidation of a substrate with concomitant emission of light, when brought in close proximity[19]. The two fragments are fused to two proteins of which a specific interaction is expected, in this case $G\alpha_q$ and PLC-β3. Probes, based on SLC, have become valuable tools for the quantification of PPI in general[20-22], but also in the field of GPCR research. In this context, SLC was successfully applied to probe the interaction of β-arrestins with GPCRs[23-25] and to the quantification of second messengers such as cAMP[26] and IP_3[6,26]. Advantages of SLC involve a high signal-to-background (S/B) ratio, enabling live cell and *in vivo* imaging[27] and the availability of luciferases catalysing chemical reactions, accompanied by the emission of bright light of different wavelengths (broad spectral diversity)[28-30].

We applied SLC to probe the $G\alpha_q$/PLC-β3 interaction (Fig. 3.1A) by means of a modified luciferase from the click-beetle *Pyrophorus plagiophthalamus* (λ_{max} = 613 nm). The enzyme was split into two fragments, a larger N-terminal fragment (CBRN) consisting of the amino acids 1-416 and a smaller C-terminal fragment (CBRC) composed of amino acids 395-542. We generated two sets of fusion proteins of which the first one represents CBRN fused either N-, or C-terminally to PLC-β3 and in the second one CBRC was fused terminally to $G\alpha_q$. As both termini of Gα subunits are known to be crucial not only for interactions with a respective GPCR, the βγ-complex but also for the association with the cellular membrane[31-34], CBRC was also integrated in three different flexible loop regions of $G\alpha_q$. The combination of those fusion proteins, giving the highest S/B ratio upon complementation was used as a sensor to probe the activation of different $G\alpha_q$-coupled receptors. We demonstrate that the new probe is of value for the functional characterisation of GPCR ligands and for imaging receptor activation in live cells.

3.2 Material & Methods

3.2.1 Materials

Dulbecco's modified Eagle's medium (DMEM) with and without phenol red and phosphate-buffered saline (PBS) were from Sigma (Taufkrichen, Germany). Leibovitz' L-15 medium (L-15) and Hank's balanced salt solution (HBSS) were from Gibco (Nidderau, Germany). Fura-2 AM, fetal calf serum (FCS), trypsin and geneticin (G418) were from Merck Biochrom (Darmstadt, Germany). D-Luciferin was purchased as potassium salt either from Wako (Tokyo, Japan) or from Pierce (Nidderau, Germany) and was dissolved in HBSS at a concentration of 400 mM. Puromycin was obtained from Invivogen (Toulouse, France). The pCBR-control vector and the Bright-Glo luciferase assay reagent were from Promega (Tokyo, Japan and Mannheim, Germany). The pcDNA4 vector was from Thermo Scientific (Nidderau, Germany), whereas the pIRESpuro3 vector was from Clontech (Saint-Germain-en-Laye, France). Depending on their physicochemical properties, when possible, ligands were dissolved in H_2O; otherwise DMSO (Darmstadt, Merck) was used as solvent. Histamine dihydrochloride (his), was from Acros Organics (Geel, Belgium), betahistine dihydrochloride (betahis), diphenhydramine hydrochloride (diph), cyproheptadine hydrochloride (cyp), maprotiline hydrochloride (map), carbachol chloride (car), iperoxo iodide (iper), N-methylscopolamine bromide (NMS), atropine (atr), propantheline bromide (prop) and pirenzepine dihydrochloride (pir) were from Sigma (Taufkirchen, Germany), whereas mepyramine maleate (mep) was from Tocris Bioscience (Bristol, United Kingdom). UR-KUM530 (KUM530)[35] and histaprodifen (histapro) were kindly provided by Prof. Dr. Sigurd Elz (University of Regensburg, Germany). Oxotremorine sesquifumarate (oxo) was from MP Biomedicals (Eschwege, Germany), xanomeline (xan) was synthesized in-house according to a standard procedure[36]. Neurotensin (8-13) (NT(8-13)) was from Synpeptide (Shanghai, China). SR142948A was gift from Dr. Harald Hübner (University of Erlangen, Germany). FR900359 was purchased from the Institute of Pharmaceutical Biology, University of Bonn (Germany).

3.2.2 Cell cultivation

In this study, the HEK293T cell line, obtained from the German collection of microorganisms and cell cultures (DSMZ, Braunschweig, Germany), was used. Cells were routinely monitored for mycoplasma contamination using the Venor GeM Mycoplasma Detection Kit (Minerva Biolabs, Berlin, Germany) and were negative. Unless otherwise stated, the cells were cultivated in DMEM containing 10% FCS (full medium) at 37 °C in a water-saturated atmosphere containing 5% CO_2.

3.2.3 Generation of plasmids

Plasmids encoding different human GPCRs were obtained from the Missouri cDNA resource center (Rolla, MO, USA). The other plasmids used were generated by standard PCR and restriction techniques within the pcDNA backbone, unless otherwise stated. A plasmid encoding the red-emitting click-beetle luciferase (pCBR-control) was used as a template in different polymerase chain reactions (PCR) to generate the sequences encoding the two slightly overlapping N-terminal (*CBRN*, encoding amino acids 1-416) and C-terminal (*CBRC*, encoding amino acids 394-542) fragments of the luciferase. *CBRN* was then used to prepare plasmids encoding fusion proteins consisting of PLC-β3 fused either N- or C-terminally to CBRN. *CBRC* was used to generate plasmids of five different fusion proteins in which CBRC was fused to both termini of $G\alpha_q$ or integrated into the $G\alpha_q$ sequence after amino acids 66, 97 ($G\alpha_q$(97)) and 123 ($G\alpha_q$(123)), respectively. The linker sequences used to connect the luciferase fragments to either PLC-β3 or $G\alpha_q$ consisted of flexible Gly and Ser residues. The cDNA encoding the $G\alpha_q$(123) fusion protein and the N-terminally-tagged PLC-β3 were then subcloned into a pIRESpuro3 vector separated by a P2A autoproteolysis site[37], yielding the pIRESpuro3 CBRN-PLC-β3-2A-$G\alpha_q$(123) vector. Cleavage of the P2A site was controlled by immunoblotting (Fig. A2). All plasmids were quality controlled by means of enzyme restriction analysis and sequencing.

3.2.4 Identification of the best pair of $G\alpha_q$ and PLC-β3 fusion proteins

HEK293T cells were seeded on a 6-well plate (Sarstedt, Nümbrecht, Germany) at a density of $7 \cdot 10^5$ cell/well. The next day, the cells were transfected with plasmids encoding the different combinations of fusion proteins and the human histamine H_1 receptor (hH_1R). After 48 h of incubation, the cells were detached by trypsinisation, centrifuged and resuspended in DMEM devoid of phenol red, supplemented with FCS (5%). The concentration was adjusted to $1.11 \cdot 10^6$ cells/mL; 90 µL of this suspension were seeded into each well of a white 96-well plate (Greiner Bio One, Frickenhausen, Germany), and the cells were incubated overnight. To induce interaction of the two fusion proteins, histamine was added at a concentration of 10 µM to the cells. In a control experiment, only DMEM without phenol red, the vehicle of histamine, was applied. After 30 min, 50 µL of medium were aspirated and replaced by 50 µL of Bright-Glo luciferase reagent. The cells were vigorously shaken for 2 min before luminescence was detected using a Genios Pro plate reader (Tecan, Crailsheim, Deutschland) for 1 s per well.

3.2.5 Generation of stable expression cell lines

HEK293T cells were transfected with the pIRESpuro3 CBRN-PLC-β3-2A-$G\alpha_q$(123) vector as described above. After two days of incubation, the cells were detached using trypsin and were seeded into a 75-cm^2 cell culture flask. Then, the cells were allowed to attach and puromycin was added at a concentration of 0.75 µg/mL. The cells were cultured upon changing the medium at regular intervals until

stable growth was observed again. Subsequently, plasmids encoding cDNAs of GPCRs were transfected in the same way, with the exception that selection was achieved in the presence of 600 µg/mL G418.

3.2.6 Characterisation of standard agonists and antagonists using the developed probe

Cells, expressing the developed $G\alpha_q$-PLC-β3 sensor in combination with one of the GPCRs, were detached from a 75-cm^2 flask by trypsinisation and centrifuged (700 g for 5 min). The pellet was resuspended in assay medium consisting of L-15 with 5% FCS and the density of the suspension was adjusted to $1.25 \cdot 10^6$ cells/mL. Then, 80 µL of this suspension were seeded into each well of a white 96-well plate, and the plate was incubated at 37 °C in a humidified atmosphere (without additional CO_2) overnight. On the next day, 10 µL of 10 mM D-luciferin (Pierce) were added to the cells, and the plate was transferred into a pre-warmed microplate luminescence reader (either a Genios Pro or an EnSpire (Perkin-Elmer, Rodgau, Germany)). The cells were allowed to equilibrate inside the reader for 10 min, before the basal luminescence was determined by recording the luminescence for the entire plate ten times with an integration time of 1 s per well. In the meantime, serial dilutions of agonists were prepared, the resulting solutions were also pre-warmed to 37 °C and subsequently added to the cells. Thereafter, luminescence was recorded for 30 plate repeats amounting to a time period of 50 min. Negative controls (solvent) and positive controls (reference full agonist, histamine (hH_1R), carbachol ($hM_{1,5}R$), oxotremorine (hM_3R)) eliciting a maximal response (100%) were included for subsequent normalization of the data. In case of the antagonist mode, antagonists were added 15 min prior to the initial thermal equilibration period to ensure an equilibrium between antagonists and receptors, before agonists were added. The pK_b-values of antagonists were determined according to the Cheng-Prusoff equation[38]. FR900359 was pre-incubated for 20 min, before cells were stimulated with agonists. After acquisition of the data, the peak luminescence intensities obtained after stimulation were used for quantitative analysis using Prism 5 (Graph Pad, La Jolla, CA, USA).

3.2.7 Fura-2 Ca^{2+} assay

HEK293T cells expressing either the hH_1R alone, or co-expressing the $G\alpha_q$-PLC-β3 sensor, were incubated with Fura-2 AM and analysed in cuvettes using a LS50 B luminescence spectrophotometer (Perkin-Elmer, Rodgau, Germany). Fura-2 calcium assays were essentially performed as described previously[39].

3.2.8 Live cell luminescence microscopy

HEK293T cells, expressing hM_3R and the $G\alpha_q$-PLC-β3 sensor, were seeded on a 35-mm cell culture dish (Iwaki, Japan) in full medium at a density of 10^6 cells/dish and were incubated overnight. The next day, 30 µL of 1 M HEPES buffer (pH 7.4) and 7.5 µL of 400 mM D-luciferin (Wako) were added. The cells

were transferred to an IX-81 microscope (Olympus, Tokyo, Japan), equipped with a super-cooled EM-CCD camera (Hamamatsu photonics K.K., Hamamatsu, Japan), with its stage heated to 37 °C, and bioluminescence microscopy was performed essentially as described[25]. Briefly, the images were acquired with an exposure time of 5 min per frame. After the first frame, oxotremorine was added to a final concentration of 100 nM. In case of the antagonist mode, atropine was added to a final concentration of 100 nM prior to the very first frame.

3.3 Results and discussion

3.3.1 Development of the Gαq activation sensor

In a conventional approach to develop a SLC-based PPI probe, a set of fusion proteins, comprising the luciferase fragments and the two host proteins is engineered and expressed. Usually, both luciferase fragments are fused to both termini of the host proteins and all combinations of the resulting fusion proteins are analysed with respect to their ability to restore the luminescence signal.

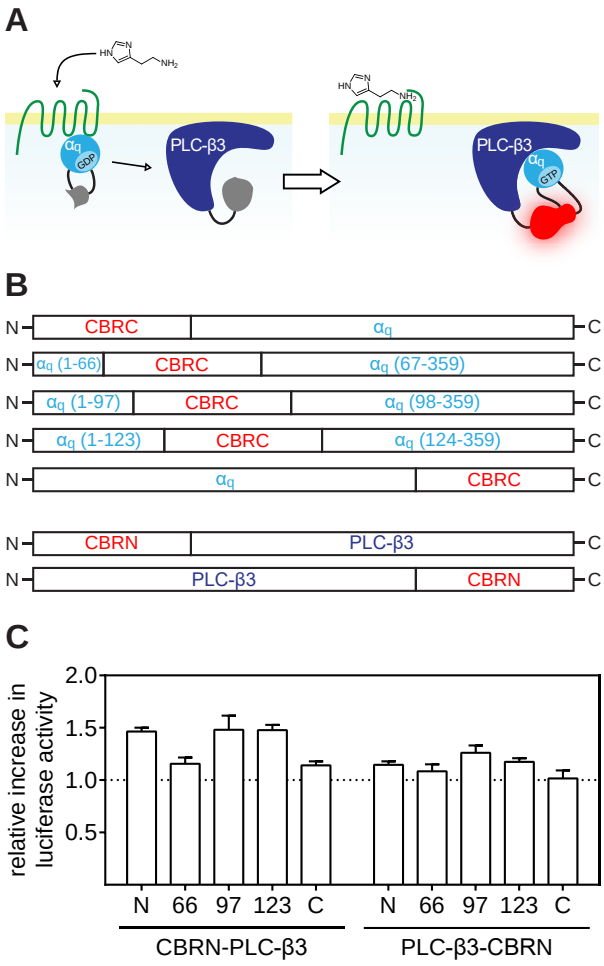

Fig. 3.1: Schematic illustration of the sensor principle and the fusion protein library used to determine the best combination of proteins. The activation of the $G\alpha_q$ pathway was probed by fusing complementary luciferase fragments to $G\alpha_q$ and PLC-β3 (**A**). A fusion protein library was generated by fusing CBRC to $G\alpha_q$ terminally and in three loop regions (numbers in parentheses denote amino acid positions) and by fusing CBRN either N-, or C-terminally to PLC-β3 (**B**). The different combinations of $G\alpha_q$ and PLC-β3 fusion proteins were expressed in HEK293T cells, co-expressing the hH_1R. The relative increase in luminescence of cells stimulated with 10 µM histamine compared to unstimulated cells is shown for each combination (**C**). Data are presented as means ± SEM from three independent experiments, performed in triplicate.

As our aim was to probe the $G\alpha_q$/PLC-β3 interaction (Fig. 3.1A), and because $G\alpha_q$ is a rather small protein of which it is well known that both termini are of major importance for interactions with βγ-subunits, with a GPCR and the association with the cell membrane[31-34], we pursued a slightly different strategy: we fused the smaller luciferase fragment (CBRC) to $G\alpha_q$ and incorporated CBRC into three different flexible loop regions, localized within the helical domain of $G\alpha_q$[40] (Fig. 3.1B). The complementing part of the luciferase (CBRN) was fused either to the N-, or the C-terminus of PLC-β3 (Fig. 3.1B). To identify the best combination of fusion proteins in terms of luminescence intensity and S/B ratio, we expressed all combinations of $G\alpha_q$ and PLC-β3 fusion proteins shown in Fig. 3.1B in HEK293T cells co-expressing the human histamine H_1 receptor (hH_1R). The resulting transfectants were stimulated with 10 µM histamine for 25 min before the cells were lysed and the substrate was added. The detected luminescence was normalized i.e. divided by the luminescence intensity emitted from unstimulated cells. The low normalized luminescence shown in Fig. 3.1C suggests that the C-terminus of PLC-β3 is rather far away from the interaction site with $G\alpha_q$. This is supported by the

crystal structure of the $G\alpha_q$/PLC-β3 complex[40]. The CBRN-PLC-β3 fusion protein gave higher S/B ratios, especially when used in combination with the $G\alpha_q$ variant, in which CBRC was incorporated after amino acid 97 or 123. However, the overall luminescence intensity was higher for $G\alpha_q$(123) (Fig. A1).

Although the construct, in which CBRC was N-terminally fused to $G\alpha_q$, showed higher luminescence (Fig. A1), but only an S/B ratio comparable to that of $G\alpha_q$(97) and $G\alpha_q$(123), respectively, this fusion protein was not considered, because Yu et al. reported that an N-terminal fusion of green fluorescent protein to $G\alpha_s$ resulted in a lack of association with the cell membrane[34]. Therefore, we favoured $G\alpha_q$(123) in combination with CBRN-PLC-β3.

We further optimized the sensor mainly with respect to handling. For this purpose, a vector plasmid, enabling convenient multi-cistronic expression of both fusion proteins in a fixed stoichiometry (1:1), using a self-cleaving P2A peptide sequence[37], separating CBRN-PLC-β3 and $G\alpha_q$(123), was constructed. Furthermore, we fabricated a HEK293T cell line, characterized by stable integration of the aforementioned plasmid into the genome as a versatile platform for the analysis of different GPCRs upon co-transfection. Cleavage of the P2A sequence was proven by immunoblotting using an anti-$G\alpha_q$ antibody (Fig. A2). The western blots also revealed that the expression level of the modified $G\alpha_q$ was similar to that of endogenous $G\alpha_q$ in HEK293T cells (Fig. A2).

3.3.2 Characterization of the new probe

To overcome the low S/B ratio, we added the substrate D-luciferin to live cells (in culture medium) rather than performing endpoint measurements after lysis of the cells. Thereby, we were able to follow the kinetics of the reaction (Fig. 3.2A). The sensor responded to an activation of the hH_1R by increasing the concentration of histamine with a gradual increase in luminescence, which can be converted to a concentration-response-curve (CRC), yielding an EC_{50} value in very good agreement with data obtained from canonical assays[3,16].

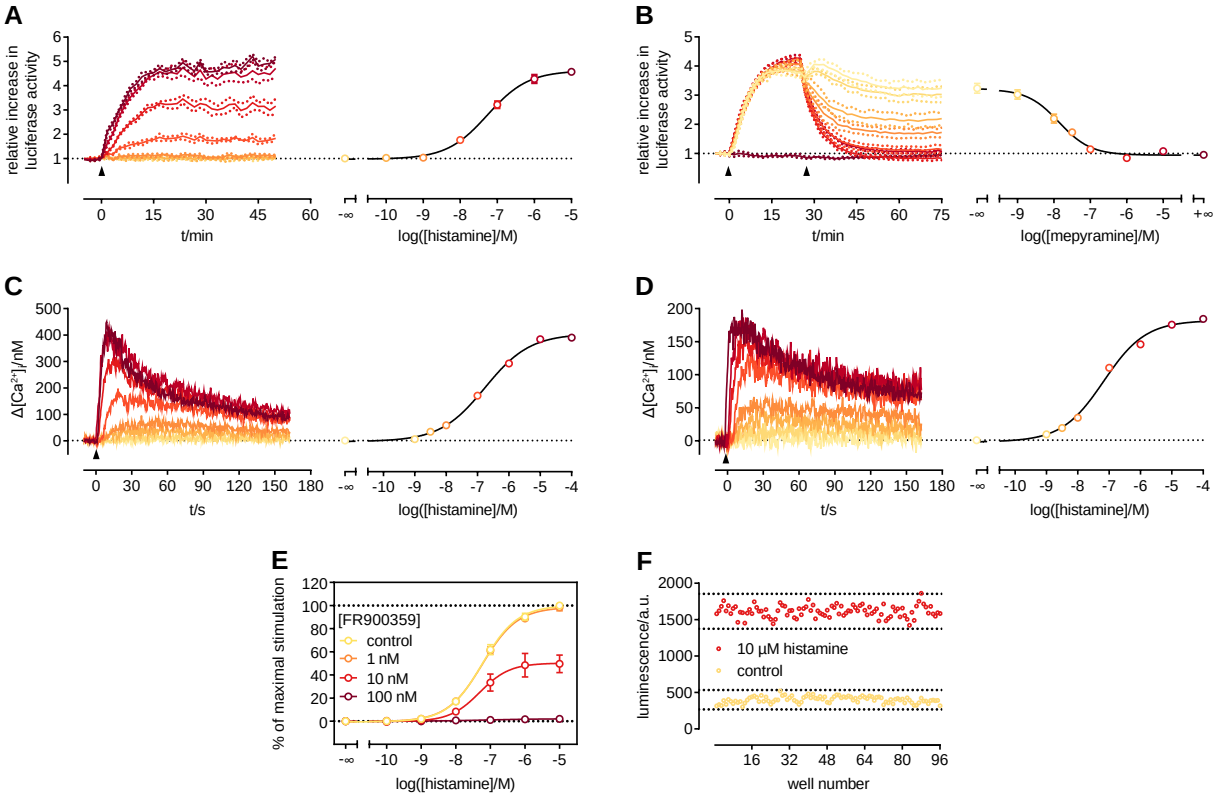

Fig. 3.2: Characterization of the Gα$_q$ activation sensor. All experiments were performed with HEK293T cells, expressing the Gα$_q$ sensor and the hH$_1$R, except for **C** were the sensor was not present. Increasing concentrations of histamine (addition indicated by arrow) lead to proportionally increasing luminescence emitted from the cells, which could be converted to a CRC (**A**). The opposite (a gradual decrease in luminescence) became obvious, when stimulated cells (300 nM histamine, first arrow) were subsequently treated with the selective hH$_1$R agonist mepyramine (second arrow) (**B**). In case of the highest concentration, luminescence decreased to basal levels, indicating full reversibility of the sensor interaction. Since the observed activation kinetics in **A** were slower than expected for G protein activation, a kinetic Fura-2 assay for the quantification of $[Ca^{2+}]_i$ was performed, to guarantee that the sensor does not negatively influence downstream signalling. In cells, in which the sensor was present, the kinetics were the same (**C**) when compared to cells devoid of the sensor (**D**). The concentration-dependent response to histamine (addition indicated by arrow) was similar (hH$_1$R alone: pEC$_{50}$: 7.1 ± 0.1; Gα$_q$ sensor present: pEC$_{50}$: 6.8 ± 0.1), too. Furthermore, we were able to show that the modified Gα$_q$ as part of the sensor was still prone to inhibition by FR900359 (**E**). The sensor shows an exceptionally good Z' of 0.7 (**F**). Data in **A-D** are representative of at least two independent experiments. Data in **E** are presented as mean along with their SEM from five independent experiments performed in triplicate. Data in **F** was obtained from an entire 96-well plate.

Additionally, we could show that the interaction of the two sensor proteins was fully reversible as demonstrated in Fig. 3.2B. The addition of mepyramine, an hH$_1$R-specific antagonist, after activation of the receptor with histamine (300 nM) led to a concentration-dependent decrease in luminescence, down to the background level.

Similar experiments were performed with a sensor in which Gα$_q$(123) was replaced by Gα$_q$(97). The concentration-dependent response to histamine and the reversibility of the interaction of the two sensor proteins were still given, but the S/B ratio was approx. 3-fold lower (Fig. A3).

It turned out that the quality of D-luciferin, the pH of the surrounding medium and the temperature were critical for the validity of the results. D-luciferin from different suppliers was compared (data not shown) as a substrate of the developed probe, and only those products are listed in the method section, which afforded robust results. When experiments were performed at RT instead at 37 °C or in

DMEM, in equilibrium with atmospheric CO_2 (around 450 ppm), no or only very weak luminescence was detected (data not shown).

However, as shown in Fig. 3.2A, onset kinetics of the sensor were slower than expected for the activation of Gα subunits[18,41]. We hypothesize that the observed slowdown is related to the folding of the full-length luciferase (maturation) upon association of the two fragments[22], thereby neither affecting the $G\alpha_q$/PLC-β3 interaction itself nor downstream signalling. To prove this, we performed a Fura-2 Ca^{2+} assay, affording kinetic information on the transient increase in cytosolic Ca^{2+} with a high temporal resolution. Although the amplitudes of the Ca^{2+} transients were higher in the presence of the sensor (Fig. 3.2C) – presumably due to differences in cell density and/or by an additional expression of exogenous $G\alpha_q$ and PLC-β3 proteins – the kinetics of intracellular Ca^{2+} mobilization observed were nearly identical to that obtained from cells expressing the hH_1R alone (Fig. 3.2D). Accordingly, the histamine concentration-dependent response was not influenced by the presence of the sensor.

The $G\alpha_q$ inhibitor FR900359 is a valuable tool for analysing signalling pathways involving $G\alpha_q$[3,42]. Therefore, we examined the susceptibility of the modified $G\alpha_q$ to inhibition by FR900359 (Fig. 3.2E). We were able to inhibit sensor activation stepwise by applying FR900359 at increasing concentrations until the signal was totally abolished at a concentration of 100 nM.

Furthermore, we were interested in the performance of the sensor, when applied in an assay for ligand characterization. With S/B ratios around 5 (Fig. A4) and a Z' value of 0.7 (Fig. 3.2F) the new probe should give excellent robust readouts in functional assays.

3.3.3 Characterization of reference ligands at five different GPCRs

Aiming at a sensor, broadly applicable to diverse $G\alpha_q$-coupled GPCRs, especially to pharmacologically characterize ligands of the respective receptors, we analysed five different GPCRs of the histamine (hH_1R), muscarinic acetylcholine ($hM_{1,3,5}R$) and neurotensin ($hNTS_1R$) family. Our focus lied on literature-described standard agonists in terms of potencies (pEC_{50}) and efficacies (E_{max}), as well as on antagonists concerning their antagonistic activity (pK_b) (cf. Fig. A5). The characterization always included a reference agonist that was able to maximally activate the receptor (defined as 100%). This was either the endogenous agonist or a pharmacologically comparable compound at the respective receptor. All other analysed ligands were normalized regarding their efficacy to the particular reference agonist (Table 3.1).

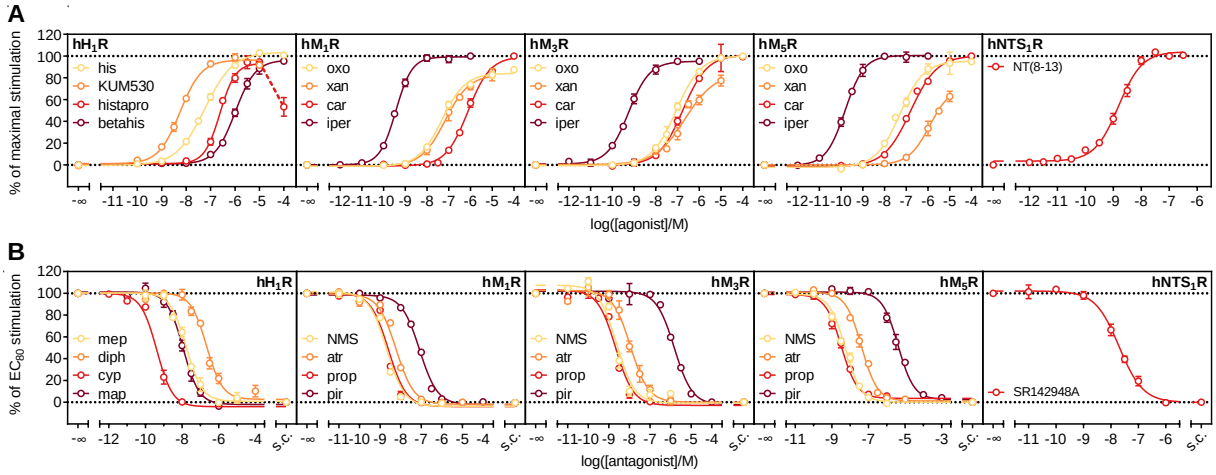

Fig. 3.3: Characterization of standard ligands at the hH$_1$R, the hM$_{1,3,5}$R and the hNTS$_1$R. Live HEK293T cells, stably expressing the developed sensor and the indicated receptor, were analysed regarding their response to standard agonists (**A**) and antagonists (**B**) for the respective receptors. The substrate D-luciferin was added directly to the cells, and the experiment was carried out at 37 °C. Agonist data was normalized to a reference full agonist for each receptor, maximal stimulation of which was defined as 100% (hH$_1$R: histamine, hM$_{1,5}$R: carbachol, hM$_3$R: oxotremorine). pEC$_{50}$, E$_{max}$ and pK$_B$ values are listed in Table 3.1 and were in good accordance with data described in literature. Data are presented as means ± SEM from at least three independent experiments, each performed in triplicate. s.c.: solvent control.

At the hH$_1$R, the endogenous agonist histamine, the slightly more potent phenylhistamine derivative UR-KUM530, histaprodifen and betahistine, a drug approved for the treatment of Ménière's disease, were analysed (Fig. 3.3A). Except for histaprodifen, where luminescence decreased after having reached a plateau, compounds gave robust CRCs. For histaprodifen and derivatives thereof, at higher concentrations toxic effects were reported[3], which might compromise the luminescence signal. The obtained potencies – with no more than half an order of magnitude difference in EC$_{50}$ – and efficacies were in good agreement with values obtained from the [^{32}P]GTPase assay[35,43] and results from assays addressing alternative signalling pathways, second messengers and holistic methods[3]. The only exception was histaprodifen, which was not always described as a full agonist as in our case[3,16,35,44,45]. Antagonistic activities of the reference ligands mepyramine, diphenhydramine, cyproheptadine and maprotiline also aligned well with values described in literature. The corresponding pK$_b$-values differed no more than half a log unit, although especially cyproheptadine was described controversially with at least one and a half orders of magnitude difference in activity across different functional and competition binding assays[3,43,46,47]. For this compound, our data align best with those from competition binding and functional holistic assays[3,46].

In literature, controversial data were reported for the analysed agonists at the muscarinic receptors, i.e. the ranges of potencies and efficacies for several compounds are very wide (Table A8.1). The potencies, we determined, fit well into the reported ranges, and, with a few exceptions, the efficacies too. For e.g. xanomeline at the hM$_3$R, or oxotremorine at the hM$_5$R, different E$_{max}$ values were reported. Although the developed sensor delivers a readout proximal to the receptor, a potential receptor reserve might still influence the observed ligand efficacies[48], which might be an explanation for the

aforementioned discrepancies. This can, of course, also apply to most of the literature reported data. The determined activities (pK_b values) of the hM_xR antagonists were comparable to those obtained from other functional assays or pK_i values from radioligand competition binding, with differences not greater than half an order of magnitude[49-56].

In case of the peptidergic $hNTS_1R$, the potency of NT(8-13) was comparable to that determined by BRET between G protein subunits[57], or in a MAPK-dependent reporter gene assay[58]. The same holds true for the antagonist SR142948A, the pK_b of which matches well with values obtained by IP_3 quantification or radioligand binding[59,60].

Table 3.1: pEC_{50}, E_{max} and pK_b values of compounds analysed at the hH_1R, the $hM_{1,3,5}Rs$ and the $hNTS_1R$. Live HEK293T cells, expressing the developed sensor and the indicated receptor, were investigated regarding their response to standard agonists and antagonist. Data are given as mean ± SEM. *N* denotes the number of biological replicates, each determined in triplicate.

	compound	pEC_{50}	$\%E_{max}$	*N*	pK_b	*N*
hH_1R	histamine	7.21 ± 0.07	100	8		
	UR-KUM530	8.22 ± 0.04	97.8 ± 3.6	7		
	histaprodifen	6.54 ± 0.07	95.6 ± 1.0	4		
	betahistine	5.95 ± 0.07	98.3 ± 2.1	4		
	mepyramine				8.48 ± 0.07	4
	diphenhydramine				7.36 ± 0.07	5
	cyproheptadine				10.12 ± 0.06	3
	maprotiline				8.74 ± 0.10	4
hM_1R	carbachol	6.12 ± 0.08	100	4		
	xanomeline	7.19 ± 0.17	80.6 ± 3.2	3		
	oxotremorine	7.32 ± 0.05	83.6 ± 1.8	3		
	iperoxo	9.42 ± 0.05	99.8 ± 2.3	4		
	N'-methylscopolamine				9.35 ± 0.07	3
	atropine				8.93 ± 0.05	3
	propantheline				9.26 ± 0.05	3
	pirenzepine				7.76 ± 0.05	3
hM_3R	oxotremorine	7.09 ± 0.09	100	8		
	xanomeline	6.51 ± 0.11	87.2 ± 6.0	5		
	carbachol	6.65 ± 0.06	101 ± 4.9	5		
	iperoxo	9.24 ± 0.10	96.4 ± 1.3	4		
	N'-methylscopolamine				9.34 ± 0.04	5
	atropine				8.69 ± 0.08	5
	propantheline				9.37 ± 0.05	5
	pirenzepine				6.57 ± 0.03	5
hM_5R	carbachol	6.78 ± 0.06	100	5		
	xanomeline	5.88 ± 0.14	73.3 ± 2.8	4		
	oxotremorine	7.19 ± 0.06	101.4 ± 4.3	4		
	iperoxo	9.80 ± 0.07	101.4 ± 1.1	4		
	N'-methylscopolamine				9.52 ± 0.08	5
	atropine				8.66 ± 0.05	5
	propantheline				9.82 ± 0.08	5
	pirenzepine				6.65 ± 0.09	5
$hNTS_1R$	neurotensin (8-13)	8.79 ± 0.09	100	8		
	SR142948A				8.20 ± 0.06	4

3.3.4 Live cell luminescence

To explore the potential of the developed probe in view of future applications, such as multiparametric measurements, e.g. in combination with impedance-based cell sensing, and imaging in laboratory animals, we decided to do live cell bioluminescence microscopy. For this purpose, cells, expressing the hM_3R and the sensor, were investigated under an inverted microscope equipped with a super-cooled EM-CCD camera. Stimulation of the cells resulted in an increase in luminescence over time, whereas pre-incubation with the antagonist atropine abolished sensor activation completely, as shown in Fig. 3.4. Although confocal resolution was not reached, luminescence was predominantly observed on the edges of the cells, indicating sensor activation associated with the cellular membrane. These observations are in agreement with the fact that both sensor proteins are membrane associated either due to palmytoylation as in case of $G\alpha_q$ or via hydrophobic regions as in the catalytic core of PLC-β3[40].

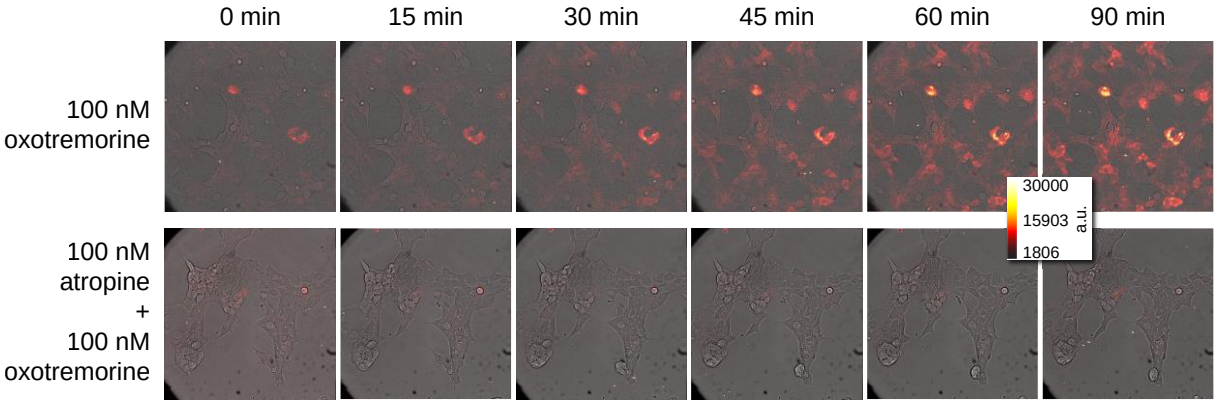

Fig. 3.4: Live cell luminescence imaging of $G\alpha_q$ sensor-expressing HEK293T cells stimulated via the hM_3R. Shown are the results of one experiment, performed in the agonist (*N* = 3) and the antagonist (*N* = 2) mode, respectively. D-luciferin was added to the cells before they were transferred to the bioluminescence microscope with its stage warmed to 37 °C. The first frame always shows cells before stimulation. All images were taken with an exposure time of 5 min and are presented as arbitrary light units in false colour. Upon stimulation with 100 nM oxotremorine (approx. EC_{60}), a constant saturable increase in luminescence was observed leading to a plateau after approx. 45 min (cf. Fig. A6). No increase was detectable, when the cells were pre-incubated with atropine (100 nM).

3.4 Conclusion

The SLC approach was applied to the interaction of $G\alpha_q$ and PLC-β3 involved in the signalling cascade of GPCRs. This led, to the best of our knowledge, to the first described SLC-based probe, in which one of the two luciferase fragments was incorporated into the protein sequence of one of the host proteins rather than attached to the termini. As a probe for the $G\alpha_q$/PLC-β3 interaction that makes genetical receptor modifications unnecessary and with its excellent Z' value of 0.7, the sensor is very suitable for ligand characterization, which was shown for five different GPCRs. Furthermore, the sensor proved to be useful for imaging, as shown for live cell bioluminescence microscopy. Beyond the here described applications the sensor might become a valuable tool for de-orphanisation and subsequent determination of signalling pathways of orphan GPCRs, the analysis of $G\alpha_q$ activation in cells endogenously expressing $G\alpha_q$ protein-coupled receptors and imaging in laboratory animals.

3.5 References

1 Katritch, V., Cherezov, V. & Stevens, R. C. Structure-function of the G protein-coupled receptor superfamily. *Annu Rev Pharmacol Toxicol* **53**, 531-556, doi:10.1146/annurev-pharmtox-032112-135923 (2013).

2 Hauser, A. S., Attwood, M. M., Rask-Andersen, M., Schiöth, H. B. & Gloriam, D. E. Trends in GPCR drug discovery: new agents, targets and indications. *Nat Rev Drug Discov* **16**, 829-842, doi:10.1038/nrd.2017.178 (2017).

3 Lieb, S., Littmann, T., Plank, N., Felixberger, J., Tanaka, M., Schäfer, T., Krief, S., Elz, S., Friedland, K., Bernhardt, G., Wegener, J., Ozawa, T. & Buschauer, A. Label-free versus conventional cellular assays: Functional investigations on the human histamine H_1 receptor. *Pharmacol Res* **114**, 13-26, doi:10.1016/j.phrs.2016.10.010 (2016).

4 Benjamin, E. R., Haftl, S. L., Xanthos, D. N., Crumley, G., Hachicha, M. & Valenzano, K. J. A miniaturized column chromatography method for measuring receptor-mediated inositol phosphate accumulation. *J Biomol Screen* **9**, 343-353, doi:10.1177/1087057103262841 (2004).

5 Trinquet, E., Fink, M., Bazin, H., Grillet, F., Maurin, F., Bourrier, E., Ansanay, H., Leroy, C., Michaud, A., Durroux, T., Maurel, D., Malhaire, F., Goudet, C., Pin, J. P., Naval, M., Hernout, O., Chrétien, F., Chapleur, Y. & Mathis, G. D-*myo*-inositol 1-phosphate as a surrogate of D-*myo*-inositol 1,4,5-tris phosphate to monitor G protein-coupled receptor activation. *Anal Biochem* **358**, 126-135, doi:10.1016/j.ab.2006.08.002 (2006).

6 Ataei, F., Torkzadeh-Mahani, M. & Hosseinkhani, S. A novel luminescent biosensor for rapid monitoring of IP_3 by split-luciferase complementary assay. *Biosens Bioelectron* **41**, 642-648, doi:10.1016/j.bios.2012.09.037 (2013).

7 Hulme, E. C. *Receptor-Effector Coupling: A Practical Approach*. Vol. 68 (Oxford University Press, 1990).

8 Grynkiewicz, G., Poenie, M. & Tsien, R. Y. A new generation of Ca^{2+} indicators with greatly improved fluorescence properties. *J Biol Chem* **260**, 3440-3450 (1985).

9 Gee, K. R., Brown, K. A., Chen, W. N., Bishop-Stewart, J., Gray, D. & Johnson, I. Chemical and physiological characterization of fluo-4 Ca^{2+}-indicator dyes. *Cell Calcium* **27**, 97-106, doi:10.1054/ceca.1999.0095 (2000).

10 McCormack, J. G. & Cobbold, P. H. *Cellular Calcium: A Practical Approach*. Vol. 80 (Oxford University Press, 1991).

11 Schrage, R., De Min, A., Hochheiser, K., Kostenis, E. & Mohr, K. Superagonism at G protein-coupled receptors and beyond. *Br J Pharmacol* **173**, 3018-3027, doi:10.1111/bph.13278 (2016).

12 Nordemann, U., Wifling, D., Schnell, D., Bernhardt, G., Stark, H., Seifert, R. & Buschauer, A. Luciferase reporter gene assay on human, murine and rat histamine H_4 receptor orthologs: correlations and discrepancies between distal and proximal readouts. *PLoS One* **8**, e73961, doi:10.1371/journal.pone.0073961 (2013).

13 Manglik, A., Lin, H., Aryal, D. K., McCorvy, J. D., Dengler, D., Corder, G., Levit, A., Kling, R. C., Bernat, V., Hübner, H., Huang, X. P., Sassano, M. F., Giguere, P. M., Löber, S., Da, D., Scherrer, G., Kobilka, B. K., Gmeiner, P., Roth, B. L. & Shoichet, B. K. Structure-based discovery of opioid analgesics with reduced side effects. *Nature* **537**, 185-190, doi:10.1038/nature19112 (2016).

14 Kenakin, T. & Christopoulos, A. Signalling bias in new drug discovery: detection, quantification and therapeutic impact. *Nat Rev Drug Discov* **12**, 205-216, doi:10.1038/nrd3954 (2013).

15 Hilf, G., Gierschik, P. & Jakobs, K. H. Muscarinic acetylcholine receptor-stimulated binding of guanosine 5'-O-(3-thiotriphosphate) to guanine-nucleotide-binding proteins in cardiac membranes. *Eur J Biochem* **186**, 725-731 (1989).

16 Strasser, A., Striegl, B., Wittmann, H. J. & Seifert, R. Pharmacological profile of histaprodifens at four recombinant histamine H_1 receptor species isoforms. *J Pharmacol Exp Ther* **324**, 60-71, doi:10.1124/jpet.107.129601 (2008).

17 Bünemann, M., Frank, M. & Lohse, M. J. Gi protein activation in intact cells involves subunit rearrangement rather than dissociation. *Proc Natl Acad Sci U S A* **100**, 16077-16082, doi:10.1073/pnas.2536719100 (2003).

18 Galés, C., Rebois, R. V., Hogue, M., Trieu, P., Breit, A., Hébert, T. E. & Bouvier, M. Real-time monitoring of receptor and G-protein interactions in living cells. *Nat Methods* **2**, 177-184, doi:10.1038/nmeth743 (2005).

19 Yoshimura, H. & Ozawa, T. Methods of split reporter reconstitution for the analysis of biomolecules. *Chem Rec* **14**, 492-501, doi:10.1002/tcr.201402001 (2014).

20 Paulmurugan, R. & Gambhir, S. S. Monitoring protein-protein interactions using split synthetic renilla luciferase protein-fragment-assisted complementation. *Anal Chem* **75**, 1584-1589 (2003).

21 Hirohama, M., Voet, A. R., Ozawa, T., Saitoh, H., Nakao, Y., Zhang, K. Y., Ito, A. & Yoshida, M. Assay methods for small ubiquitin-like modifier (SUMO)-SUMO-interacting motif (SIM) interactions in vivo and in vitro using a split-luciferase complementation system. *Anal Biochem* **448**, 92-94, doi:10.1016/j.ab.2013.12.009 (2014).

22 Hattori, M. & Ozawa, T. Split luciferase complementation for analysis of intracellular signaling. *Anal Sci* **30**, 539-544 (2014).

23 Dixon, A. S., Schwinn, M. K., Hall, M. P., Zimmerman, K., Otto, P., Lubben, T. H., Butler, B. L., Binkowski, B. F., Machleidt, T., Kirkland, T. A., Wood, M. G., Eggers, C. T., Encell, L. P. & Wood, K. V. NanoLuc Complementation Reporter Optimized for Accurate Measurement of Protein Interactions in Cells. *ACS Chem Biol* **11**, 400-408, doi:10.1021/acschembio.5b00753 (2016).

24 Littmann, T., Göttle, M., Reinartz, M. T., Kälble, S., Wainer, I. W., Ozawa, T. & Seifert, R. Recruitment of β-arrestin 1 and 2 to the β_2-adrenoceptor: analysis of 65 ligands. *J Pharmacol Exp Ther* **355**, 183-190, doi:10.1124/jpet.115.227959 (2015).

25 Misawa, N., Kafi, A. K., Hattori, M., Miura, K., Masuda, K. & Ozawa, T. Rapid and high-sensitivity cell-based assays of protein-protein interactions using split click beetle luciferase complementation: an approach to the study of G-protein-coupled receptors. *Anal Chem* **82**, 2552-2560, doi:10.1021/ac100104q (2010).

26 Takeuchi, M., Nagaoka, Y., Yamada, T., Takakura, H. & Ozawa, T. Ratiometric bioluminescence indicators for monitoring cyclic adenosine 3',5'-monophosphate in live cells based on luciferase-fragment complementation. *Anal Chem* **82**, 9306-9313, doi:10.1021/ac102692u (2010).

27 Takakura, H., Hattori, M., Takeuchi, M. & Ozawa, T. Visualization and quantitative analysis of G protein-coupled receptor-β-arrestin interaction in single cells and specific organs of living mice using split luciferase complementation. *ACS Chem Biol* **7**, 901-910, doi:10.1021/cb200360z (2012).

28 Nakajima, Y., Kimura, T., Sugata, K., Enomoto, T., Asakawa, A., Kubota, H., Ikeda, M. & Ohmiya, Y. Multicolor luciferase assay system: one-step monitoring of multiple gene expressions with a single substrate. *Biotechniques* **38**, 891-894 (2005).

29 Hida, N., Awais, M., Takeuchi, M., Ueno, N., Tashiro, M., Takagi, C., Singh, T., Hayashi, M., Ohmiya, Y. & Ozawa, T. High-sensitivity real-time imaging of dual protein-protein interactions in living subjects using multicolor luciferases. *PLoS One* **4**, e5868, doi:10.1371/journal.pone.0005868 (2009).

30 Villalobos, V., Naik, S., Bruinsma, M., Dothager, R. S., Pan, M. H., Samrakandi, M., Moss, B., Elhammali, A. & Piwnica-Worms, D. Dual-color click beetle luciferase heteroprotein fragment complementation assays. *Chem Biol* **17**, 1018-1029, doi:10.1016/j.chembiol.2010.06.018 (2010).

31 Conklin, B. R., Farfel, Z., Lustig, K. D., Julius, D. & Bourne, H. R. Substitution of three amino acids switches receptor specificity of $G_q\alpha$ to that of $G_i\alpha$. *Nature* **363**, 274-276, doi:10.1038/363274a0 (1993).

32 Hepler, J. R., Biddlecome, G. H., Kleuss, C., Camp, L. A., Hofmann, S. L., Ross, E. M. & Gilman, A. G. Functional importance of the amino terminus of $G_{q\alpha}$. *J Biol Chem* **271**, 496-504 (1996).

33 Rasmussen, S. G., DeVree, B. T., Zou, Y., Kruse, A. C., Chung, K. Y., Kobilka, T. S., Thian, F. S., Chae, P. S., Pardon, E., Calinski, D., Mathiesen, J. M., Shah, S. T., Lyons, J. A., Caffrey, M., Gellman, S. H., Steyaert, J., Skiniotis, G., Weis, W. I., Sunahara, R. K. & Kobilka, B. K. Crystal structure of the β_2 adrenergic receptor-G_s protein complex. *Nature* **477**, 549-555, doi:10.1038/nature10361 (2011).

34 Yu, J. Z. & Rasenick, M. M. Real-time visualization of a fluorescent $G\alpha_s$: Dissociation of the activated G protein from plasma membrane. *Mol Pharmacol* **61**, 352-359 (2002).

35 Strasser, A., Wittmann, H. J., Kunze, M., Elz, S. & Seifert, R. Molecular basis for the selective interaction of synthetic agonists with the human histamine H_1-receptor compared with the guinea pig H_1-receptor. *Mol Pharmacol* **75**, 454-465, doi:10.1124/mol.108.053009 (2009).

36 Kane, B. E., Grant, M. K., El-Fakahany, E. E. & Ferguson, D. M. Synthesis and evaluation of xanomeline analogs - probing the wash-resistant phenomenon at the M_1 muscarinic acetylcholine receptor. *Bioorg Med Chem* **16**, 1376-1392, doi:10.1016/j.bmc.2007.10.058 (2008).

37 Kim, J. H., Lee, S. R., Li, L. H., Park, H. J., Park, J. H., Lee, K. Y., Kim, M. K., Shin, B. A. & Choi, S. Y. High cleavage efficiency of a 2A peptide derived from porcine teschovirus-1 in human cell lines, zebrafish and mice. *PLoS One* **6**, e18556, doi:10.1371/journal.pone.0018556 (2011).

38 Cheng, Y. & Prusoff, W. H. Relationship between the inhibition constant (K_1) and the concentration of inhibitor which causes 50 per cent inhibition (I_{50}) of an enzymatic reaction. *Biochem Pharmacol* **22**, 3099-3108 (1973).

39 Müller, M., Knieps, S., Gessele, K., Dove, S., Bernhardt, G. & Buschauer, A. Synthesis and neuropeptide Y Y_1 receptor antagonistic activity of *N*,*N*-disubstituted ω-guanidino- and ω-aminoalkanoic acid amides. *Arch Pharm (Weinheim)* **330**, 333-342 (1997).

40 Lyon, A. M., Dutta, S., Boguth, C. A., Skiniotis, G. & Tesmer, J. J. Full-length $G\alpha_q$-phospholipase C-β3 structure reveals interfaces of the C-terminal coiled-coil domain. *Nat Struct Mol Biol* **20**, 355-362, doi:10.1038/nsmb.2497 (2013).

41 Milde, M., Rinne, A., Wunder, F., Engelhardt, S. & Bünemann, M. Dynamics of $G\alpha_{i1}$ interaction with type 5 adenylate cyclase reveal the molecular basis for high sensitivity of G_i-mediated inhibition of cAMP production. *Biochem J* **454**, 515-523, doi:10.1042/BJ20130554 (2013).

42 Schrage, R., Schmitz, A. L., Gaffal, E., Annala, S., Kehraus, S., Wenzel, D., Büllesbach, K. M., Bald, T., Inoue, A., Shinjo, Y., Galandrin, S., Shridhar, N., Hesse, M., Grundmann, M., Merten, N., Charpentier, T. H., Martz, M., Butcher, A. J., Slodczyk, T., Armando, S., Effern, M., Namkung, Y., Jenkins, L., Horn, V., Stößel, A., Dargatz, H., Tietze, D., Imhof, D., Galés, C., Drewke, C., Müller, C. E., Hölzel, M., Milligan, G., Tobin, A. B., Gomeza, J., Dohlman, H. G., Sondek, J., Harden, T. K., Bouvier, M., Laporte, S. A., Aoki, J., Fleischmann, B. K., Mohr, K., König, G. M., Tüting, T. & Kostenis, E. The experimental power of FR900359 to study Gq-regulated biological processes. *Nat Commun* **6**, 10156, doi:10.1038/ncomms10156 (2015).

43 Seifert, R., Wenzel-Seifert, K., Bürckstümmer, T., Pertz, H. H., Schunack, W., Dove, S., Buschauer, A. & Elz, S. Multiple differences in agonist and antagonist pharmacology between human and guinea pig histamine H_1-receptor. *J Pharmacol Exp Ther* **305**, 1104-1115, doi:10.1124/jpet.103.049619 (2003).

44 Lim, H. D., van Rijn, R. M., Ling, P., Bakker, R. A., Thurmond, R. L. & Leurs, R. Evaluation of histamine H_1-, H_2-, and H_3-receptor ligands at the human histamine H_4 receptor: identification of 4-methylhistamine as the first potent and selective H_4 receptor agonist. *J Pharmacol Exp Ther* **314**, 1310-1321, doi:10.1124/jpet.105.087965 (2005).

45 Patil, R., Elz, S. & Reiser, O. Side-chain modified analogues of histaprodifen: asymmetric synthesis and histamine H_1-receptor activity. *Bioorg Med Chem Lett* **16**, 672-676, doi:10.1016/j.bmcl.2005.10.030 (2006).

46 Moguilevsky, N., Varsalona, F., Noyer, M., Gillard, M., Guillaume, J. P., Garcia, L., Szpirer, C., Szpirer, J. & Bollen, A. Stable expression of human H_1-histamine-receptor cDNA in Chinese hamster ovary cells. Pharmacological characterisation of the protein, tissue distribution of messenger RNA and chromosomal localisation of the gene. *Eur J Biochem* **224**, 489-495 (1994).

47 Appl, H., Holzammer, T., Dove, S., Haen, E., Strasser, A. & Seifert, R. Interactions of recombinant human histamine H_1R, H_2R, H_3R, and H_4R receptors with 34 antidepressants and antipsychotics. *Naunyn Schmiedebergs Arch Pharmacol* **385**, 145-170, doi:10.1007/s00210-011-0704-0 (2012).

48 Bräuner-Osborne, H., Ebert, B., Brann, M. R., Falch, E. & Krogsgaard-Larsen, P. Functional partial agonism at cloned human muscarinic acetylcholine receptors. *Eur J Pharmacol* **313**, 145-150 (1996).

49 Bolden, C., Cusack, B. & Richelson, E. Antagonism by antimuscarinic and neuroleptic compounds at the five cloned human muscarinic cholinergic receptors expressed in Chinese hamster ovary cells. *J Pharmacol Exp Ther* **260**, 576-580 (1992).

50 Bräuner-Osborne, H. & Brann, M. R. Pharmacology of muscarinic acetylcholine receptor subtypes (m1-m5): high throughput assays in mammalian cells. *Eur J Pharmacol* **295**, 93-102 (1996).

51 Burstein, E. S., Spalding, T. A. & Brann, M. R. Pharmacology of muscarinic receptor subtypes constitutively activated by G proteins. *Mol Pharmacol* **51**, 312-319 (1997).

52 Christopoulos, A., Pierce, T. L., Sorman, J. L. & El-Fakahany, E. E. On the unique binding and activating properties of xanomeline at the M_1 muscarinic acetylcholine receptor. *Mol Pharmacol* **53**, 1120-1130 (1998).

53 Dong, G. Z., Kameyama, K., Rinken, A. & Haga, T. Ligand binding properties of muscarinic acetylcholine receptor subtypes (m1-m5) expressed in baculovirus-infected insect cells. *J Pharmacol Exp Ther* **274**, 378-384 (1995).

54 Huang, F., Buchwald, P., Browne, C. E., Farag, H. H., Wu, W. M., Ji, F., Hochhaus, G. & Bodor, N. Receptor binding studies of soft anticholinergic agents. *AAPS PharmSci* **3**, E30, doi:10.1208/ps030430 (2001).

55 Watson, N., Daniels, D. V., Ford, A. P., Eglen, R. M. & Hegde, S. S. Comparative pharmacology of recombinant human M_3 and M_5 muscarinic receptors expressed in CHO-K1 cells. *Br J Pharmacol* **127**, 590-596, doi:10.1038/sj.bjp.0702551 (1999).

56 Wess, J., Lambrecht, G., Mutschler, E., Brann, M. R. & Dörje, F. Selectivity profile of the novel muscarinic antagonist UH-AH 37 determined by the use of cloned receptors and isolated tissue preparations. *Br J Pharmacol* **102**, 246-250 (1991).

57 Besserer-Offroy, E., Brouillette, R. L., Lavenus, S., Froehlich, U., Brumwell, A., Murza, A., Longpré, J. M., Marsault, E., Grandbois, M., Sarret, P. & Leduc, R. The signaling signature of the neurotensin type 1 receptor with endogenous ligands. *Eur J Pharmacol* **805**, 1-13, doi:10.1016/j.ejphar.2017.03.046 (2017).

58 Kling, R. C., Plomer, M., Lang, C., Banerjee, A., Hübner, H. & Gmeiner, P. Development of Covalent Ligand-Receptor Pairs to Study the Binding Properties of Nonpeptidic Neurotensin Receptor 1 Antagonists. *ACS Chem Biol* **11**, 869-875, doi:10.1021/acschembio.5b00965 (2016).

59 Gully, D., Labeeuw, B., Boigegrain, R., Oury-Donat, F., Bachy, A., Poncelet, M., Steinberg, R., Suaud-Chagny, M. F., Santucci, V., Vita, N., Pecceu, F., Labbé-Jullié, C., Kitabgi, P., Soubrié, P., Le Fur, G. & Maffrand, J. P. Biochemical and pharmacological activities of SR 142948A, a new potent neurotensin receptor antagonist. *J Pharmacol Exp Ther* **280**, 802-812 (1997).

60 Keller, M., Kuhn, K. K., Einsiedel, J., Hübner, H., Biselli, S., Mollereau, C., Wifling, D., Svobodova, J., Bernhardt, G., Cabrele, C., Vanderheyden, P. M., Gmeiner, P. & Buschauer, A. Mimicking of Arginine by Functionalized N^{ω}-Carbamoylated Arginine As a New Broadly Applicable Approach to Labeled Bioactive Peptides: High Affinity Angiotensin, Neuropeptide Y, Neuropeptide FF, and Neurotensin Receptor Ligands As Examples. *J Med Chem* **59**, 1925-1945, doi:10.1021/acs.jmedchem.5b01495 (2016).

4. Towards probing the interactions of $G\alpha_s$ and $G\alpha_i$ with adenylyl cyclases using split-luciferase complementation

4.1 Introduction

Probing the interaction of Gα subunits with their effector proteins should be a generally applicable approach, not only for the interaction of $G\alpha_q$ with the PLC-β3 (cf. chapter 3[1]). Two other major Gα subtypes, namely $G\alpha_s$ and $G\alpha_i$, interact with integral membrane proteins from the AC class[2-5], which catalyse the formation of cAMP from ATP[6-8]. Analogously to the $G\alpha_q$ pathway, assays developed for the characterisation of ligands at $G\alpha_s$ and $G\alpha_i$-coupled receptors mostly rely on the quantification of the second messenger cAMP[9-13] or on the usage of radiolabelled [^{35}S]-GTPγS to assess Gα activation[14,15]. However, as pointed out before, quantification of second messengers is unfavourable for applications, such as precise efficacy determination[16], or agonist bias detection. An additional drawback, when $G\alpha_i$-dependent effects on the intracellular cAMP concentration are quantified, is the very marginal influence on basal cAMP making a pre-stimulation with forskolin necessary[7,13]. Therefore, proximal detection techniques of GPCR activation, ideally on the G protein level, are needed. But, due to increasing problems with the availability and quality of radiolabelled compounds, as well as a poor assay performance with certain receptors[14], the [^{35}S]-GTPγS incorporation assay is also becoming more and more impracticable.

Aiming at a technique that can be used to quantify $G\alpha_s$ and $G\alpha_i$ activation similarly to the assay described in chapter 3[1] for $G\alpha_q$, SLC was applied to the interaction of either of the two Gα subtypes with their effector protein AC (cf. Fig. 4.1). Different libraries of vector plasmids encoding fusion proteins of $G\alpha_s$ and $G\alpha_i$ fused to CBRC, as well as AC2, AC5 and AC6 fused to CBRN were generated (cf. Fig. 4.2). The smaller luciferase fragment CBRC was fused to the termini of $G\alpha_s$ and $G\alpha_i$ and also incorporated into three different flexible loop regions chosen on the basis of crystal structures[17-19] and studies in which the Gα subunits were labelled with fluorescent proteins[20-23]. The ACs were tagged solely on either of both termini with CBRN.

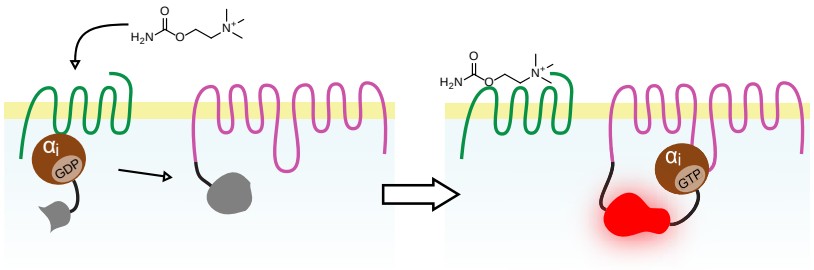

Fig. 4.1: Schematic illustration of the proposed assay setup. The human muscarinic acetylcholine M_2 receptor (hM_2R, green) is activated by binding of the agonist carbachol. This leads to the exchange of GDP for GTP, which in turn promotes the dissociation of the Gα subunit from the G protein/GPCR complex. The activated Gα subunit interacts with the effector protein AC (pink), bringing the two luciferase fragments, fused to Gα and AC, into close proximity. After maturation of the intact luciferase from the separate fragments, light is emitted. The illustration shows $G\alpha_i$, but applies to $G\alpha_s$ as well, since it also interacts with ACs.

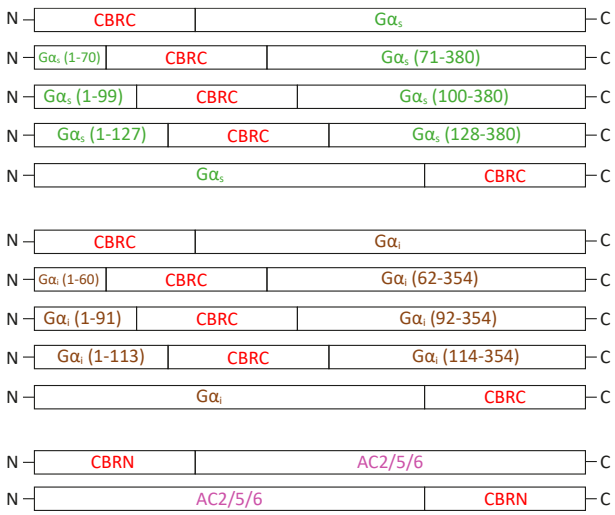

Fig. 4.2: Schematic illustration of the different $G\alpha_{s,i}$/CBRC and AC/CBRN fusion proteins.

After preparation of the plasmids, the encoded fusion proteins were examined with respect to their ability to interact with each other. HEK293T cells were transfected with different combinations of plasmids encoding the Gα and AC fusion proteins together with a plasmid encoding the human histamine H_2 receptor (hH_2R), in case of the CRBC-tagged $G\alpha_s$ proteins. The $G\alpha_i$/AC interaction was analysed either with the human muscarinic acetylcholine M_2 receptor (hM_2R), the human histamine H_3 receptor (hH_3R) or the human histamine H_4 receptor (hH_4R). After stimulation with histamine ($hH_{2,3,4}R$) or carbachol (hM_2R), the change in luciferase activity was quantified. Furthermore, the subcellular localisation of the AC2 and AC6 fusion proteins was analysed using fluorescence immunostaining.

4.2 Materials & Methods

4.2.1 Materials

Phosphate-buffered saline (PBS) was from Sigma (Tokyo, Germany). PBS^{++} was prepared by adding 2.03 mg of $MgCl_2 \cdot 6\ H_2O$ and 2.94 mg of $CaCl_2 \cdot 2\ H_2O$ to 20 mL of PBS. Poly-L-lysine, para-formaldehyde (4%) and gelatin from cold water fish skin (40%) were from Sigma (Tokyo, Japan). Triton X-100 was from Merck (Tokyo, Japan). The anti-V5 antibody produced in rabbit was from Abcam (Tokyo, Japan) and the anti-rabbit antibody, produced in goat and conjugated to Alexa Fluor 647, was from Thermo Scientific (Tokyo, Japan).

4.2.2 Cell cultivation

Was performed as described under 3.2.2.

4.2.3 Generation of plasmids

Plasmids, encoding different human GPCRs as well as $G\alpha_{i1}$ and the short isoform of $G\alpha_s$, were obtained from the Missouri cDNA resource center (Rolla, MO, USA). The other plasmids used were generated by standard PCR and restriction techniques within the pcDNA backbone, unless otherwise stated. A plasmid encoding the red-emitting click-beetle luciferase (pCBR-control) was used as a template in different PCRs to generate the sequences encoding the two slightly overlapping N-terminal (*CBRN*, encoding amino acids 1-416) and C-terminal (*CBRC*, encoding amino acids 394-542) fragments of the luciferase. *CBRN* was then used to prepare plasmids encoding fusion proteins consisting of AC2, AC5, or AC6 fused either N- or C-terminally to CBRN. At the C-terminus of each AC/CBRN fusion protein, a V5-tag was present. *CBRC* was used to generate plasmids of five different fusion proteins for both, $G\alpha_s$ and $G\alpha_i$, in which CBRC was fused to both termini of Gα or integrated into the Gα sequence after amino acids 70, 99 and 127, as in case of $G\alpha_s$, or after amino acids 60, 91 and 117, as in case of $G\alpha_i$. The linker sequences used to connect the luciferase fragments to either AC or Gα consisted of flexible Gly and Ser residues. All plasmids were quality-controlled by DNA sequencing.

4.2.4 Detection of interaction between $G\alpha_{s/i}$ and AC2/6 fusion proteins

Was performed as described for the $G\alpha_q$ and PLC-β3 fusion proteins under 3.2.4.

4.2.5 Fluorescence immunostaining of AC2 and AC6 fusion proteins

HEK293T cells were seeded on a poly-L-lysine coated 35-mm glass bottom dish at a density of $5 \cdot 10^5$ cells/dish. On the next day, the cells were transfected with 2 µg of plasmids encoding N- or C-terminally-tagged AC2, or AC6. An untransfected control was also included to assess unspecific binding of the antibodies. After 24 h of incubation, Hoechst 33342 was added at a concentration of 1 µg/mL, and

the cells were incubated for another 30 min. The medium was aspirated, and the cells were washed once with PBS^{++}. To fix the cells, 2 mL of para-formaldehyde (4%) were added at 37 °C for 30 min. Afterwards, the cells were washed once with PBS^{++}, before 1.5 µL of Triton X-100 (0.2%) were added at RT for 5 min, in order to permeabilize the cellular membranes. The dish was washed three times with 1 mL of PBS^{++}, before 1.5 mL blocking solution (0.2% gelatin from cold water fish skin in PBS^{++}) were added and incubated while slowly shaking at RT for 1 h. After aspiration of the blocking solution, a solution containing the primary (anti-V5) antibody (diluted 1:500 in blocking solution) was added and incubated as in the step before. The cells were washed three times with PBS^{++}, and the secondary antibody (anti-rabbit) conjugated to Alexa Fluor 647 was added (diluted 1:5000 in blocking solution) and incubated while slowly shaking for another hour. Before the fixed cells were imaged, residual secondary antibody was removed by washing another three times with PBS^{++}. Imaging was carried out using an Olympus FV-1000 (Tokyo, Japan) confocal laser scanning microscope.

4.2.6 Identification of the best pair of $G\alpha_{s/i}$ and AC5 fusion proteins

HEK293T cells were treated as described before, except for the usage of Leibovitz' L15 as medium, in order to be able to perform live cell measurements. On the day of the assay, 10 µL of D-Luciferin (10 mM) were added to the cells, and the plate was transferred into a pre-warmed EnSpire microplate luminescence reader (Perkin-Elmer, Germany). The cells were allowed to equilibrate inside the reader for 10 min, before the basal luminescence was determined by recording the luminescence of the entire plate ten times with an integration time of 1 s per well. Then, either histamine ($G\alpha_s$), or carbachol ($G\alpha_i$) and only Leibovitz' L15 (solvent control) were added to the cells. Immediately afterwards, luminescence was recorded for 50 plate repeats amounting to a time period of 70 min.

4.3 Results and discussion

4.3.1 Interaction between $G\alpha_i$ and AC6 fusion proteins

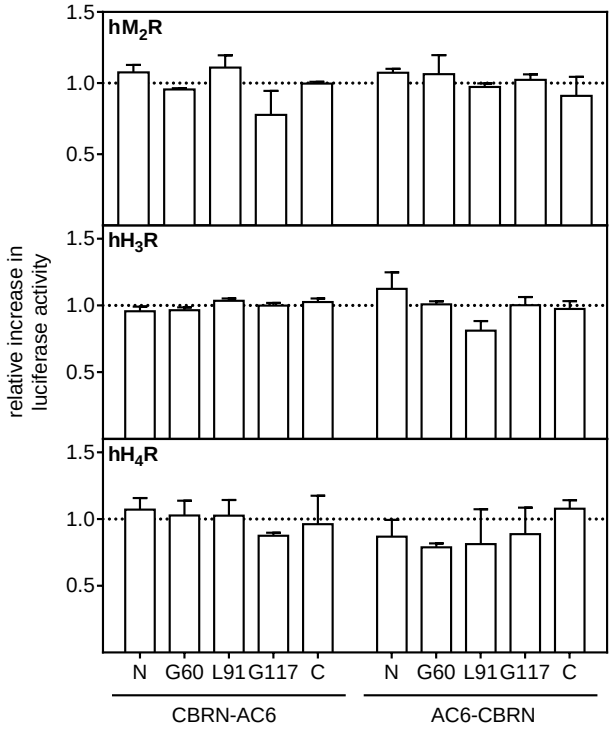

Fig. 4.3: Changes in luciferase activity for the different combinations of $G\alpha_i$ and AC6 luciferase fragment fusion proteins stimulated via the hM_2R, the hH_3R and the hH_4R. HEK293T cells were transiently transfected with plasmids encoding the indicated fusion proteins of $G\alpha_i$/CBRC and AC6/CBRN and the indicated GPCRs. After two days of transfection, the cells were stimulated with 10 µM carbachol (hM_2R), or 10 µM histamine ($hH_{3,4}R$). The resulting luminescence intensity was divided by that obtained from cells treated with a solvent control. No signal increases were detected. Data represent the means ± SEM of one to two independent experiments, each performed in triplicate.

Since the aim of this project was to establish a technique applicable to both, $G\alpha_s$ and $G\alpha_i$ proteins, the chosen AC had to be regulated by both Gα subtypes as well. In a first attempt, AC6, which was shown to be regulated by both Gα subtypes[7], was analysed together with $G\alpha_i$ and three different $G\alpha_i$-coupling GPCRs, the hM_2R, hH_3R and the hH_4R. However, as displayed in Fig. 4.3 no increases in luciferase activity were detected after stimulation of the receptors with their respective reference agonists (hM_2R: 10 µM carbachol, $hH_{3,4}R$: 10 µM histamine).

The fusion of the luciferase fragments to the $G\alpha_i$ (CBRC) and the AC6 (CBRN) might negatively influence their folding, or might block interaction surfaces of the two proteins, resulting in a loss of function of one or both proteins, which could explain the non-existent luminescence changes. In addition, membrane trafficking of the AC through the endoplasmic reticulum (ER) could be hampered by the fusion to CBRN.

4.3.2 Interaction between AC2 and either $G\alpha_s$ or $G\alpha_i$ fusion proteins

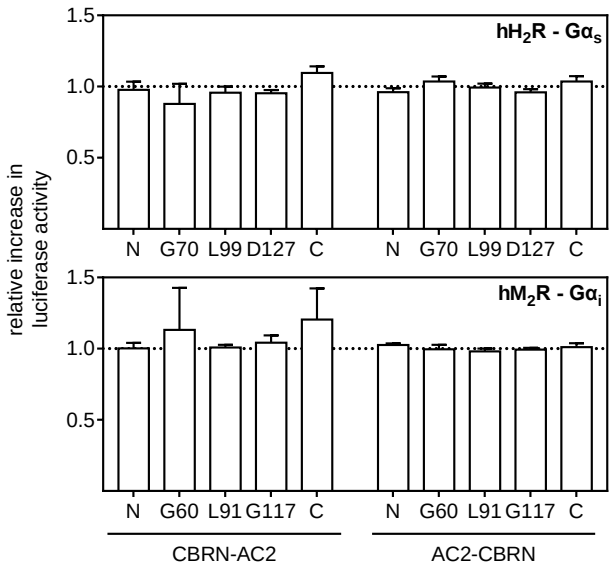

Fig. 4.4: Changes in luciferase activity for the different combinations of $G\alpha_s$, $G\alpha_i$ and AC2 luciferase fragment fusion proteins stimulated via the hH_2R ($G\alpha_s$) and the hM_2R ($G\alpha_i$). HEK293T cells were transfected with plasmids encoding the $G\alpha_s$/CBRC and AC2/CBRN fusion proteins together with the hH_2R. In another approach, $G\alpha_i$/CBRC fusion proteins were to be co-expressed with the AC2/CBRN fusion proteins and the hM_2R. As in 4.3.1, no increases in luciferase activity were detected after stimulation of the GPCR. Data represent the means ± SEM of one experiment, performed in triplicate.

A different attempt to probe the interaction between ACs and $G\alpha_s$/$G\alpha_i$ proteins was made using AC2, because it was shown to be modulated by the two Gα subtypes comparable to AC6[7]. HEK293T cells were differentially transfected: on one hand, with plasmids encoding $G\alpha_s$ and AC2 differentially fused to the CBR fragments and the hH_2R. On the other hand, with plasmids encoding the $G\alpha_i$ and AC2 fusion proteins together with a plasmid encoding the hM_2R. Again, the GPCRs were stimulated either with 100 µM histamine (hH_2R, $G\alpha_s$), or with 10 µM carbachol (hM_2R, $G\alpha_i$) and the change in luminescence was quantified in relation to a solvent control (Fig. 4.4).

As in 4.3.1, no increases in luminescence after stimulation of a GPCR were detected. Neither for $G\alpha_s$ interacting with AC2, nor for $G\alpha_i$.

4.3.3 Cellular localisation of AC2 and the AC6 fusion proteins

Since both attempts to probe the interaction between an adenylyl cyclase and the $G\alpha_s$ and $G\alpha_i$ proteins applying the SLC approach failed, the cellular localisation of the fusion proteins, consisting of either AC2, or AC6 together with CBRN, was determined. HEK293T cells transfected with the four different AC/CBRN fusion proteins were subjected to fluorescence immunostaining by making use of the V5-tag at the C-terminus of the fusion constructs. As displayed in Fig. 4.5, the staining revealed an intracellular localisation of the AC/CBRN fusion proteins, which could be an explanation for the lack in interaction with the Gα proteins.

Localisation at the cellular membrane is absolutely necessary for an interaction with the Gα proteins[20,24]. ACs are large in size and consist of 12 transmembrane helices[8]. Therefore, the proteins are translated into the ER were protein folding and trafficking into the cellular membrane occur[25]. Integration of multi-spanning transmembrane proteins into the ER-membrane is a complex process, initiated by the signal-recognition particle (SRP)[26], which recognises either targeting sequences[27] or hydrophobic elements in

putative transmembrane domains during translation at the ribosome[25]. Binding of SRP facilitates a slow-down of translation via its M-domain and the translocation of the ribosome to the ER by a direct interaction with the SRP receptor[26]. The ribosome with its immature protein is then transferred to a Sec61 channel[28]. These channels are responsible for the integration of hydrophobic sequences, such as transmembrane helices, into the membrane of the ER[25,28]. Following finalisation of the translation, the protein is targeted via the Golgi apparatus to the plasma membrane[29].

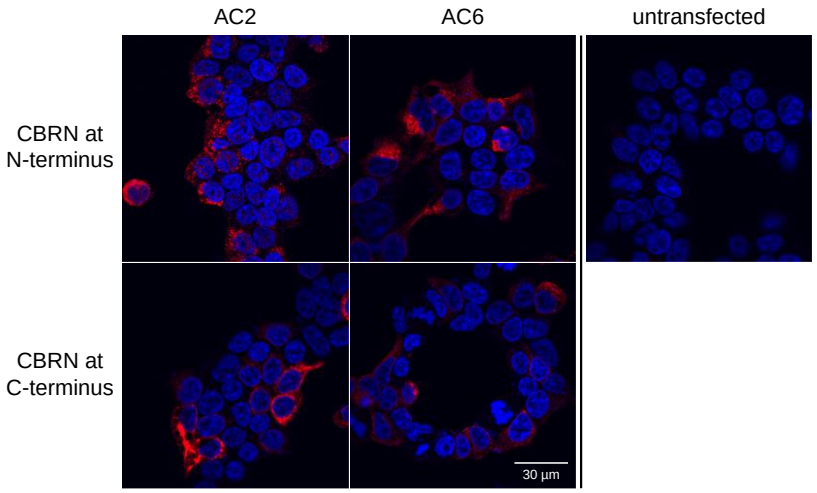

Fig. 4.5: Fluorescence immunostaining of the AC/CBRN fusion proteins using the C-terminal V5-tag. HEK293T cells were transfected with the genes of the different AC/CBRN fusion proteins, and fluorescence immunostaining was performed according to 4.2.5. The C-terminal V5-tag was stained using an anti-V5 primary antibody and an Alexa Fluor 647-conjugated secondary antibody shown in red. Nuclei were counterstained using Hoechst 33342, represented in blue. The absence of unspecific binding was demonstrated with untransfected HE293T cells, subjected to the same staining procedure. ACs are integral membrane proteins consisting of 12 transmembrane helices. However, the immunostaining of the CBRN fusion proteins reveals an intracellular localisation, presumably in the ER.

Therefore, folding of a protein such as an AC, having numerous transmembrane helices, is presumably very complex on its own. In addition, the CBRN tags are present on the termini, which might abolish the recognition of the immature protein by the SRP. Furthermore, the overexpression of the proteins, might lead to misfolding and aggregation inside the ER. Taken together, this probably overstrains the capabilities of the ER, being in line with the fact that overexpression of ACs in *Sf9* insect cells for crystallisation attempts failed[24]. Consequently, an aggregation of the unfolded proteins inside the ER would explain the results of the immunostaining experiments.

4.3.4 Interaction of AC5 with $G\alpha_s$ and $G\alpha_i$ fusion proteins

In two studies, the AC5 isoform was shown to be associated with the cell membrane, also when overexpressed, and when fused with a fluorescent protein[4,20]. Therefore, in a final attempt, AC5 was used as a CBRN fusion protein to probe its interaction with $G\alpha_s$ and $G\alpha_i$. HEK293T cells were treated as described before, but were analysed as live cells with D-luciferin added to the surrounding medium. In Fig. 4.6 the result of one experiment, using both Gα subtypes and the corresponding receptors is displayed. Increases in luminescence could be detected and since live cell measurements were performed, also the time-dependent development of the luminescence was recorded.

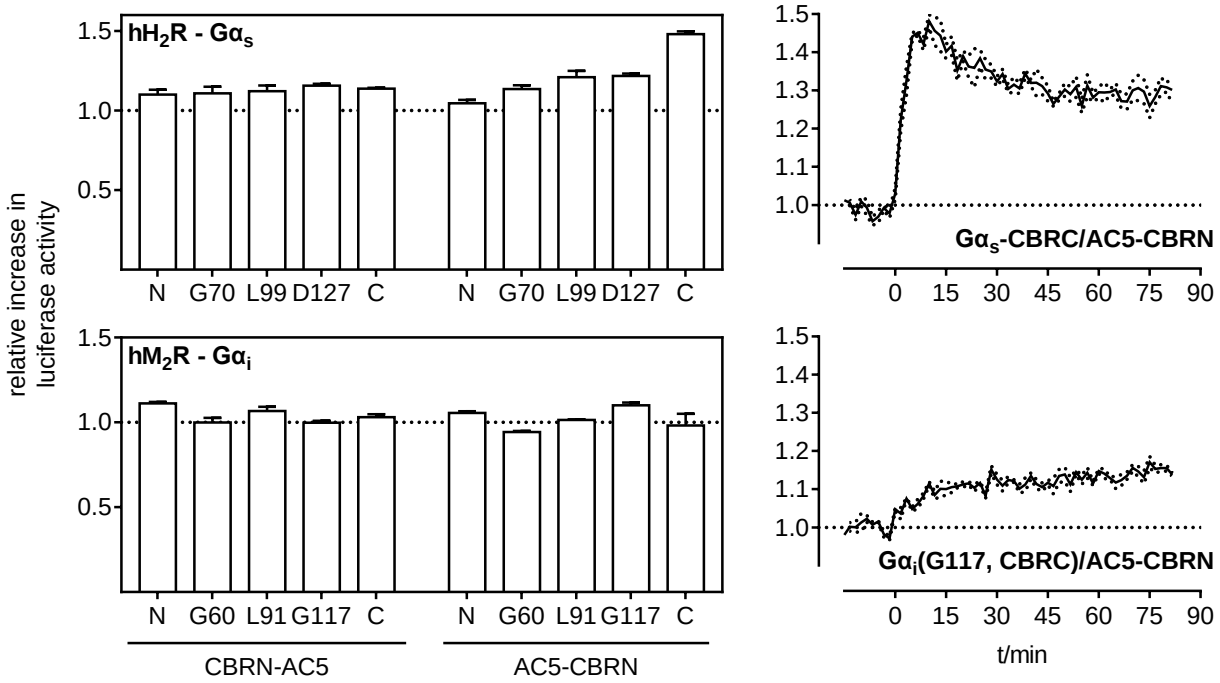

Fig. 4.6: Changes in luciferase activity of the different combinations of $G\alpha_s$, $G\alpha_i$ and AC5 luciferase fragment fusion proteins stimulated via the hH_2R ($G\alpha_s$) and the hM_2R ($G\alpha_i$) and exemplary time courses. HEK293T cells were transfected with plasmids encoding the $G\alpha_s$/CBRC and AC5/CBRN fusion proteins together with the hH_2R. In another approach, $G\alpha_i$/CBRC fusion proteins were co-expressed along with the AC5/CBRN fusion proteins and the hM_2R. In contrast to 4.3.1 and 4.3.2, analysis was carried out using live cells. The cells were stimulated with 100 µM histamine (hH_2R) and 100 µM carbachol (hM_2R), respectively. Displayed graphs represent the detected luminescence intensity 10 min (hH_2R) and 15 min (hM_2R), respectively, after addition of the agonist, divided by luminescence of a solvent control at the corresponding time point. In the representative time course diagrams, agonist was added at time point zero. Data represent the means ± SEM of one experiment, performed in triplicate.

Unfortunately, the results were irreproducible. Several combinations of fusion proteins of $G\alpha_s$/$G\alpha_i$ and AC5 responded with luminescence intensity increases after stimulation with an agonist. The time-dependent analysis revealed that increases began with agonist addition, persisted over time and were not associated with differences in cell density between stimulated and control cells. This suggests that the measured effects might have actually resulted from an interaction of the two sensor proteins. However, since the increases in luminescence intensity were very small compared to those of the $G\alpha_q$/PLC-β3 combination (cf. chapter 3[1]), and since the preliminary results were irreproducible, a lot of optimisation will be necessary, to follow this approach to characterize GPCR ligands.

The most probable reason for the aforementioned problems, is the lacking or insufficient membrane expression of the AC. To overcome this limitation, artificial signalling sequences could be added N-terminally to the AC/CBRN fusion proteins to improve trafficking to the membrane. This strategy was proven useful in the context with N-terminal fusion proteins of GPCRs[30,31]. A different approach could be the design of a synthetic AC fragment consisting only of its soluble catalytic domain fused to CBRN, since both Gα isoforms were proposed to bind directly to this specific domain[2,3,32]. The latter is also supported by a crystal structure of $G\alpha_s$ with an engineered catalytic domain[17]. Another solution could be the application of serum starvation before conducting the experiments. HEK293T cells endogenously express several GPCRs[33] and FCS, a constituent of the assay medium, contains numerous ingredients[34] from which

many are still even unknown[35]. Since the assay is not restricted to a specific receptor and is therefore activated by any $G\alpha_s$-, or $G\alpha_i$-coupled receptor expressed by the cell[33], unspecific activation through serum components, like hormones or other small molecules[34], might occur. The α_{2A} adrenoceptor, for example, can be activated by serum components[20]. Activation of Gα proteins through serum components means that the basal interaction between Gα and AC proteins is already high, which would reduce the dynamic range of the assay.

4.4 Conclusion

The translation of the approach, described in chapter 3[1], to probe Gα interaction with their effector proteins for studying GPCR function failed in case of $G\alpha_s$ and $G\alpha_i$. Several attempts were made to probe the interaction between the two Gα subtypes with different ACs. Two ACs fused to CBRN showed poor membrane expression, being the most probable reason for the lacking interaction with Gα. In case of AC5, a single experiment yielded increases in luciferase activity after stimulation of the Gα/AC interaction through a GPCR, but the results could not be reproduced. Future studies to improve the assay performance could involve the usage of artificial signalling sequences to enhance membrane targeting, the generation of a synthetic and soluble AC surrogate fused to CBRN, making membrane targeting unnecessary, or serum starvation of the cells.

4.5 References

1 Littmann, T., Ozawa, T., Hoffmann, C., Buschauer, A. & Bernhardt, G. A split luciferase-based probe for quantitative proximal determination of $G\alpha_q$ signalling in live cells. *Sci Rep* **8**, 17179, doi:10.1038/s41598-018-35615-w (2018).

2 Yan, S. Z., Huang, Z. H., Rao, V. D., Hurley, J. H. & Tang, W. J. Three discrete regions of mammalian adenylyl cyclase form a site for $G_{s\alpha}$ activation. *J Biol Chem* **272**, 18849-18854 (1997).

3 Dessauer, C. W., Tesmer, J. J., Sprang, S. R. & Gilman, A. G. Identification of a $G_{i\alpha}$ binding site on type V adenylyl cyclase. *J Biol Chem* **273**, 25831-25839 (1998).

4 Sadana, R., Dascal, N. & Dessauer, C. W. N terminus of type 5 adenylyl cyclase scaffolds G_s heterotrimer. *Mol Pharmacol* **76**, 1256-1264, doi:10.1124/mol.109.058370 (2009).

5 Chen-Goodspeed, M., Lukan, A. N. & Dessauer, C. W. Modeling of $G\alpha_s$ and $G\alpha_i$ regulation of human type V and VI adenylyl cyclase. *J Biol Chem* **280**, 1808-1816, doi:10.1074/jbc.M409172200 (2005).

6 Tang, W. J. & Hurley, J. H. Catalytic mechanism and regulation of mammalian adenylyl cyclases. *Mol Pharmacol* **54**, 231-240 (1998).

7 Taussig, R., Tang, W. J., Hepler, J. R. & Gilman, A. G. Distinct patterns of bidirectional regulation of mammalian adenylyl cyclases. *J Biol Chem* **269**, 6093-6100 (1994).

8 Halls, M. L. & Cooper, D. M. Adenylyl cyclase signalling complexes - Pharmacological challenges and opportunities. *Pharmacol Ther* **172**, 171-180, doi:10.1016/j.pharmthera.2017.01.001 (2017).

9 Adams, S. R., Harootunian, A. T., Buechler, Y. J., Taylor, S. S. & Tsien, R. Y. Fluorescence ratio imaging of cyclic AMP in single cells. *Nature* **349**, 694-697, doi:10.1038/349694a0 (1991).

10 Nikolaev, V. O., Bünemann, M., Hein, L., Hannawacker, A. & Lohse, M. J. Novel single chain cAMP sensors for receptor-induced signal propagation. *J Biol Chem* **279**, 37215-37218, doi:10.1074/jbc.C400302200 (2004).

11 Gabriel, D., Vernier, M., Pfeifer, M. J., Dasen, B., Tenaillon, L. & Bouhelal, R. High throughput screening technologies for direct cyclic AMP measurement. *Assay Drug Dev Technol* **1**, 291-303, doi:10.1089/15406580360545107 (2003).

12 Brunskole-Hummel, I., Reinartz, M. T., Kälble, S., Burhenne, H., Schwede, F., Buschauer, A. & Seifert, R. Dissociations in the effects of β_2-adrenergic receptor agonists on cAMP formation and superoxide production in human neutrophils: support for the concept of functional selectivity. *PLoS One* **8**, e64556, doi:10.1371/journal.pone.0064556 (2013).

13 Nordemann, U., Wifling, D., Schnell, D., Bernhardt, G., Stark, H., Seifert, R. & Buschauer, A. Luciferase reporter gene assay on human, murine and rat histamine H_4 receptor orthologs: correlations and discrepancies between distal and proximal readouts. *PLoS One* **8**, e73961, doi:10.1371/journal.pone.0073961 (2013).

14 Harrison, C. & Traynor, J. R. The [^{35}S]GTPγS binding assay: approaches and applications in pharmacology. *Life Sciences* **74**, 489-508, doi:10.1016/j.lfs.2003.07.005 (2003).

15 Hilf, G., Gierschik, P. & Jakobs, K. H. Muscarinic acetylcholine receptor-stimulated binding of guanosine 5'-O-(3-thiotriphosphate) to guanine-nucleotide-binding proteins in cardiac membranes. *Eur J Biochem* **186**, 725-731 (1989).

16 Smith, N. J., Bennett, K. A. & Milligan, G. When simple agonism is not enough: emerging modalities of GPCR ligands. *Mol Cell Endocrinol* **331**, 241-247, doi:10.1016/j.mce.2010.07.009 (2011).

17 Tesmer, J. J., Sunahara, R. K., Gilman, A. G. & Sprang, S. R. Crystal structure of the catalytic domains of adenylyl cyclase in a complex with $G_{s\alpha}$-GTPγS. *Science* **278**, 1907-1916 (1997).

18 Thaker, T. M., Sarwar, M., Preininger, A. M., Hamm, H. E. & Iverson, T. M. A transient interaction between the phosphate binding loop and switch I contributes to the allosteric network between receptor and nucleotide in $G\alpha_{i1}$. *J Biol Chem* **289**, 11331-11341, doi:10.1074/jbc.M113.539064 (2014).

19 Rasmussen, S. G., DeVree, B. T., Zou, Y., Kruse, A. C., Chung, K. Y., Kobilka, T. S., Thian, F. S., Chae, P. S., Pardon, E., Calinski, D., Mathiesen, J. M., Shah, S. T., Lyons, J. A., Caffrey, M., Gellman, S. H., Steyaert, J., Skiniotis, G., Weis, W. I., Sunahara, R. K. & Kobilka, B. K. Crystal structure of the β_2 adrenergic receptor-G_s protein complex. *Nature* **477**, 549-555, doi:10.1038/nature10361 (2011).

20 Milde, M., Rinne, A., Wunder, F., Engelhardt, S. & Bünemann, M. Dynamics of $G\alpha_{i1}$ interaction with type 5 adenylate cyclase reveal the molecular basis for high sensitivity of G_i-mediated inhibition of cAMP production. *Biochem J* **454**, 515-523, doi:10.1042/BJ20130554 (2013).

21 Galés, C., Rebois, R. V., Hogue, M., Trieu, P., Breit, A., Hébert, T. E. & Bouvier, M. Real-time monitoring of receptor and G-protein interactions in living cells. *Nat Methods* **2**, 177-184, doi:10.1038/nmeth743 (2005).

22 Galés, C., Van Durm, J. J., Schaak, S., Pontier, S., Percherancier, Y., Audet, M., Paris, H. & Bouvier, M. Probing the activation-promoted structural rearrangements in preassembled receptor-G protein complexes. *Nat Struct Mol Biol* **13**, 778-786, doi:10.1038/nsmb1134 (2006).

23 Bünemann, M., Frank, M. & Lohse, M. J. Gi protein activation in intact cells involves subunit rearrangement rather than dissociation. *Proc Natl Acad Sci U S A* **100**, 16077-16082, doi:10.1073/pnas.2536719100 (2003).

24 Sadana, R. & Dessauer, C. W. Physiological roles for G protein-regulated adenylyl cyclase isoforms: insights from knockout and overexpression studies. *Neurosignals* **17**, 5-22, doi:10.1159/000166277 (2009).

25 Shao, S. & Hegde, R. S. Membrane protein insertion at the endoplasmic reticulum. *Annu Rev Cell Dev Biol* **27**, 25-56, doi:10.1146/annurev-cellbio-092910-154125 (2011).

26 Grudnik, P., Bange, G. & Sinning, I. Protein targeting by the signal recognition particle. *Biol Chem* **390**, 775-782, doi:10.1515/BC.2009.102 (2009).

27 von Heijne, G. Protein targeting signals. *Curr Opin Cell Biol* **2**, 604-608 (1990).

28 Pfeffer, S., Burbaum, L., Unverdorben, P., Pech, M., Chen, Y., Zimmermann, R., Beckmann, R. & Förster, F. Structure of the native Sec61 protein-conducting channel. *Nat Commun* **6**, 8403, doi:10.1038/ncomms9403 (2015).

29 Venditti, R., Wilson, C. & De Matteis, M. A. Exiting the ER: what we know and what we don't. *Trends Cell Biol* **24**, 9-18, doi:10.1016/j.tcb.2013.08.005 (2014).

30 Stoddart, L. A., Johnstone, E. K. M., Wheal, A. J., Goulding, J., Robers, M. B., Machleidt, T., Wood, K. V., Hill, S. J. & Pfleger, K. D. G. Application of BRET to monitor ligand binding to GPCRs. *Nat Methods* **12**, 661-663, doi:10.1038/nmeth.3398 (2015).

31 Takenouchi, O., Yoshimura, H. & Ozawa, T. Unique Roles of β-Arrestin in GPCR Trafficking Revealed by Photoinducible Dimerizers. *Sci Rep* **8**, 677, doi:10.1038/s41598-017-19130-y (2018).

32 Milde, M., Werthmann, R. C., von Hayn, K. & Bünemann, M. Dynamics of adenylate cyclase regulation via heterotrimeric G-proteins. *Biochem Soc Trans* **42**, 239-243, doi:10.1042/BST20130280 (2014).

33 Atwood, B. K., Lopez, J., Wager-Miller, J., Mackie, K. & Straiker, A. Expression of G protein-coupled receptors and related proteins in HEK293, AtT20, BV2, and N18 cell lines as revealed by microarray analysis. *BMC Genomics* **12**, 14, doi:10.1186/1471-2164-12-14 (2011).

34 Freshney, R. I. in *Culture of Animal Cells* (ed R.I. Freshney) Ch. 8, 99-114 (John Wiley & Sons, 2011).

35 Baker, M. Reproducibility: Respect your cells! *Nature* **537**, 433-435, doi:10.1038/537433a (2016).

5. A split luciferase-based assay for simultaneous analyses of the ligand concentration- and time-dependent recruitment of β-arrestin2

Prior to the submission of this thesis, parts of this chapter have been submitted for publication:

Littmann, T., Buschauer, A. & Bernhardt, G. Split luciferase-based assay for simultaneous analyses of the ligand concentration- and time-dependent recruitment of β-arrestin2. (2018) submitted

Author contributions: T.L. conceived the project with input from A.B. and G.B.. T.L. performed experiments and data analysis with continuous supervision by A.B. and G.B.. T.L. and G.B. wrote the manuscript.

5.1 Introduction

G protein-coupled receptors are integral membrane proteins responsible for transducing extracellular stimuli across the cellular membrane. This renders them one of the most important classes of drug targets[1]. GPCRs comprise seven transmembrane helices, which rearrange upon agonist binding[2], mainly promoting two different intracellular responses: on one hand, the heterotrimeric G proteins become activated by an exchange of GDP by GTP within their α-subunit, leading to the dissociation of the GPCR/G protein complex into the Gα subunit, the Gβγ dimer and the GPCR[3]. Both constituents of a heterotrimeric G protein (Gα and Gβγ) are then capable of activating different effector proteins such as ACs[3,4], PLCs[5] or ion channels[3,6]. On the other hand, mainly GRKs[7], but also other protein kinases[8], phosphorylate activated GPCRs at their C-terminus and intracellular loop regions[9], resulting in an increased affinity of the activated receptor to β-arrestins[10]. Subsequently, the binding of β-arrestins to phosphorylated receptors facilitates binding of clathrins[11] and associated proteins, leading to the internalization of the GPCR/β-arrestin complex[12]. At the same time, however, this complex can activate its own distinct signalling pathways by means of β-arrestin functioning as a scaffolding protein, bringing e.g. kinases and other proteins, involved in signalling, in close proximity[13-15]. Accordingly, supported by experimental evidence, a new concept with respect to the activation of GPCRs has arisen, which veers away from the classical understanding of a receptor as a simple toggle switch (on/off)[16]. Several GPCR ligands were reported that showed selective activation of one or a bias towards one of the two described signalling pathways[17-21], involving agonist-specific receptor conformations[22]. Therefore, biased agonists are expected to improve pharmacotherapy, e.g. due to reduced adverse drug effects[23,24].

To analyse newly developed ligands with respect to their functionally-selective activation of GPCRs, sensitive techniques are needed. Commercial assays, currently employed to determine β-arrestin recruitment with high throughput, require specialised equipment and/or do not give temporal information about the GPCR/β-arrestin interaction[25]. Split reporter assays, for example, often have readouts either requiring cell lysis[26,27] or the kinetics of the probed protein/protein interaction is masked by

comparatively long maturation times of the functional reporter protein[28]. The TANGO assay measures β-arrestin recruitment by utilising a transcription factor, which is cleaved off a GPCR, when a protease-tagged β-arrestin becomes recruited[25]. Then, the transcription factor triggers the expression of β-lactamase[29]. Therefore, no temporal information about the GPCR/β-arrestin interaction can be obtained and beyond that, the readout is heavily affected by signal amplification. By contrast, tagging β-arrestin with a fluorescent label, allows the analysis of its intracellular distribution over time[30]. This approach delivers unparalleled spatiotemporal information on the GPCR/β-arrestin interaction, provided that either a confocal microscope[30] (limiting throughput) or an expensive high content imager is available[25]. A last, frequently used class of assays is based on resonance energy transfer[31]. Generally, these exhibit excellent temporal resolution, but are often limited in throughput.

We aimed at a technique to quantify of β-arrestin2 recruitment, which can not only be used to construct concentration-response-curves with high throughput, but gives at the same time information on the time course of the GPCR/β-arrestin2 interaction in real time. Furthermore, it should be economical and easily applicable in combination with other luminometric or impedimetric assays for prospective multiparametric measurements. For this purpose, we applied split-luciferase complementation by using the NLuc[32], which exhibits a bright blue light emission (λ_{max} = 460 nm) after addition of the substrate[33]. "Dissection" of the luciferase led to two fragments, strongly differing in size, i.e. one fragment comprising 158 amino acids (NLucN), whereas the other consists of only 11 amino acids (NLucC)[32]. By fusing either one of the two fragments to the C-terminus of the receptor and the complementary one to the N-terminus of β-arrestin2, the GPCR/β-arrestin interaction was probed (cf. Fig. 5.1). Since the presence of such tags alters the natural protein sequence, there might be an influence on overall protein function. Thus, we thoroughly investigated the β-arrestin2 recruitment process in a ligand concentration- and time-dependent manner in case of the hH_1R, $hM_{1,5}R$ and $hNTS_1R$. To identify a possible influence on downstream signalling, we monitored the mobilisation of intracellular Ca^{2+}, provoked by the stimulation of the modified receptors. Furthermore, we analysed, if overexpression of GRK2 has an effect on the β-arrestin2 recruitment process.

5.2 Material & Methods

5.2.1 Materials

The pcDNA3.1 and pcDNA4 vectors were from Thermo Scientific (Nidderau, Germany). Furimazine was from Promega (Mannheim, Germany).

5.2.2 Cell cultivation

Was performed as described under 3.2.2.

5.2.3 Generation of plasmids

The plasmids encoding the luciferase fragments (NlucN, NLucC) were from Promega (Mannheim, Germany). The plasmids used were generated by standard PCR and restriction techniques within the pcDNA backbone. A set of pcDNA4 vectors, which encode the different GPCRs with their C-termini fused either to NLucN, or NLucC, separated by a flexible linker consisting of glycine and serine residues, was prepared. Similarly, two pcDNA3.1 vectors, encoding either NLucN or NLucC, fused to the N-terminus of β-arrestin2, were generated. A cDNA encoding GRK2 was obtained by mRNA isolation from MCF-7 cells and subsequent reverse transcription and was subcloned into pcDNA3.1. All plasmids were quality controlled by means of enzyme restriction analysis and/or colony PCR and sequencing.

5.2.4 Generation of stable transfectants

HEK293T cells seeded on a 6-well plate, were either transfected with 2 µg of the pcDNA3.1 NLucN-β-arrestin2, or of the pcDNA3.1 NLucC-β-arrestin2 vector. After two days of incubation, the cells were detached using trypsin/EDTA, seeded into a 75-cm^2 cell culture flask, and G418 was added at a concentration of 1000 µg/mL. The cells were cultured upon changing the medium at regular intervals until stable growth was observed again. Subsequently, cells were transfected with pcDNA4 vectors, encoding cDNAs of the GPCR fusion proteins (GPCR-NLucC or GPCR-NLucN), in the same way, with the exception that selection was achieved in the presence of zeocin (400 µg/mL).

5.2.5 Characterisation of standard agonists and antagonists using the developed probes

Cells, expressing one of the tagged β-arrestin2 and one of the complementary-tagged GPCRs, were detached from a 75-cm^2 flask by trypsinisation and centrifuged (700 g for 5 min). The pellet was resuspended in assay medium consisting of L-15 with 5% FCS, and the density of the suspension was adjusted to $1.25 \cdot 10^6$ cells/mL. Then, 80 µL of this suspension were seeded into each well of a white 96-well plate, and the plate was incubated at 37 °C in a humidified atmosphere (without additional CO_2) overnight. On the next day, 10 µL of furimazine were added to the cells, and the plate was transferred into a pre-

warmed (37 °C) EnSpire microplate luminescence reader. The cells were allowed to equilibrate inside the reader for 10 min, before the basal luminescence was determined, by recording the luminescence of the entire plate 20 times with an integration time of 100 ms per well. In the meantime, serial dilutions of agonists were prepared, the resulting solutions were also pre-warmed to 37 °C and subsequently added to the cells. Thereafter, luminescence was recorded for 100 plate repeats amounting to a time period of 50 min. Negative controls (solvent) and positive controls (reference full agonist, histamine (hH_1R) and carbachol ($hM_{1,5}R$)) eliciting a maximal response (100%) were included for subsequent normalization of the data. In case of the antagonist mode, antagonists were added 15 min prior to the initial thermal equilibration period to ensure an equilibrium between antagonists and receptors, before agonists were added. The pK_b-values of antagonists were determined according to the Cheng-Prusoff equation[34]. After acquisition, the data was corrected for the baseline drift caused by the flash kinetic of the luciferase reaction by dividing all curves by the one recorded for the solvent control using Prism 5 (Graph Pad, La Jolla, CA, USA). Subsequently, peaks of the obtained time courses were used for the conversion into CRCs. In case of the co-expression of exogenous GRK2, the cells were transfected with 2 µg of pcDNA3.1 GRK2 per well of a 6-well plate two days prior to the experiment.

5.2.6 Fura-2 Ca^{2+} assay

Fura-2 calcium assays were performed as described previously using a LS50 B luminescence spectrophotometer (Perkin-Elmer, Rodgau, Germany)[35]. HEK293T cells, expressing the different combinations of tagged β-arrestin2 and the tagged GPCRs were detached by repeatedly rinsing the culture flask with loading buffer and not by trypsinisation to avoid proteolytic cleavage of the receptors.

5.3 Results and discussion

5.3.1 Assay characteristics

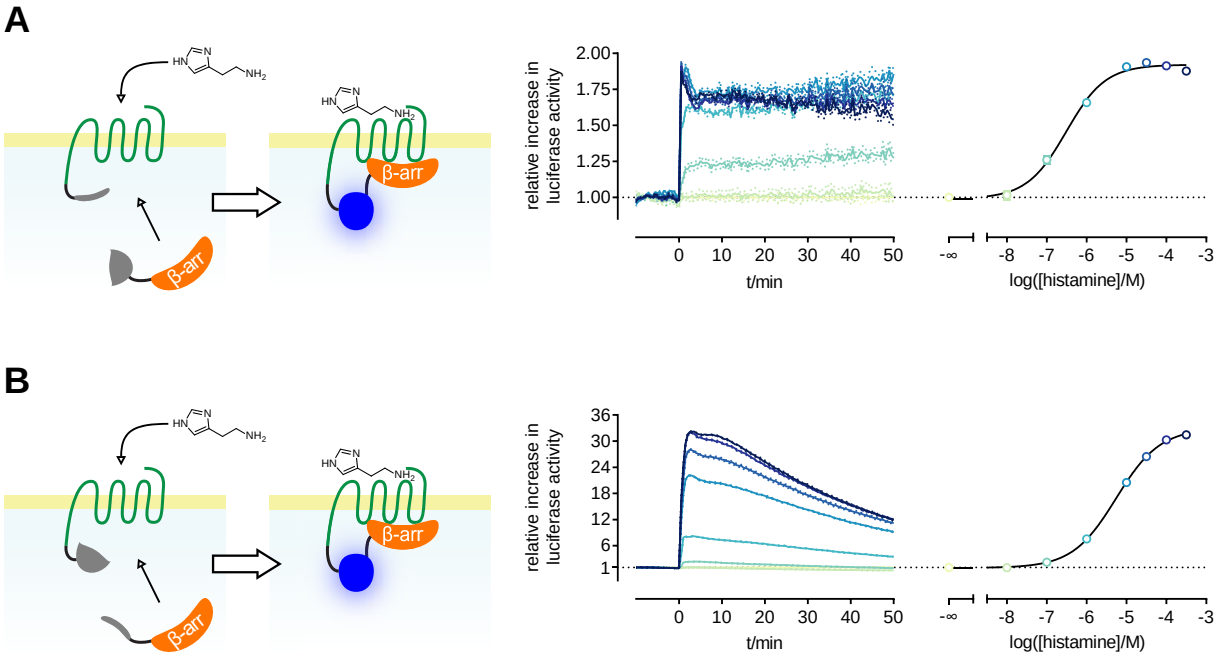

Fig. 5.1: Schematic illustration of the assay principle and exemplary results. HEK293T cells stably expressing the NLucC-tagged hH_1R and NLucN-tagged β-arrestin2 (**A**), or vice versa (**B**), were analysed with respect to their response to histamine using a microplate reader. In case of the NLucC-tagged hH_1R, the S/B ratio is drastically reduced in comparison to the NLucN-tagged receptor. However, the larger tag in case of the latter seems to negatively influence the concentration-dependent response of the receptor. Data are shown as means ± SEM from one representative experiment performed in triplicate of at least seven independent experiments.

Four different GPCRs were genetically modified to generate fusion proteins with either one of the luciferase fragments NLucN, or NLucC fused to the C-terminus of each receptor. In a similar manner, the luciferase fragments were fused to the N-terminus of β-arrestin2. Different cell lines were generated, stably expressing the GPCR fusion protein and the complementary β-arrestin2 fusion protein. The response of the cells to agonist stimulation was detected using a luminescence microplate reader in a time-resolved manner. Representative results for the hH_1R are shown in Fig. 5.1.

The S/B ratio was higher in case of the NLucN-tagged receptor in comparison to the NLucC-tagged receptor, which is the case for all of the

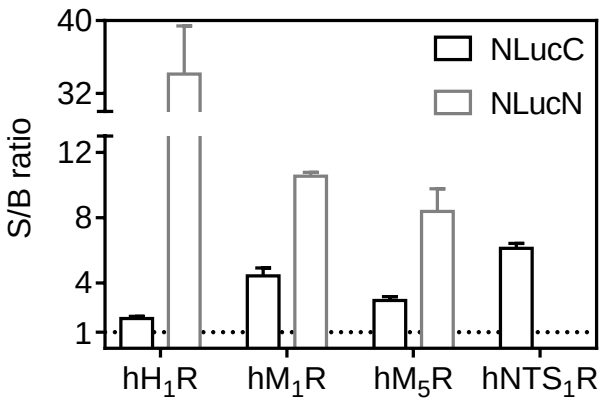

Fig. 5.2: S/B ratios of all analysed receptors with either NLucC, or NLucN fused to their C-termini. HEK293T cells were stably transfected with the indicated receptors and the indicated NLuc fragment fused to their C-termini. Each complementary fragment was fused to the N-terminus of β-arrestin2. The cells were stimulated using either 300 µM histamine (hH_1R), 1 mM carbachol ($hM_{1,5}R$), or 1 µM NT(8-13) ($hNTS_1R$) and the resulting peak response was divided by that of a solvent control. In case of NLucN fused to the C-termini of the receptors the S/B ratios were higher. Data are presented as means ± SEM from at least four independent experiments performed in triplicate.

herein analysed receptors (cf. Fig. 5.2). When comparing the effects provoked by different concentrations of histamine at the different hH_1R fusion proteins, a difference of one order of magnitude becomes obvious.

5.3.2 Influence of the luciferase fragment position on β-arrestin2 recruitment and downstream signalling

We were interested, if the difference in potency (cf. 5.3.1), with respect to the β-arrestin2 recruitment, depending on the C-terminal fusion protein, could also be observed for other receptors and, if the C-terminal modification influences downstream signalling. Therefore, we analysed different standard (cf. Fig. A7) ligands at the hH_1R, the $hM_{1,5}R$ and the $hNTS_1R$ in the developed β-arrestin2 recruitment assay, as well as in the Fura-2-based intracellular Ca^{2+} assay (cf. Fig. 5.3 and Table 5.1).

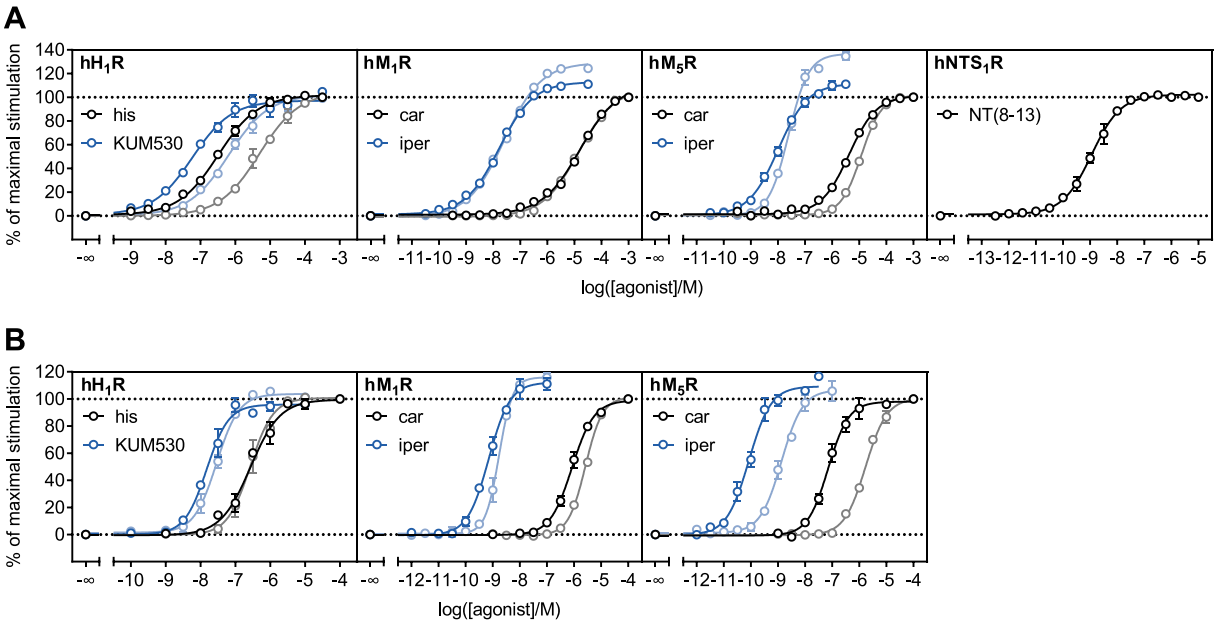

Fig. 5.3: Characterization of standard agonist in the β-arrestin2 recruitment assay (A) and the Fura-2-based intracellular Ca^{2+} assay (B). HEK293T cells, stably expressing the indicated receptor and either NLucC (dark colours), or NLucN (light colours) fused to its C-terminus, as well as the complementary-tagged β-arrestin2 were analysed with respect to β-arrestin2 recruitment (**A**), or the intracellular Ca^{2+} mobilization (**B**) upon agonist stimulation. No clear pattern could be observed, however, when a difference in potency was visible, it was always lower in case of the larger NLucN fragment at the C-terminus of the GPCR. The corresponding pEC_{50} and E_{max} values are given in Table 5.1. Data are presented as means ± SEM from at least three independent experiments.

Whereas β-arrestin2 recruitment to the hH_1R and the hM_5R was affected by the NLucN tag at their C-termini, in case of the hH_1R, no difference in the mobilisation of intracellular Ca^{2+} was observed. The opposite was true for the hM_1R, were β-arrestin2 recruitment seemed not to be negatively influenced by the NLucN tag, but intracellular Ca^{2+} mobilisation was. No general pattern became obvious, however, when a difference between the differentially-tagged receptors was detected, the NLucN tag always negatively affected the potency of the analysed agonists. This was not only true for the reference agonists histamine and carbachol, but also, in a similar order of potency, for UR-KUM530 and iperoxo, respectively. Probably, due to its size, the larger NLucN fragment reduces the affinity of the activated receptor

towards intracellular signalling partners. The fact that the pK_b values of the analysed antagonists were only hardly affected, suggests that the conformation of the receptor in the region of the binding site remains unchanged (cf. Fig. A8 and Table 5.1).

With respect to β-arrestin2 recruitment to the hH_1R, two studies described substantially different potencies for histamine, differing by two orders of magnitude. One study from our group, also using luciferase complementation, but with a different luciferase (firefly-type), reported a pEC_{50} value of 7.74 for histamine[36]. This value is one order of magnitude higher than those obtained by G protein-dependent assays[36,37]. A similar phenomenon was described for UR-KUM530[36]. The higher potencies might be explained by autoaffinity between the two firefly-type luciferase fragments, since, in contrast to the split NLuc system[32], the split firefly-type luciferase system was not optimized. Another study using RLuc-based BRET, a technique in which complementation of enzyme fragments in not involved, and therefore, autoaffinity is not an issue, reported a pEC_{50} for histamine of 5.70[38]. This is on a par with our data described for the hH_1R-NLucN setup. The large size of RLuc, fused to the C-terminus of the hH_1R could be an explanation why the obtained pEC_{50} value is similar to the one we obtained with NLucN fused to the C-terminus of the receptor. Our herein described results for the hH_1R-NLucC setup range in between the literature-described pEC_{50} values with a value of 6.49 ± 0.06. This fits well to data obtained by proximal detection of G protein activation by the GTPase assay[37], but also to data from a luciferase reporter gene assay[36]. Due to the small tag at the C-terminus of the receptor and the similarity of the pEC_{50} values of histamine and UR-KUM530 to the values obtained by G protein-dependent assays, we feel that the hH_1R-NLucC construct resembles the native interaction between hH_1R and β-arrestin2 the most.

At the hM_1R, the pEC_{50} of the β-arrestin2 recruitment for carbachol aligns well with data obtained from a commercially available enzyme complementation assay[39] and a BRET-based determination of β-arrestin2 recruitment[40]. We did not see differences between the two differentially-tagged hM_1R variants, suggesting that β-arrestin2 recruitment to the receptor is not altered by a C-terminal fusion, which is in line with the fact that a hM_1R-RLuc fusion protein[40] delivers a similar potency for carbachol. However, since the intracellular Ca^{2+} mobilisation is negatively influenced by the presence of the larger NLucN tag, the NLucC-tagged receptor should be the better choice.

To the best of our knowledge, no β-arrestin2 recruitment data has been reported for the hM_5R. Our data suggests that the receptor does not tolerate large proteins fused to its C-terminus, since both, the β-arrestin2 recruitment process, and the mobilisation of intracellular Ca^{2+} were negatively influenced, when NLucN was fused to the C-terminus of hM_5R. The fact that the pEC_{50} for carbachol at the NLucC-fused receptor obtained in the Ca^{2+} assay fits very well to data obtained for carbachol at the wildtype receptor in different $G\alpha_q$-dependent assays[5,41], supports the assumption that tagging with NLucC does not impair receptor function.

Iperoxo, originally described as a hM_2R superagonist[42,43], exhibited a higher E_{max} at the hM_1R and the hM_5R with respect to β-arrestin2 recruitment than carbachol. Superagonism or supraphysiological efficacies must be interpreted very carefully, since these effects are usually very small and can also be generated, or masked by signal amplification, which makes proximal readouts, such as the herein analysed β-arrestin2 recruitment, absolutely necessary[44]. Therefore, our data suggest that iperoxo is a superagonist at the hM_1R and the hM_5R also with respect to β-arrestin2 recruitment.

The pEC_{50} value obtained for NT(8-13) at the $hNTS_1R$ is not only in good agreement with data obtained by a proximal $G\alpha_q$ activation assay[5], but also with reported data on β-arrestin2 recruitment by BRET[45]. The latter suggest that the $hNTS_1R$ tolerates larger proteins fused to its C-terminus, too.

Table 5.1: pEC_{50}, E_{max} and pK_b values of the compounds analysed in this study. Data are presented as means ± SEM. *N* denotes the number of independent biological replicates. (N.D.: not determined.)

			β-arrestin2 recruitment				$Ca^{2+}{}_i$ mobilisation		
receptor	**C-terminal tag**	**compound**	**pEC_{50}**	**$\%E_{max}$**	**pK_b**	***N***	**pEC_{50}**	**$\%E_{max}$**	***N***
hH_1R	NLucC	histamine	6.49 ± 0.06	100		7	6.51 ± 0.14	100	3
		UR-KUM530	7.27 ± 0.04	100.6 ± 2.4		4	7.75 ± 0.12	95.5 ± 1.5	3
		mepyramine			8.41 ± 0.15	3			
		diphenhydramine			7.09 ± 0.13	3			
	NLucN	histamine	5.26 ± 0.07	100		8	6.57 ± 0.15	100	4
		UR-KUM530	6.21 ± 0.06	102.4 ± 1.8		4	7.59 ± 0.09	102.1 ± 0.5	4
		mepyramine			8.00 ± 0.09	4			
		diphenhydramine			6.83 ± 0.01	3			
hM_1R	NLucC	carbachol	4.73 ± 0.07	100		10	6.05 ± 0.11	100	3
		iperoxo	7.74 ± 0.04	114.1 ± 1.3		5	9.14 ± 0.07	113.4 ± 3.5	3
		N'-methylscopolamine			8.96 ± 0.07	3			
		atropine			8.73 ± 0.03	3			
	NLucN	carbachol	4.77 ± 0.06	100		10	5.60 ± 0.03	100	3
		iperoxo	7.55 ± 0.04	131.0 ± 2.1		5	8.64 ± 0.21	117.4 ± 3.2	3
		N'-methylscopolamine			9.35 ± 0.04	3			
		atropine			9.00 ± 0.10	4			
hM_5R	NLucC	carbachol	5.37 ± 0.05	100		8	7.14 ± 0.07	100	3
		iperoxo	8.02 ± 0.04	111.8 ± 1.9		6	10.12 ± 0.03	107.5 ± 3.3	3
		N'-methylscopolamine			9.32 ± 0.07	3			
		atropine			9.02 ± 0.04	4			
	NLucN	carbachol	4.92 ± 0.03	100		8	5.73 ± 0.08	100	3
		iperoxo	7.56 ± 0.01	139.2 ± 5.0		6	8.91 ± 0.08	107.9 ± 6	3
		N'-methylscopolamine			9.58 ± 0.03	3			
		atropine			9.24 ± 0.07	4			
$hNTS_1R$	NLucC	NT(8-13)	8.96 ± 0.1	100		8	N.D.	N.D.	
		SR142948A			8.30 ± 0.13	4			

5.3.3 Time course of β-arrestin2 recruitment

Most luciferase-based measurements, especially when split luciferase-based, require cell lysis to ensure sufficiently high luminescence signals for a reliable quantification with a microplate reader. Since the NLuc is, compared to other luciferases, a very bright luciferase[33], live cell measurements are possible. Another advantage of the herein used system is the comparatively fast time period, the luciferase needs for maturation upon association of the two fragments and that their interaction is fully reversible[32], allowing measurements in real time.

With respect to β-arrestin recruitment, GPCRs can be categorised into class A and class B receptors[46], based on the duration of the interaction between receptor and β-arrestin[47]. Short interaction times (class A) lead to a rapid recycling of the receptor back to the cellular membrane[48], whereas long interaction times (class B) promote the degradation of the receptor[49]. The herein analysed receptors belong to both classes as becomes obvious by the time course of the receptor/β-arrestin2 interaction shown in Fig. 5.4 for the NLucC-fused receptors. The receptors hH_1R, hM_1R and hM_5R behave as class A receptors, showing a rapid peak response of the interaction immediately after agonist addition, followed by a fast decline, interpreted as receptor recycling[30]. The $hNTS_1R$, however, shows a rapid onset of interaction, reaching a plateau approx. after. 2 min, which is maintained over the entire time period analysed. This is in line with other reports on this receptor[9] and indicates sustained GPCR/β-arrestin2 interaction preventing receptor recycling[50].

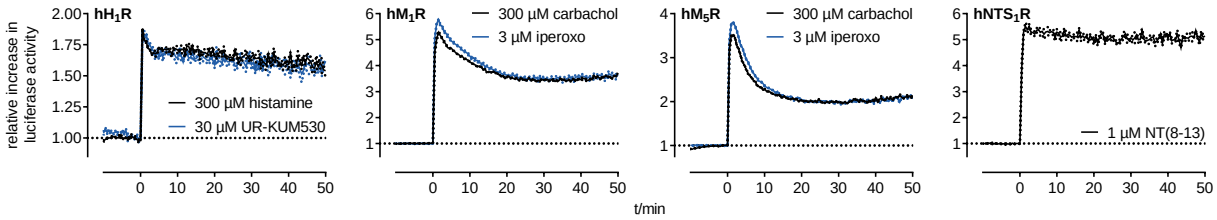

Fig. 5.4: Time course of the GPCR-NLucC/NLucN-β-arrestin2 interaction. HEK293T cells, stably co-expressing the indicated receptor and NLucC fused to its C-terminus, as well as the complementary-tagged β-arrestin2 were analysed with respect to the time-dependency of β-arrestin2 recruitment. Each indicated agonist was added at time point zero. The data was baseline-corrected for a solvent control. Whereas the hH_1R and the $hM_{1,5}R$ show a peak in receptor/β-arrestin2 interaction shortly after agonist addition followed by a rapid dissociation, presumably due to receptor recycling to the membrane, the interaction between the $hNTS_1R$ and β-arrestin2 is stable over the whole time period. Data are representative of at least four independent experiments, each performed in triplicate.

5.3.4 Influence of exogenous GRK2 co-expression on β-arrestin2 recruitment

Since GRKs are responsible for receptor phosphorylation, which is a prerequisite for β-arrestin recruitment[10], we analysed if a co-expression of exogenous GRK influences the β-arrestin2 recruitment process. We transfected the stable transfectants, described under 5.2.4, expressing the differentially-tagged receptor and β-arrestin fusion proteins, with a plasmid encoding GRK2, because this kinase was shown to have a broad substrate specificity among GPCRs[7,51]. Furthermore, GRK2 is known to interact with $G\alpha_q$[52], which is the canonical Gα subtype of all receptors analysed herein. The response of the cells to the

respective reference agonist was determined in comparison to control cells, devoid of GRK2 overexpression. As displayed in Fig. 5.5, no or only very minor differences were observed, when the kinase was co-expressed, which suggests that endogenous GRK expression in the HEK293T cells is sufficient to ensure β-arrestin recruitment.

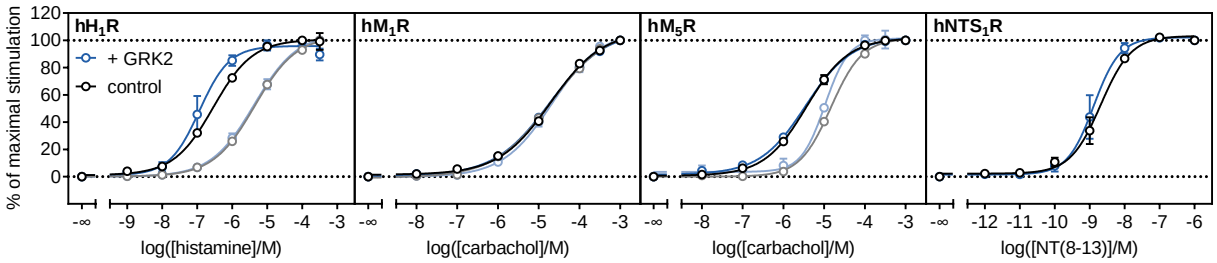

Fig. 5.5: Influence of exogenous GRK2 co-expression on β-arrestin2 recruitment. HEK293T cells, stably co-expressing the indicated receptor and either NLucC (dark colors), or NLucN (light colors) fused to its C-terminus, as well as the complementary-tagged β-arrestin2 were analysed with respect to the influence of co-expression of exogenous GRK2. The overexpression of GRK2 did not, or only very minorly, alter the potency of the analysed ligands. Data are presented as means ± SEM from at least three independent experiments, each performed in triplicate.

5.4 Conclusion

We developed a split luciferase-based β-arrestin2 recruitment assay for the hH_1R, $hM_{1,5}R$ and $hNTS_1R$, applicable in live HEK293T cells. Despite lower S/B ratios, the combination of GPCR-NLucC/NLucN-β-arrestin2 proved superior to the GPCR-NLucN/NLucC-β-arrestin2 combination: the larger NLucN, fused to the C-terminus, negatively influenced the function of several receptors, becoming apparent not only when β-arrestin2 recruitment was analysed, but also on the second messenger level. Therefore, solely focusing on S/B ratios in the initial phase of the development of split luciferase assays, as often practiced[53-55], might lead to assays, which do not reflect the physiological behaviour of the analysed proteins anymore. The assay based on GPCR-NLucC was proven to be useful for determining ligand potencies and efficacies, and was sensitive enough to identify iperoxo as a putative superagonist at the hM_1R and the hM_5R with respect to β-arrestin2 recruitment. We further demonstrated that temporal analyses of the receptor/β-arrestin2 interaction can be performed to e.g. discriminate between receptors that only transiently interact with arrestins after activation, presumably because they recycle to the plasma membrane very fast, and those that show sustained interaction. The assay principle should be broadly applicable to other GPCRs, and, due to the high sensitivity and the very proximal readout, our assay can be of high value for the identification of biased agonists, e.g. in multiparametric assays.

5.5 References

1 Hauser, A. S., Attwood, M. M., Rask-Andersen, M., Schiöth, H. B. & Gloriam, D. E. Trends in GPCR drug discovery: new agents, targets and indications. *Nat Rev Drug Discov* **16**, 829-842, doi:10.1038/nrd.2017.178 (2017).

2 Rasmussen, S. G., DeVree, B. T., Zou, Y., Kruse, A. C., Chung, K. Y., Kobilka, T. S., Thian, F. S., Chae, P. S., Pardon, E., Calinski, D., Mathiesen, J. M., Shah, S. T., Lyons, J. A., Caffrey, M., Gellman, S. H., Steyaert, J., Skiniotis, G., Weis, W. I., Sunahara, R. K. & Kobilka, B. K. Crystal structure of the β_2 adrenergic receptor-G_s protein complex. *Nature* **477**, 549-555, doi:10.1038/nature10361 (2011).

3 Hilger, D., Masureel, M. & Kobilka, B. K. Structure and dynamics of GPCR signaling complexes. *Nat Struct Mol Biol* **25**, 4-12, doi:10.1038/s41594-017-0011-7 (2018).

4 Sadana, R., Dascal, N. & Dessauer, C. W. N terminus of type 5 adenylyl cyclase scaffolds G_s heterotrimer. *Mol Pharmacol* **76**, 1256-1264, doi:10.1124/mol.109.058370 (2009).

5 Littmann, T., Ozawa, T., Hoffmann, C., Buschauer, A. & Bernhardt, G. A split luciferase-based probe for quantitative proximal determination of $G\alpha_q$ signalling in live cells. *Sci Rep* **8**, 17179, doi:10.1038/s41598-018-35615-w (2018).

6 Hommers, L. G., Lohse, M. J. & Bünemann, M. Regulation of the inward rectifying properties of G-protein-activated inwardly rectifying K^+ (GIRK) channels by Gβγ subunits. *J Biol Chem* **278**, 1037-1043, doi:10.1074/jbc.M205325200 (2003).

7 Inagaki, S., Ghirlando, R., Vishnivetskiy, S. A., Homan, K. T., White, J. F., Tesmer, J. J., Gurevich, V. V. & Grisshammer, R. G Protein-Coupled Receptor Kinase 2 (GRK2) and 5 (GRK5) Exhibit Selective Phosphorylation of the Neurotensin Receptor in Vitro. *Biochemistry* **54**, 4320-4329, doi:10.1021/acs.biochem.5b00285 (2015).

8 Yang, Z., Yang, F., Zhang, D., Liu, Z., Lin, A., Liu, C., Xiao, P., Yu, X. & Sun, J. P. Phosphorylation of G Protein-Coupled Receptors: From the Barcode Hypothesis to the Flute Model. *Mol Pharmacol* **92**, 201-210, doi:10.1124/mol.116.107839 (2017).

9 Oakley, R. H., Laporte, S. A., Holt, J. A., Barak, L. S. & Caron, M. G. Molecular determinants underlying the formation of stable intracellular G protein-coupled receptor-β-arrestin complexes after receptor endocytosis. *J Biol Chem* **276**, 19452-19460, doi:10.1074/jbc.M101450200 (2001).

10 Lohse, M. J., Benovic, J. L., Codina, J., Caron, M. G. & Lefkowitz, R. J. β-Arrestin: a protein that regulates β-adrenergic receptor function. *Science* **248**, 1547-1550 (1990).

11 Goodman, O. B., Jr., Krupnick, J. G., Santini, F., Gurevich, V. V., Penn, R. B., Gagnon, A. W., Keen, J. H. & Benovic, J. L. β-Arrestin acts as a clathrin adaptor in endocytosis of the β_2-adrenergic receptor. *Nature* **383**, 447-450, doi:10.1038/383447a0 (1996).

12 Ferguson, S. S., Downey, W. E., 3rd, Colapietro, A. M., Barak, L. S., Ménard, L. & Caron, M. G. Role of β-arrestin in mediating agonist-promoted G protein-coupled receptor internalization. *Science* **271**, 363-366 (1996).

13 Luttrell, L. M., Ferguson, S. S. G., Daaka, Y., Miller, W. E., Maudsley, S., Della Rocca, G. J., Lin, F. T., Kawakatsu, H., Owada, K., Luttrell, D. K., Caron, M. G. & Lefkowitz, R. J. β-Arrestin-Dependent Formation of β_2-Adrenergic Receptor-Src Protein Kinase Complexes. *Science* **283**, 655-661, doi:10.1126/science.283.5402.655 (1999).

14 Shenoy, S. K., Drake, M. T., Nelson, C. D., Houtz, D. A., Xiao, K., Madabushi, S., Reiter, E., Premont, R. T., Lichtarge, O. & Lefkowitz, R. J. β-Arrestin-dependent, G protein-independent ERK1/2 activation by the β_2 adrenergic receptor. *J Biol Chem* **281**, 1261-1273, doi:10.1074/jbc.M506576200 (2006).

15 Shukla, A. K., Xiao, K. & Lefkowitz, R. J. Emerging paradigms of β-arrestin-dependent seven transmembrane receptor signaling. *Trends Biochem Sci* **36**, 457-469, doi:10.1016/j.tibs.2011.06.003 (2011).

16 Seifert, R. Functional selectivity of G-protein-coupled receptors: from recombinant systems to native human cells. *Biochem Pharmacol* **86**, 853-861, doi:10.1016/j.bcp.2013.07.029 (2013).

17 Wacker, D., Wang, C., Katritch, V., Han, G. W., Huang, X. P., Vardy, E., McCorvy, J. D., Jiang, Y., Chu, M., Siu, F. Y., Liu, W., Xu, H. E., Cherezov, V., Roth, B. L. & Stevens, R. C. Structural features for functional selectivity at serotonin receptors. *Science* **340**, 615-619, doi:10.1126/science.1232808 (2013).

18 Reinartz, M. T., Kälble, S., Littmann, T., Ozawa, T., Dove, S., Kaever, V., Wainer, I. W. & Seifert, R. Structure-bias relationships for fenoterol stereoisomers in six molecular and cellular assays at the β_2-adrenoceptor. *Naunyn Schmiedebergs Arch Pharmacol* **388**, 51-65, doi:10.1007/s00210-014-1054-5 (2015).

19 White, K. L., Scopton, A. P., Rives, M. L., Bikbulatov, R. V., Polepally, P. R., Brown, P. J., Kenakin, T., Javitch, J. A., Zjawiony, J. K. & Roth, B. L. Identification of novel functionally selective κ-opioid receptor scaffolds. *Mol Pharmacol* **85**, 83-90, doi:10.1124/mol.113.089649 (2014).

20 Patel, C. B., Noor, N. & Rockman, H. A. Functional selectivity in adrenergic and angiotensin signaling systems. *Mol Pharmacol* **78**, 983-992, doi:10.1124/mol.110.067066 (2010).

21 Manglik, A., Lin, H., Aryal, D. K., McCorvy, J. D., Dengler, D., Corder, G., Levit, A., Kling, R. C., Bernat, V., Hübner, H., Huang, X. P., Sassano, M. F., Giguere, P. M., Löber, S., Da, D., Scherrer, G., Kobilka, B. K., Gmeiner, P., Roth, B. L. & Shoichet, B. K. Structure-based discovery of opioid analgesics with reduced side effects. *Nature* **537**, 185-190, doi:10.1038/nature19112 (2016).

22 Correll, C. C. & McKittrick, B. A. Biased ligand modulation of seven transmembrane receptors (7TMRs): functional implications for drug discovery. *J Med Chem* **57**, 6887-6896, doi:10.1021/jm401677g (2014).

23 Michel, M. C. & Charlton, S. J. Biased agonism in drug discovery - is it too soon to choose a path? *Mol Pharmacol* **93**, 259-265, doi:10.1124/mol.117.110890 (2018).

24 Rankovic, Z., Brust, T. F. & Bohn, L. M. Biased agonism: An emerging paradigm in GPCR drug discovery. *Bioorg Med Chem Lett* **26**, 241-250, doi:10.1016/j.bmcl.2015.12.024 (2016).

25 Zhang, R. & Xie, X. Tools for GPCR drug discovery. *Acta Pharmacol Sin* **33**, 372-384, doi:10.1038/aps.2011.173 (2012).

26 Misawa, N., Kafi, A. K., Hattori, M., Miura, K., Masuda, K. & Ozawa, T. Rapid and high-sensitivity cell-based assays of protein-protein interactions using split click beetle luciferase complementation: an approach to the study of G-protein-coupled receptors. *Anal Chem* **82**, 2552-2560, doi:10.1021/ac100104q (2010).

27 Hübner, H., Schellhorn, T., Gienger, M., Schaab, C., Kaindl, J., Leeb, L., Clark, T., Möller, D. & Gmeiner, P. Structure-guided development of heterodimer-selective GPCR ligands. *Nat Commun* **7**, 12298, doi:10.1038/ncomms12298 (2016).

28 Song, Y. B., Park, C. O., Jeong, J. Y. & Huh, W. K. Monitoring G protein-coupled receptor activation using an adenovirus-based β-arrestin bimolecular fluorescence complementation assay. *Anal Biochem* **449**, 32-41, doi:10.1016/j.ab.2013.12.017 (2014).

29 Dogra, S., Sona, C., Kumar, A. & Yadav, P. N. Tango assay for ligand-induced GPCR-β-arrestin2 interaction: Application in drug discovery. *Methods Cell Biol* **132**, 233-254, doi:10.1016/bs.mcb.2015.11.001 (2016).

30 Oakley, R. H., Laporte, S. A., Holt, J. A., Barak, L. S. & Caron, M. G. Association of β-arrestin with G protein-coupled receptors during clathrin-mediated endocytosis dictates the profile of receptor resensitization. *J Biol Chem* **274**, 32248-32257 (1999).

31 Lohse, M. J., Nuber, S. & Hoffmann, C. Fluorescence/bioluminescence resonance energy transfer techniques to study G-protein-coupled receptor activation and signaling. *Pharmacol Rev* **64**, 299-336, doi:10.1124/pr.110.004309 (2012).

32 Dixon, A. S., Schwinn, M. K., Hall, M. P., Zimmerman, K., Otto, P., Lubben, T. H., Butler, B. L., Binkowski, B. F., Machleidt, T., Kirkland, T. A., Wood, M. G., Eggers, C. T., Encell, L. P. & Wood, K. V. NanoLuc Complementation Reporter Optimized for Accurate Measurement of Protein Interactions in Cells. *ACS Chem Biol* **11**, 400-408, doi:10.1021/acschembio.5b00753 (2016).

33 Hall, M. P., Unch, J., Binkowski, B. F., Valley, M. P., Butler, B. L., Wood, M. G., Otto, P., Zimmerman, K., Vidugiris, G., Machleidt, T., Robers, M. B., Benink, H. A., Eggers, C. T., Slater, M. R., Meisenheimer, P. L., Klaubert, D. H., Fan, F., Encell, L. P. & Wood, K. V. Engineered luciferase reporter from a deep sea shrimp utilizing a novel imidazopyrazinone substrate. *ACS Chem Biol* **7**, 1848-1857, doi:10.1021/cb3002478 (2012).

34 Cheng, Y. & Prusoff, W. H. Relationship between the inhibition constant (K_1) and the concentration of inhibitor which causes 50 per cent inhibition (I_{50}) of an enzymatic reaction. *Biochem Pharmacol* **22**, 3099-3108 (1973).

35 Müller, M., Knieps, S., Gessele, K., Dove, S., Bernhardt, G. & Buschauer, A. Synthesis and neuropeptide Y Y_1 receptor antagonistic activity of *N*,*N*-disubstituted ω-guanidino- and ω-aminoalkanoic acid amides. *Arch Pharm (Weinheim)* **330**, 333-342 (1997).

36 Lieb, S., Littmann, T., Plank, N., Felixberger, J., Tanaka, M., Schäfer, T., Krief, S., Elz, S., Friedland, K., Bernhardt, G., Wegener, J., Ozawa, T. & Buschauer, A. Label-free versus conventional cellular assays: Functional investigations on the human histamine H_1 receptor. *Pharmacol Res* **114**, 13-26, doi:10.1016/j.phrs.2016.10.010 (2016).

37 Strasser, A., Wittmann, H. J., Kunze, M., Elz, S. & Seifert, R. Molecular basis for the selective interaction of synthetic agonists with the human histamine H_1-receptor compared with the guinea pig H_1-receptor. *Mol Pharmacol* **75**, 454-465, doi:10.1124/mol.108.053009 (2009).

38 Bosma, R., Moritani, R., Leurs, R. & Vischer, H. F. BRET-based β-arrestin2 recruitment to the histamine H_1 receptor for investigating antihistamine binding kinetics. *Pharmacol Res* **111**, 679-687, doi:10.1016/j.phrs.2016.07.034 (2016).

39 Digby, G. J., Noetzel, M. J., Bubser, M., Utley, T. J., Walker, A. G., Byun, N. E., Lebois, E. P., Xiang, Z., Sheffler, D. J., Cho, H. P., Davis, A. A., Nemirovsky, N. E., Mennenga, S. E., Camp, B. W., Bimonte-Nelson, H. A., Bode, J., Italiano, K., Morrison, R., Daniels, J. S., Niswender, C. M., Olive, M. F., Lindsley, C. W., Jones, C. K. & Conn, P. J. Novel allosteric agonists of M_1 muscarinic acetylcholine receptors induce brain region-specific responses that correspond with behavioral effects in animal models. *J Neurosci* **32**, 8532-8544, doi:10.1523/JNEUROSCI.0337-12.2012 (2012).

40 Yeatman, H. R., Lane, J. R., Choy, K. H., Lambert, N. A., Sexton, P. M., Christopoulos, A. & Canals, M. Allosteric modulation of M_1 muscarinic acetylcholine receptor internalization and subcellular trafficking. *J Biol Chem* **289**, 15856-15866, doi:10.1074/jbc.M113.536672 (2014).

41 Bräuner-Osborne, H. & Brann, M. R. Pharmacology of muscarinic acetylcholine receptor subtypes (m1-m5): high throughput assays in mammalian cells. *Eur J Pharmacol* **295**, 93-102 (1996).

42 Kruse, A. C., Ring, A. M., Manglik, A., Hu, J., Hu, K., Eitel, K., Hübner, H., Pardon, E., Valant, C., Sexton, P. M., Christopoulos, A., Felder, C. C., Gmeiner, P., Steyaert, J., Weis, W. I., Garcia, K. C., Wess, J. & Kobilka, B. K. Activation and allosteric modulation of a muscarinic acetylcholine receptor. *Nature* **504**, 101-106, doi:10.1038/nature12735 (2013).

43 Schrage, R., Seemann, W. K., Klöckner, J., Dallanoce, C., Racke, K., Kostenis, E., De Amici, M., Holzgrabe, U. & Mohr, K. Agonists with supraphysiological efficacy at the muscarinic M_2 ACh receptor. *Br J Pharmacol* **169**, 357-370, doi:10.1111/bph.12003 (2013).

44 Schrage, R., De Min, A., Hochheiser, K., Kostenis, E. & Mohr, K. Superagonism at G protein-coupled receptors and beyond. *Br J Pharmacol* **173**, 3018-3027, doi:10.1111/bph.13278 (2016).

45 Besserer-Offroy, E., Brouillette, R. L., Lavenus, S., Froehlich, U., Brumwell, A., Murza, A., Longpré, J. M., Marsault, E., Grandbois, M., Sarret, P. & Leduc, R. The signaling signature of the neurotensin type 1 receptor with endogenous ligands. *Eur J Pharmacol* **805**, 1-13, doi:10.1016/j.ejphar.2017.03.046 (2017).

46 Kendall, R. T. & Luttrell, L. M. Diversity in arrestin function. *Cell Mol Life Sci* **66**, 2953-2973, doi:10.1007/s00018-009-0088-1 (2009).

47 Oakley, R. H., Laporte, S. A., Holt, J. A., Caron, M. G. & Barak, L. S. Differential affinities of visual arrestin, β-arrestin1, and β-arrestin2 for G protein-coupled receptors delineate two major classes of receptors. *J Biol Chem* **275**, 17201-17210, doi:10.1074/jbc.M910348199 (2000).

48 Takenouchi, O., Yoshimura, H. & Ozawa, T. Unique Roles of β-Arrestin in GPCR Trafficking Revealed by Photoinducible Dimerizers. *Sci Rep* **8**, 677, doi:10.1038/s41598-017-19130-y (2018).

49 Martin, N. P., Lefkowitz, R. J. & Shenoy, S. K. Regulation of V2 vasopressin receptor degradation by agonist-promoted ubiquitination. *J Biol Chem* **278**, 45954-45959, doi:10.1074/jbc.M308285200 (2003).

50 Zhang, J., Barak, L. S., Anborgh, P. H., Laporte, S. A., Caron, M. G. & Ferguson, S. S. Cellular trafficking of G protein-coupled receptor/β-arrestin endocytic complexes. *J Biol Chem* **274**, 10999-11006 (1999).

51 Li, L., Homan, K. T., Vishnivetskiy, S. A., Manglik, A., Tesmer, J. J., Gurevich, V. V. & Gurevich, E. V. G Protein-coupled Receptor Kinases of the GRK4 Protein Subfamily Phosphorylate Inactive G Protein-coupled Receptors (GPCRs). *J Biol Chem* **290**, 10775-10790, doi:10.1074/jbc.M115.644773 (2015).

52 Tesmer, V. M., Kawano, T., Shankaranarayanan, A., Kozasa, T. & Tesmer, J. J. Snapshot of activated G proteins at the membrane: the $G\alpha_q$-GRK2-Gβγ complex. *Science* **310**, 1686-1690, doi:10.1126/science.1118890 (2005).

53 Deng, Q., Wang, D., Xiang, X., Gao, X., Hardwidge, P. R., Kaushik, R. S., Wolff, T., Chakravarty, S. & Li, F. Application of a split luciferase complementation assay for the detection of viral protein-protein interactions. *J Virol Methods* **176**, 108-111, doi:10.1016/j.jviromet.2011.04.028 (2011).

54 Cannaert, A., Storme, J., Franz, F., Auwärter, V. & Stove, C. P. Detection and Activity Profiling of Synthetic Cannabinoids and Their Metabolites with a Newly Developed Bioassay. *Anal Chem* **88**, 11476-11485, doi:10.1021/acs.analchem.6b02600 (2016).

55 Cannaert, A., Vasudevan, L., Friscia, M., Mohr, A. L. A., Wille, S. M. R. & Stove, C. P. Activity-Based Concept to Screen Biological Matrices for Opiates and (Synthetic) Opioids. *Clin Chem* **64**, 1221-1229, doi:10.1373/clinchem.2018.289496 (2018).

6. Simultaneous quantification of G protein activation and β-arrestin2 recruitment

6.1 Introduction

The determination of agonist bias between Gα- and β-arrestin-dependent signalling at GPCRs becomes increasingly important, since biased drugs are expected to perform superior in pharmacotherapy, e.g. due to reduction of adverse drug effects[1,2]. In addition, several receptors were found to have different endogenous agonists, thereby exhibiting natural biased agonism[3-7].

Currently, the analysis of agonist bias comprises the application of two different assay systems[2,8,9]. In most cases, this is accompanied by the use of different receptor sources (i.e. intact cells, membranes), which can not only drastically differ in the level of receptor expression, but also in the abundance of signalling proteins involved in GPCR-dependent signalling cascades[10,11]. Several reports described that such differences are responsible for discrepancies in potency and/or efficacy of the analysed agonists[12-15]. Therefore, results obtained from such assays can mistakenly be interpreted as agonist bias[8].

Furthermore, $G\alpha_q$ activation is frequently assessed downstream on the second messenger level by measuring IP_3 formation[16-18] or Ca^{2+} influx[19-21] into the cytosol, whereas the recruitment of β-arrestin is determined by directly measuring its interaction with the GPCR[4,22-24]. However, in a comparison of rather distal second messenger data, which can be effected by signal amplification[25], with proximal results from β-arrestin recruitment assays, the G protein-dependent pathway can be overrepresented, since the amplification can lead to apparently increased potencies and/or efficacies[25].

A proximal determination of $G\alpha_q$ activation is generally favourable, but as mentioned in chapter 3, suitable techniques for proximal determinations are often compromised by e.g. the requirement of cell lysis ([^{35}S]-GTPγS incorporation assay[26,27]) or a limited throughput (FRET[28]- and BRET[29,30]-based methods). In lysis-based methods, the absent membrane potential can influence receptor function, as shown, e.g. for the α_{2A} adrenoceptor, the activation of which is altered by changes in the membrane potential[31]. This can again be misleading, when comparing results from lysis-based methods with results from β-arrestin recruitment assays, in which agonist stimulation, if not the entire measurement, is usually performed with intact cells[24,32-35].

Taken together, these shortcomings can lead to significant misinterpretations in the determination of agonist bias between $G\alpha_q$ activation and β-arrestin recruitment. Therefore, aiming at a technique for a more robust determination of agonist bias between the two pathways in live cells, a multiparametric assay was developed, which also decreases the time needed for the measurement. The independently developed and characterised methods described in chapters 3[36] and 5 were combined in a single assay (cf. Fig. 6.1). Both assays were designed with a potential multiparametric application in mind, which determined the selection of the luciferases. The red light-emitting CBR[37] (λ_{max} = 613 nm) was chosen for the $G\alpha_q$ activation sensor and the blue light-emitting NLuc[38] (λ_{max} = 460 nm) was used to measure β-arrestin recruitment, in order to have a maximal difference between the emission spectra of the luciferases. By applying appropriate optical filters, a discrimination between the two luciferases, expressed in the same cell population, was achieved.

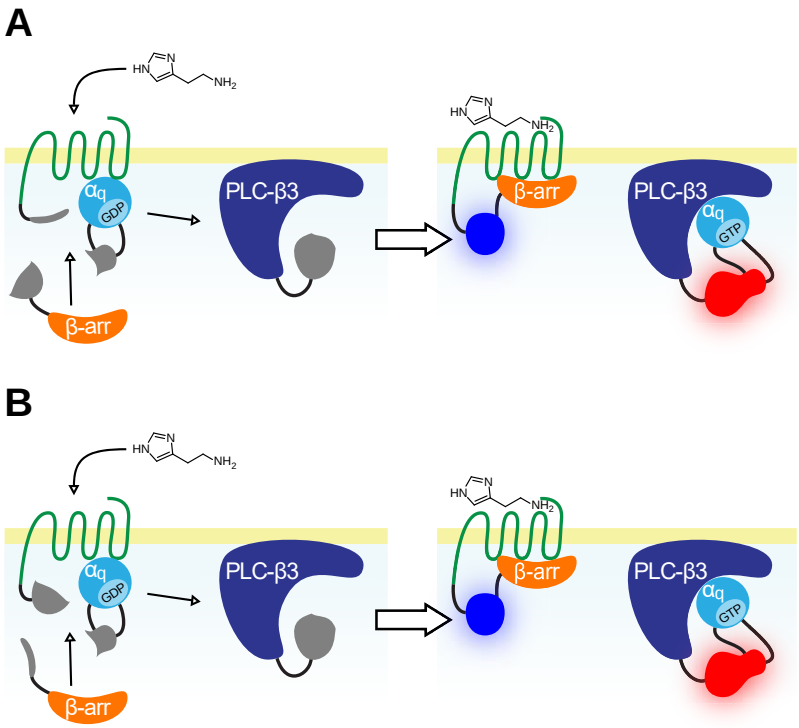

Fig. 6.1: Schematic illustration of the two employed assay setups. Multiparametric determination of $G\alpha_q$ activation and β-arrestin2 recruitment was achieved by co-expressing the $G\alpha_q$/PLC-β3 probe together with either the GPCR-NLucC/NLucN-β-arrestin2-based (**A**), or with the GPCR-NLucN/NLucC-β-arrestin2-based (**B**) assay for assessing β-arrestin recruitment in the same HEK293T cell population.

Results from the multiparametric approach were obtained from the exact same receptor-expressing cell population, and both readouts originated from a comparable proximal stage within each signalling cascade. The two developed sensors were stably co-expressed in HEK293T cells, activated through the hH_1R, the hM_1R, the hM_5R and the $hNTS_1R$. Different standard ligands were characterised in the multiparametric assay with respect to their potencies and efficacies or antagonistic activities.

6.2 Materials & Methods

6.2.1 Materials

Please refer to 3.2.1 and 5.2.1.

6.2.2 Cell cultivation

Was performed as described under 3.2.2.

6.2.3 Generation of stable transfectants

The, in chapter 5 described, HEK293T cells, developed for the NLuc complementation-based detection of β-arrestin2 recruitment, were stably co-transfected with the pIRESpuro3 CBRN-PLC-β3-2A-Gα_q(123) vector (chapter 3[36]). Transfection and subsequent selection using puromycin (1 µg/mL) was carried out as described in chapter 3[36].

6.2.4 Determination of spectral cross-talk

Discrimination between the two luciferases was achieved by applying a 610 nm long-pass (610 LP) filter for the red light-emitting CBR of the Gα_q-PLC-β3 sensor and a 460/50 nm band-pass (460/50 BP) filter for the β-arrestin2 recruitment probe. In order to determine the spectral bleed-through of one luciferase into the other channel, experiments were performed in which only one of the luciferases was present. The monoparametric assays, described in chapters 3[36] and 5, were separately conducted, and luminescence was quantified through both filters. Afterwards, the amount of light detected from the CBR luciferase in the Gα_q/PLC-β3 probe through the 460/50 BP filter was divided by that of the 610 LP filter. For the NLuc-based β-arrestin2 sensor this was done vice versa.

6.2.5 Quantification of agonistic potencies and antagonistic activities in the developed multiparametric assay

Cells, expressing the Gα_q-PLC-β3 sensor in combination with one of the GPCR/β-arrestin2 recruitment sensors, were detached from a 75-cm^2 flask by trypsinisation and centrifuged (700 g for 5 min). The pellet was resuspended in assay medium, consisting of L-15 with 5% FCS, and the density of the suspension was adjusted to 1.25 · 10^6 cells/mL. Then, 80 µL of this suspension were seeded into each well of a white 96-well plate, and the plate was incubated at 37 °C in a humidified atmosphere (without additional CO_2) overnight. On the next day, 10 µL of a mixture of 10 mM D-luciferin (Pierce) and furimazine were added to the cells, and the plate was transferred into a pre-warmed microplate luminescence reader (Genios Pro). The cells were allowed to equilibrate inside the reader for 10 min, before the basal luminescence was measured, by recording the luminescence for the entire plate eight times. Luminescence was quantified through both filters for 500 ms each, before the next well was analysed. In the meantime, serial

dilutions of agonists were prepared, the resulting solutions were also pre-warmed to 37 °C and subsequently added to the cells. Thereafter, luminescence was recorded for 20 plate repeats amounting to a time period of 50 min. Negative controls (solvent) and positive controls (reference full agonist, histamine (hH_1R), carbachol ($hM_{1,5}R$)) eliciting a maximal response (100%) were included for subsequent normalization of the data. In case of the antagonist mode, antagonists were added 15 min prior to the initial thermal equilibration period to ensure an equilibrium between antagonists and receptors, before agonists were added. The pK_b-values of antagonists were determined according to the Cheng-Prusoff equation[39].

6.3 Results and discussion

6.3.1 Spectral cross-talk

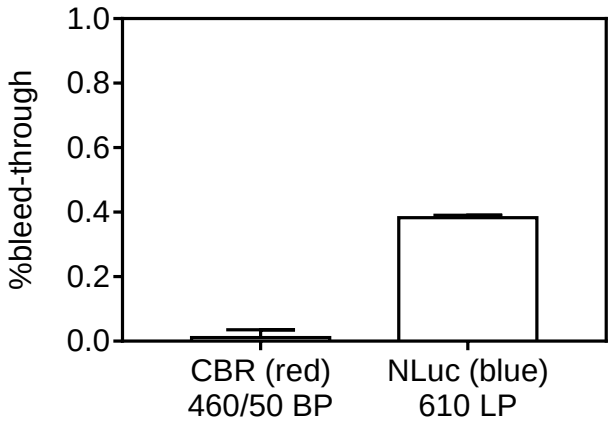

Fig. 6.2: Spectral bleed-through determined for CBR and NLuc through the respective other filter. The CBR-based $G\alpha_q$/PLC-β3 probe and the NLuc-based β-arrestin2 recruitment sensor were analysed separately and their luminescence was detected through a 460/50 BP filter and a 610 LP filter. Luminescence emitted from CBR was exclusively detected through the 610 LP filter, whereas a very small amount (0.4%) of luminescence from the NLuc was detected through the 610 LP filter. Data represent means ± SEM from three wells over 25 cycles each.

Optical filters were employed to discriminate between the two luciferases (CBR: 610 LP, NLuc: 460/50 BP). Although the luciferases were chosen based on their large difference in λ_{max}, luciferases exhibit rather broad emission spectra[37]. Therefore, spectral bleed-through might be observed. By conducting the assays described in chapters 3[36] and 5 separately and detecting the emitted luminescence through both filters, this cross-talk was determined. Fig. 6.2 shows that no bleed-through was detected from the CBR luciferase used in the $G\alpha_q$/PLC-β3 probe through the 460/50 BP filter and only very small cross-talk (0.4%) was determined from the NLuc, employed in the β-arrestin2 recruitment sensor, through the 610 LP filter. Since the intensities of the two probes in the multiparametric assay were expected to be on a similar level, no calculations to correct for the small NLuc bleed-through were necessary.

6.3.2 Characteristics of the multiparametric assay

Two approaches were pursued for the multiparametric assay by applying the β-arrestin2 recruitment assay in both setups, similar to chapter 5. Each receptor, except for the $hNTS_1R$, was C-terminally either tagged with NLucC, or NLucN and β-arrestin2 with the corresponding complementing luciferase fragment. The agonist concentration-dependent response and S/B ratios of the two co-expressed sensors were analysed using the reference agonists histamine (hH_1R), carbachol ($hM_{1,5}R$) and NT(8-13) ($hNTS_1R$).

At the hH_1R, increasing concentrations of histamine led to a gradual increase in luminescence of both sensors (cf. Fig. 6.3), except for the setup, in which the hH_1R-NLucC/NLucN-β-arrestin2 combination was used to probe β-arrestin2 recruitment (Fig. 6.3A). This combination of NLuc fusion proteins already showed the lowest S/B ratio, when analysed alone (cf. Fig. 5.2), barely reaching a two-fold increase in luminescence upon stimulation with histamine. Presumably, by using the band-pass filter for the detection, decreasing sensitivity, the small increase in the signal cannot be resolved anymore. The S/B ratio of the $G\alpha_q$/PLC-β3 probe was not affected by the co-expression of the β-arrestin2 recruitment sensors, and detection with the two emission filters. The same holds true for the hH_1R-NLucN-based β-arrestin2 recruitment probe. Nevertheless, CRCs could be constructed from the signals originating from the $G\alpha_q$/PLC-β3 sensor and the hH_1R-NLucN-based β-arrestin2 probe.

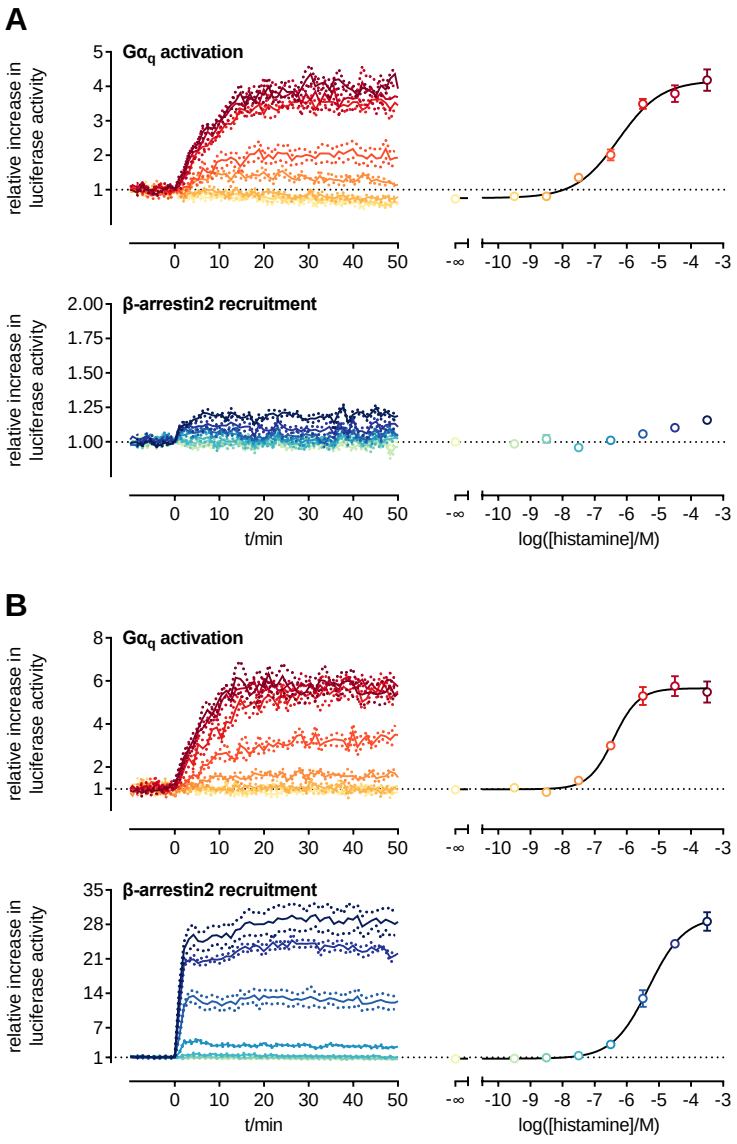

Fig. 6.3: Histamine concentration-dependent increase in luminescence of both sensors activated by the hH_1R expressed in HEK293T cells. The $G\alpha_q$/PLC-β3 interaction sensor was co-expressed either with the hH_1R-NLucC-based (**A**) or with the hH_1R-NLucN-based (**B**) β-arrestin2 recruitment sensor, and the response of the sensors to increasing concentrations of histamine were analysed. Shown are the results of one representative experiment each, determined in triplicate. The total number of biological replicates is given in Table 6.1.

The stimulation of the hM_1R, expressed as two different fusion proteins in two different HEK293T cell populations, using carbachol also triggered a gradual increase in luciferase activity (cf. Fig. 6.4). The S/B ratio of the $G\alpha_q$/PLC-β3 probe was reduced as compared to the monoparametric assay, but it was still above a factor of six in case of carbachol concentrations around E_{max}. The hM_1R-NLucC-based β-arrestin2 probe delivered S/B ratios comparable to those from the monoparametric setup, as opposed to the hM_1R-NLucN-based probe, which showed an S/B ratio decrease by a factor of approx. 4. Nevertheless, all probes delivered robust results and allowed the construction of CRCs.

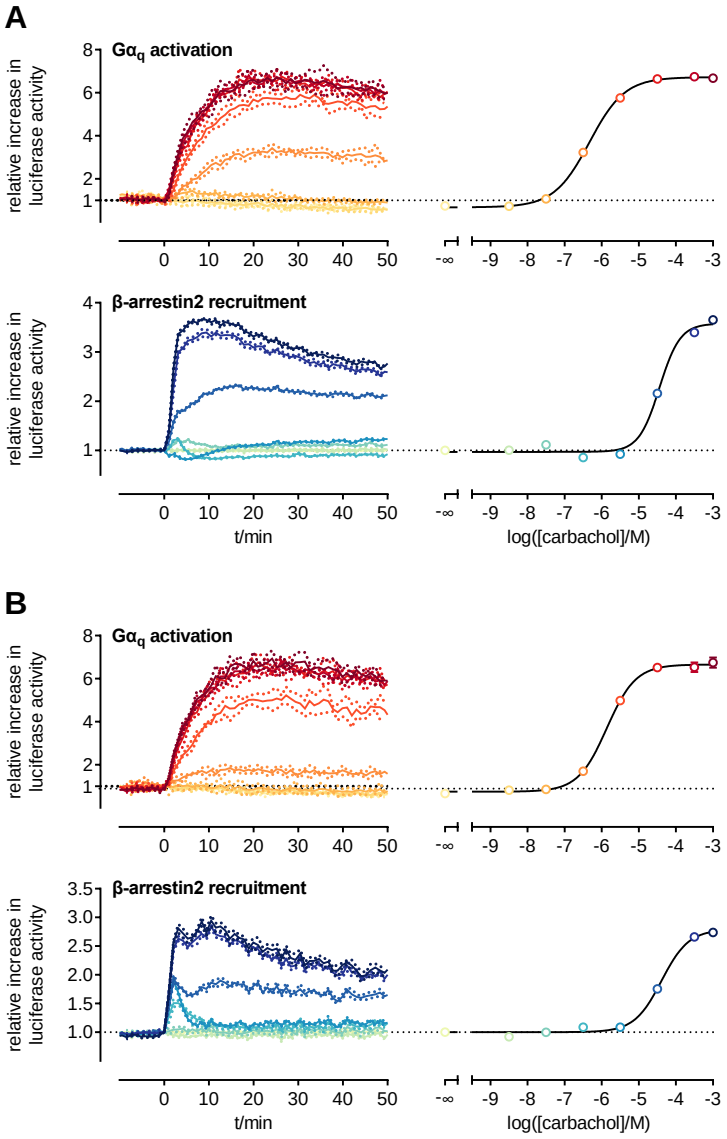

Fig. 6.4: Carbachol concentration-dependent increase in luminescence of both sensors activated by the hM_1R expressed in HEK293T cells. The $G\alpha_q$/PLC-β3 interaction sensor was co-expressed either with the hM_1R-NLucC-based (**A**) or with the hM_1R-NLucN-based (**B**) β-arrestin2 recruitment sensor, and the response of the sensors to increasing concentrations of carbachol were analysed. Shown are the results of one representative experiment each, determined in triplicate. The total number of biological replicates is given in Table 6.1.

Activation of the $G\alpha_q$/PLC-β3 probe via the two different hM_5R fusion proteins led to a fourfold increase in S/B ratio compared to the monoparametric assay (cf. Fig. 6.5). The hM_5R-NLucC-based β-arrestin2 recruitment assay applied in the multiparametric approach delivered a comparable S/B ratio (Fig. 6.5A), whereas the hM_5R-NLucN-based assay also showed a fourfold-increased S/B ratio, compared to the monoparametric setup (Fig. 6.5B). Both approaches allowed the construction of CRCs.

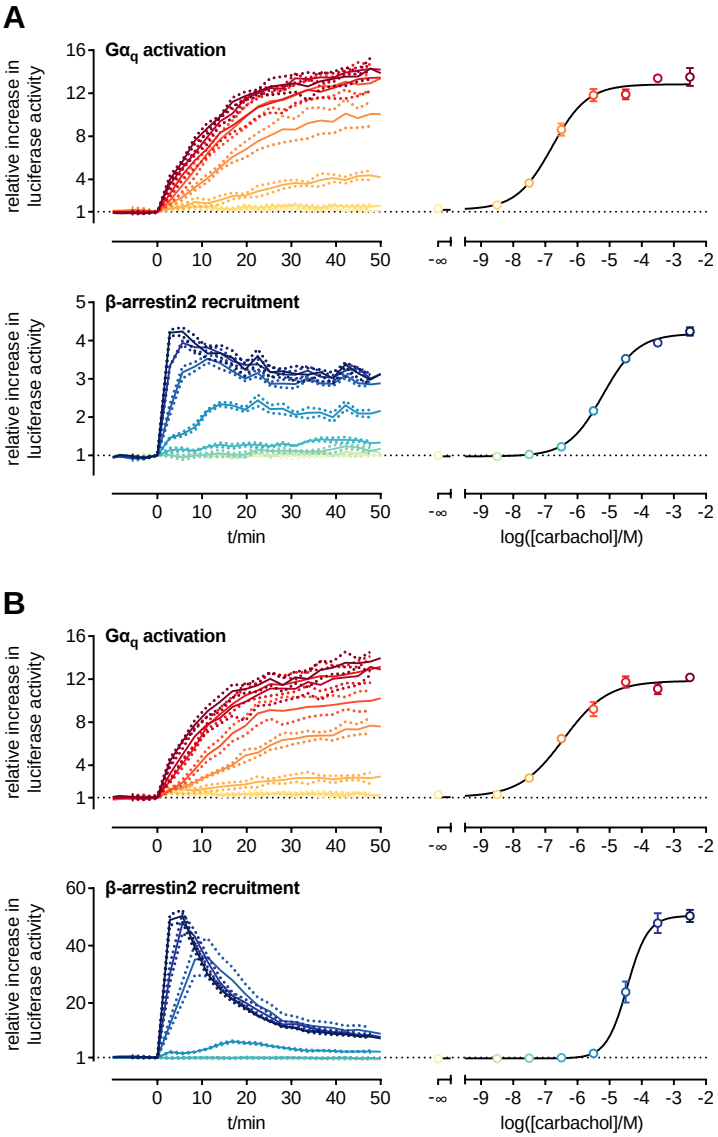

Fig. 6.5: Carbachol concentration-dependent increase in luminescence of both sensors activated by the hM_5R expressed in HEK293T cells. The $G\alpha_q$/PLC-β3 interaction sensor was co-expressed either with the hM_5R-NLucC-based (**A**) or with the hM_5R-NLucN-based (**B**) β-arrestin2 recruitment sensor, and the response of the sensors to increasing concentrations of carbachol were analysed. Shown are the results of one representative experiment each, determined in triplicate. The total number of biological replicates is given in Table 6.1.

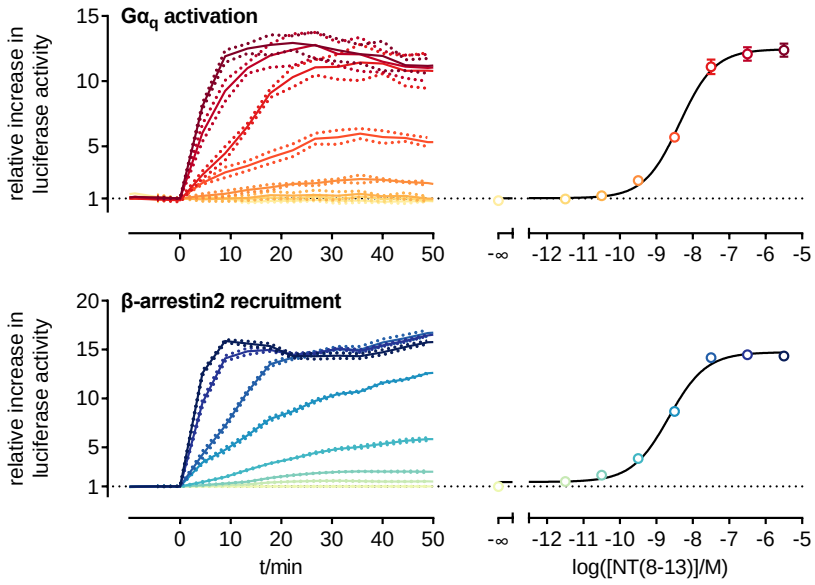

Fig. 6.6: NT(8-13) concentration-dependent increase in luminescence of both sensors activated by the hNTS$_1$R-NLucC expressed in HEK293T cells. The Gα$_q$/PLC-β3 interaction sensor was co-expressed with the hNTS$_1$R-NLucC-based β-arrestin2 recruitment sensor and their responses to increasing concentrations of NT(8-13) were analysed. Shown are the results of one representative experiment, determined in triplicate. The total number of biological replicates is given in Table 6.1.

In case of the hNTS$_1$R, which was analysed only with the hNTS$_1$R-NLucC/NLucN-β-arrestin2 combination for measuring β-arrestin2 recruitment, the S/B ratios of both probes increased as compared to the monoparametric assays and CRCs could also be constructed (cf. Fig. 6.6).

For all analysed receptors, the observed kinetic traces were also in agreement to those obtained by each monoparametric assay. On one hand, the Gα$_q$/PLC-β3 probe responded with an increase in luminescence after agonist addition, leading to a plateau after 10-15 min in case of all receptors. On the other hand, the kinetics observed for the interaction of the NLucC-tagged GPCRs with β-arrestin2 were in agreement with those obtained with the β-arrestin2 assay alone. The hM$_1$R and hM$_5$R showed kinetics characteristic of class A GPCRs[40,41], whereas the hNTS$_1$R exhibited kinetics resulting in a plateau, typical for class B GPCRs[40,41].

A possible reason for the differences observed in the S/B ratios could be variations in protein expression levels, since all experiments were performed in polyclonal stably-expressing cell populations. High abundancies of certain proteins might cause lower S/B ratios, as this would increase the probability of unspecific co-localisations of proteins and would therefore cause higher background luminescence intensities[15].

6.3.3 Analysis of standard agonists and antagonists in the multiparametric assay

To evaluate the multiparametric assay for potential ligand characterisation, different standard agonists and antagonists were analysed (cf. Fig. 6.7 and Table 6.1). The pEC$_{50}$ values determined at the two muscarinic receptors and the hNTS$_1$R were in good agreement – with a maximum difference of half an order of magnitude – to those obtained, when both assays were performed separately. The discrepancies observed for the differentially-tagged receptors (either with NLucC, or NLucN) became apparent in the same manner as reported in chapter 5 (cf. Fig. 5.3 and Table 5.1). At the hM$_1$R, where the nature of the tag did not alter the β-arrestin2 recruitment process, but the Gα$_q$-dependent Ca^{2+} response, the potency determined using the Gα$_q$/PLC-β3 probe was reduced for both agonists, when the larger NLucN tag was

fused to the hM_1R. For the hM_5R, the opposite was observed, meaning that the $G\alpha_q$/PLC-β3 interaction was not influenced by the type of tag at the receptor, but the β-arrestin2 recruitment was, which also corresponds to the data presented in chapter 5. Additionally, the superagonistic effects detected for iperoxo with respect to β-arrestin2 recruitment were confirmed using the multiparametric assay. The antagonistic activities (pK_b values) were in good accordance with those obtained using each monoparametric assay.

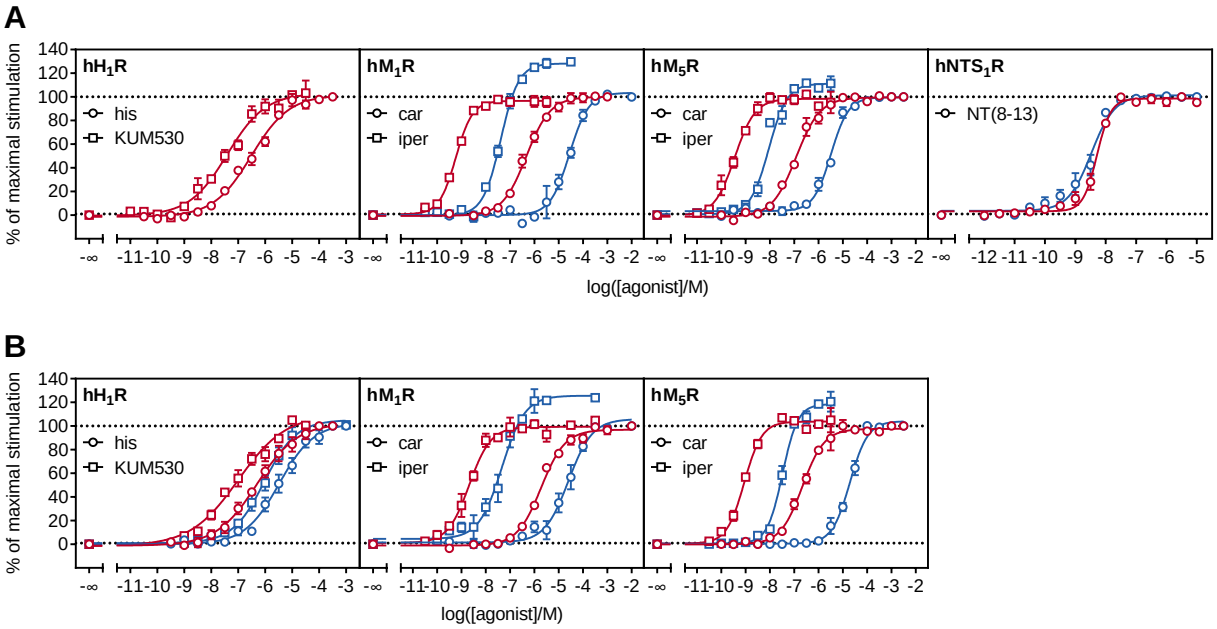

Fig. 6.7: Characterisation of standard agonists at the hH_1R, $hM_{1,5}R$ and the $hNTS_1R$ using the developed multiparametric assay for $G\alpha_q$ activation and β-arrestin2 recruitment. The $G\alpha_q$/PLC-β3 interaction sensor was co-expressed either with the GPCR-NLucC-based (**A**) or with the GPCR-NLucN-based (**B**) β-arrestin2 recruitment sensor, and the response of the sensors to increasing concentrations of standard agonists were analysed. The data corresponding to the $G\alpha_q$/PLC-β3 interaction probe is displayed in red, whereas the data obtained using the sensor for β-arrestin2 recruitment is shown in blue.

Interestingly, differences in the pEC_{50} values between the $G\alpha_q$ activation and the β-arrestin2 recruitment of approx. one log-unit were observed for both agonists, analysed at the two muscarinic receptors, whereas NT(8-13) at the $hNTS_1R$, activated both pathways with a comparable potency. Most probably, differential affinities of the activated receptor for the two intracellular effectors caused these differences in potency[42]. This might be connected to the aforementioned fact that the two muscarinic receptors were identified as class A receptors, whereas the $hNTS_1R$ is a class B receptor[40]. This classification was originally not only made due to different interaction kinetics between GPCRs and β-arrestins[40,41], but also because of differential affinities of β-arrestin2 for the two classes of GPCRs[40], which seem to play a role here as well. One can only speculate about the physiological relevance of such a phenomenon, but it might be associated with the prevention of cells against an overstimulation upon continuous presence of agonists[43], being more important for cells expressing $hNTS_1Rs$ than for those expressing the two muscarinic receptors.

Table 6.1: pEC_{50}, E_{max} and pK_b values of the compounds analysed using the multiparametric assay. Data are presented as means ± SEM. *N* denotes the number of independent biological replicates from which each was performed in triplicate. (N.S.: no signal)

			$G\alpha_q$ activation			β-arrestin2 recruitment			
receptor	**C-terminal tag**	**compound**	**pEC_{50}**	**$\%E_{max}$**	**pK_b**	**pEC_{50}**	**$\%E_{max}$**	**pK_b**	***N***
hH_1R	NLucC	histamine	6.48 ± 0.09	100		N.S.	N.S.		6
		UR-KUM530	7.33 ± 0.12	103.1 ± 4.2		N.S.	N.S.		4
		mepyramine			7.63 ± 0.07			N.S.	3
		diphenhydramine			7.08 ± 0.64			N.S.	3
	NLucN	histamine	6.28 ± 0.13	100		5.32 ± 0.14	100		6
		UR-KUM530	7.03 ± 0.17	109.9 ± 7		5.90 ± 0.17	105.2 ± 5.8		4
		mepyramine			8.13 ± 0.14			8.06 ± 0.03	3
		diphenhydramine			6.80 ± 0.12			6.91 ± 0.11	3
hM_1R	NLucC	carbachol	6.33 ± 0.06	100		4.49 ± 0.10	100		6
		iperoxo	9.24 ± 0.02	96.1 ± 1.6		7.39 ± 0.05	128.3 ± 1.7		4
		N'-methylscopolamine			9.72 ± 0.04			9.01 ± 0.09	3
		atropine			9.30 ± 0.04			8.76 ± 0.23	3
	NLucN	carbachol	5.70 ± 0.03	100		4.47 ± 0.25	100		5
		iperoxo	8.72 ± 0.06	98.9 ± 2.7		7.27 ± 0.06	131.1 ± 8.8		3
		N'-methylscopolamine			9.66 ± 0.07			9.14 ± 0.17	3
		atropine			9.20 ± 0.08			8.61 ± 0.16	3
hM_5R	NLucC	carbachol	6.90 ± 0.08	100		5.49 ± 0.08	100		7
		iperoxo	9.47 ± 0.05	98.6 ± 0.7		8.01 ± 0.12	111.6 ± 2.1		4
		N'-methylscopolamine			9.18 ± 0.15			9.19 ± 0.13	3
		atropine			8.81 ± 0.36			9.05 ± 0.15	3
	NLucN	carbachol	6.64 ± 0.06	100		4.70 ± 0.08	100		5
		iperoxo	9.05 ± 0.04	103.9 ± 3.6		7.45 ± 0.11	122.8 ± 7.2		4
		N'-methylscopolamine			9.38 ± 0.10			9.30 ± 0.19	3
		atropine			8.71 ± 0.13			9.11 ± 0.02	3
$hNTS_1R$	NLucC	NT(8-13)	8.31 ± 0.06	100		8.55 ± 0.13	100		6
		SR142948A			8.09 ± 0.05			7.85 ± 0.21	2

Unfortunately, the pEC_{50} values of the agonists and, to a lesser extent, also the pK_b values of the antagonists obtained at the hH_1R differ up to one order of magnitude compared to the monoparametric assays. Again, differences in protein expression could be the reason for these discrepancies. Several reports described that the expression level of intracellular effector proteins of GPCRs can influence the observed potencies of the analysed agonists[13,15].

To further enhance the robustness of the developed multiparametric assay, a different expression system of the proteins might be beneficial. One approach could be similar to the one already employed in chapter 3[36] for the construction of the $G\alpha_q$/PLC-β3 probe, which involved the multicistronic expression of both sensor proteins encoded on one vector separated by a P2A autoproteolysis site. By adding the NLucN fragment-tagged β-arrestin2 to the vector, separated by another P2A site, a fixed 1:1:1 ratio[44] of all intracellular effector proteins of the GPCR expressed in a recombinant cell line, could be achieved. This would at least ensure that both probes are expressed at a similar level, avoiding an unbalanced expression of only one of the two probes, which could (artificially) pretend bias[13,15]. Finally, a cell population stably transfected with such a vector plasmid should undergo single clone selection. The selection, exploiting the transient transfection of a GPCR, should be focused on the S/B ratios of both probes, the potencies of standard agonists and an expression of the probes as comparable as possible to the endogenous level of their unmodified counterparts (i.e. $G\alpha_q$, PLC-β3 and β-arrestin2). The experiments with the $G\alpha_q$/PLC-β3 probe, shown in chapter 3[36], were performed at expression levels comparable to those of endogenous $G\alpha_q$[36] (cf. Fig. A2), which demonstrates that the probe works reliably at endogenous expression levels. For the split NLuc-based β-arrestin2 recruitment assay the expression levels were not evaluated, but other assays, based on split NLuc, were shown to give reliable results, or to perform even better, when they were not overexpressed[15,45], which suggests that this could also be true for the β-arrestin2 recruitment sensor. This population could subsequently be used for transfection with different receptors, tagged with the NLucC fragment. Admittedly, such a plasmid would become very large in size and could therefore be on one hand, difficult to construct using standard cloning procedures and on the other hand, transfection could become challenging. Another shortcoming would be that the expression levels would be fixed to the aforementioned 1:1:1 ratio, which is not necessarily the case under endogenous expression conditions[10,11]. For the analysis of agonist bias, this could become disadvantageous, since differences in protein expression of the intracellular signalling partners of the GPCR can lead to an apparent bias[8].

Therefore, a different approach could involve the engineering of HEK293T cells by genome-editing[46]. By exchanging the genes of the proteins within a certain cell population, which are parts of the two sensors with their modified counterparts, they would be expressed on the same level as the native proteins.

By applying one of the two above-mentioned strategies, the herein described approach for simultaneous quantification of $G\alpha_q$ activation and β-arrestin2 recruitment could be further optimised to yield results as comparable to the physiological state as possible.

6.4 Conclusion

The herein presented results demonstrate that a simultaneous determination of $G\alpha_q$ activation and β-arrestin2 recruitment in a single cell population can be achieved by applying split luciferase complementation with two luciferases exhibiting different emission maxima. The red light-emitting CBR luciferase was used to probe the interaction of $G\alpha_q$ with PLC-β3, whereas β-arrestin2 recruitment to a GPCR was probed by applying the blue light-emitting NLuc. The spectral separation of the employed luciferases was sufficient to allow a discrimination solely based on the application of two different emission filters without additional spectral unmixing. The approach was applied successfully to the hM_1R, the hM_5R and the $hNTS_1R$, and to a lesser extent also to the hH_1R, allowing the construction of CRCs of agonists and the determination of antagonistic activities for both, $G\alpha_q$ activation and β-arrestin2 recruitment at the same time. Results from the former three receptors suggest that both sensors do not interfere with each other under co-expression.

The results obtained at the hH_1R, however, suggest that protein abundance, and therefore, gene expression levels influence the observed S/B ratios and more importantly, the pEC_{50} values. Therefore, to further improve the value of the developed technique, expression levels of the sensors need to be optimised, ideally by restricting them to the endogenous expression level of their native counterparts.

Nevertheless, the advantages of the simultaneous detection lie, on one hand, in a marked reduction of time needed for the measurements, since instead of two assays only one is necessary. On the other hand, in the unification of experimental conditions (common cellular background and receptor expression levels). Therefore, in future, the assay will certainly be of high value for the reliable determination of agonist bias at various GPCRs between the $G\alpha_q$ and the β-arrestin pathways.

6.5 References

1 Rankovic, Z., Brust, T. F. & Bohn, L. M. Biased agonism: An emerging paradigm in GPCR drug discovery. *Bioorg Med Chem Lett* **26**, 241-250, doi:10.1016/j.bmcl.2015.12.024 (2016).

2 Michel, M. C. & Charlton, S. J. Biased agonism in drug discovery - is it too soon to choose a path? *Mol Pharmacol* **93**, 259-265, doi:10.1124/mol.117.110890 (2018).

3 Carter, A. A. & Hill, S. J. Characterization of isoprenaline- and salmeterol-stimulated interactions between β_2-adrenoceptors and β-arrestin 2 using β-galactosidase complementation in C2C12 cells. *J Pharmacol Exp Ther* **315**, 839-848, doi:10.1124/jpet.105.088914 (2005).

4 Littmann, T., Göttle, M., Reinartz, M. T., Kälble, S., Wainer, I. W., Ozawa, T. & Seifert, R. Recruitment of β-arrestin 1 and 2 to the β_2-adrenoceptor: analysis of 65 ligands. *J Pharmacol Exp Ther* **355**, 183-190, doi:10.1124/jpet.115.227959 (2015).

5 Zidar, D. A. Endogenous ligand bias by chemokines: implications at the front lines of infection and leukocyte trafficking. *Endocr Metab Immune Disord Drug Targets* **11**, 120-131 (2011).

6 Thompson, G. L., Lane, J. R., Coudrat, T., Sexton, P. M., Christopoulos, A. & Canals, M. Biased Agonism of Endogenous Opioid Peptides at the μ-Opioid Receptor. *Mol Pharmacol* **88**, 335-346, doi:10.1124/mol.115.098848 (2015).

7 Reyes-Alcaraz, A., Lee, Y. N., Yun, S., Hwang, J. I. & Seong, J. Y. Conformational signatures in β-arrestin2 reveal natural biased agonism at a G-protein-coupled receptor. *Commun Biol* **1**, 128, doi:10.1038/s42003-018-0134-3 (2018).

8 Kenakin, T. & Christopoulos, A. Signalling bias in new drug discovery: detection, quantification and therapeutic impact. *Nat Rev Drug Discov* **12**, 205-216, doi:10.1038/nrd3954 (2013).

9 van der Westhuizen, E. T., Breton, B., Christopoulos, A. & Bouvier, M. Quantification of ligand bias for clinically relevant β_2-adrenergic receptor ligands: implications for drug taxonomy. *Mol Pharmacol* **85**, 492-509, doi:10.1124/mol.113.088880 (2014).

10 Atwood, B. K., Lopez, J., Wager-Miller, J., Mackie, K. & Straiker, A. Expression of G protein-coupled receptors and related proteins in HEK293, AtT20, BV2, and N18 cell lines as revealed by microarray analysis. *BMC Genomics* **12**, 14, doi:10.1186/1471-2164-12-14 (2011).

11 Correll, C. C. & McKittrick, B. A. Biased ligand modulation of seven transmembrane receptors (7TMRs): functional implications for drug discovery. *J Med Chem* **57**, 6887-6896, doi:10.1021/jm401677g (2014).

12 Kenakin, T., Watson, C., Muniz-Medina, V., Christopoulos, A. & Novick, S. A simple method for quantifying functional selectivity and agonist bias. *ACS Chem Neurosci* **3**, 193-203, doi:10.1021/cn200111m (2012).

13 Bräuner-Osborne, H., Ebert, B., Brann, M. R., Falch, E. & Krogsgaard-Larsen, P. Functional partial agonism at cloned human muscarinic acetylcholine receptors. *Eur J Pharmacol* **313**, 145-150 (1996).

14 Hermans, E., Challiss, R. A. & Nahorski, S. R. Effects of varying the expression level of recombinant human mGlu1α receptors on the pharmacological properties of agonists and antagonists. *Br J Pharmacol* **126**, 873-882, doi:10.1038/sj.bjp.0702359 (1999).

15 Wan, Q., Okashah, N., Inoue, A., Nehmé, R., Carpenter, B., Tate, C. G. & Lambert, N. A. Mini G protein probes for active G protein-coupled receptors (GPCRs) in live cells. *J Biol Chem* **293**, 7466-7473, doi:10.1074/jbc.RA118.001975 (2018).

16 Benjamin, E. R., Haftl, S. L., Xanthos, D. N., Crumley, G., Hachicha, M. & Valenzano, K. J. A miniaturized column chromatography method for measuring receptor-mediated inositol phosphate accumulation. *J Biomol Screen* **9**, 343-353, doi:10.1177/1087057103262841 (2004).

17 Gulyás, G., Tóth, J. T., Tóth, D. J., Kurucz, I., Hunyady, L., Balla, T. & Várnai, P. Measurement of inositol 1,4,5-trisphosphate in living cells using an improved set of resonance energy transfer-based biosensors. *PLoS One* **10**, e0125601, doi:10.1371/journal.pone.0125601 (2015).

18 Trinquet, E., Fink, M., Bazin, H., Grillet, F., Maurin, F., Bourrier, E., Ansanay, H., Leroy, C., Michaud, A., Durroux, T., Maurel, D., Malhaire, F., Goudet, C., Pin, J. P., Naval, M., Hernout, O., Chrétien, F., Chapleur, Y. & Mathis, G. D-*myo*-inositol 1-phosphate as a surrogate of D-*myo*-inositol 1,4,5-tris phosphate to monitor G protein-coupled receptor activation. *Anal Biochem* **358**, 126-135, doi:10.1016/j.ab.2006.08.002 (2006).

19 Grynkiewicz, G., Poenie, M. & Tsien, R. Y. A new generation of Ca^{2+} indicators with greatly improved fluorescence properties. *J Biol Chem* **260**, 3440-3450 (1985).

20 Suzuki, K., Kimura, T., Shinoda, H., Bai, G., Daniels, M. J., Arai, Y., Nakano, M. & Nagai, T. Five colour variants of bright luminescent protein for real-time multicolour bioimaging. *Nat Commun* **7**, 13718, doi:10.1038/ncomms13718 (2016).

21 Shimomura, O., Johnson, F. H. & Saiga, Y. Extraction, purification and properties of aequorin, a bioluminescent protein from the luminous hydromedusan, *Aequorea*. *J Cell Comp Physiol* **59**, 223-239 (1962).

22 Angers, S., Salahpour, A., Joly, E., Hilairet, S., Chelsky, D., Dennis, M. & Bouvier, M. Detection of β_2-adrenergic receptor dimerization in living cells using bioluminescence resonance energy transfer (BRET). *Proc Natl Acad Sci U S A* **97**, 3684-3689, doi:10.1073/pnas.060590697 (2000).

23 Krasel, C., Bünemann, M., Lorenz, K. & Lohse, M. J. β-Arrestin binding to the β_2-adrenergic receptor requires both receptor phosphorylation and receptor activation. *J Biol Chem* **280**, 9528-9535, doi:10.1074/jbc.M413078200 (2005).

24 Misawa, N., Kafi, A. K., Hattori, M., Miura, K., Masuda, K. & Ozawa, T. Rapid and high-sensitivity cell-based assays of protein-protein interactions using split click beetle luciferase complementation: an approach to the study of G-protein-coupled receptors. *Anal Chem* **82**, 2552-2560, doi:10.1021/ac100104q (2010).

25 Nordemann, U., Wifling, D., Schnell, D., Bernhardt, G., Stark, H., Seifert, R. & Buschauer, A. Luciferase reporter gene assay on human, murine and rat histamine H_4 receptor orthologs: correlations and discrepancies between distal and proximal readouts. *PLoS One* **8**, e73961, doi:10.1371/journal.pone.0073961 (2013).

26 Hilf, G., Gierschik, P. & Jakobs, K. H. Muscarinic acetylcholine receptor-stimulated binding of guanosine 5'-O-(3-thiotriphosphate) to guanine-nucleotide-binding proteins in cardiac membranes. *Eur J Biochem* **186**, 725-731 (1989).

27 Harrison, C. & Traynor, J. R. The [^{35}S]GTPγS binding assay: approaches and applications in pharmacology. *Life Sciences* **74**, 489-508, doi:10.1016/j.lfs.2003.07.005 (2003).

28 Bünemann, M., Frank, M. & Lohse, M. J. Gi protein activation in intact cells involves subunit rearrangement rather than dissociation. *Proc Natl Acad Sci U S A* **100**, 16077-16082, doi:10.1073/pnas.2536719100 (2003).

29 Galés, C., Rebois, R. V., Hogue, M., Trieu, P., Breit, A., Hébert, T. E. & Bouvier, M. Real-time monitoring of receptor and G-protein interactions in living cells. *Nat Methods* **2**, 177-184, doi:10.1038/nmeth743 (2005).

30 Galés, C., Van Durm, J. J., Schaak, S., Pontier, S., Percherancier, Y., Audet, M., Paris, H. & Bouvier, M. Probing the activation-promoted structural rearrangements in preassembled receptor-G protein complexes. *Nat Struct Mol Biol* **13**, 778-786, doi:10.1038/nsmb1134 (2006).

31 Rinne, A., Birk, A. & Bünemann, M. Voltage regulates adrenergic receptor function. *Proc Natl Acad Sci U S A* **110**, 1536-1541, doi:10.1073/pnas.1212656110 (2013).

32 Oakley, R. H., Hudson, C. C., Cruickshank, R. D., Meyers, D. M., Payne, R. E., Jr., Rhem, S. M. & Loomis, C. R. The cellular distribution of fluorescently labeled arrestins provides a robust, sensitive, and universal assay for screening G protein-coupled receptors. *Assay Drug Dev Technol* **1**, 21-30, doi:10.1089/154065802761001275 (2002).

33 Reiner, S., Ambrosio, M., Hoffmann, C. & Lohse, M. J. Differential signaling of the endogenous agonists at the β_2-adrenergic receptor. *J Biol Chem* **285**, 36188-36198, doi:10.1074/jbc.M110.175604 (2010).

34 Bosma, R., Moritani, R., Leurs, R. & Vischer, H. F. BRET-based β-arrestin2 recruitment to the histamine H_1 receptor for investigating antihistamine binding kinetics. *Pharmacol Res* **111**, 679-687, doi:10.1016/j.phrs.2016.07.034 (2016).

35 Dogra, S., Sona, C., Kumar, A. & Yadav, P. N. Tango assay for ligand-induced GPCR-β-arrestin2 interaction: Application in drug discovery. *Methods Cell Biol* **132**, 233-254, doi:10.1016/bs.mcb.2015.11.001 (2016).

36 Littmann, T., Ozawa, T., Hoffmann, C., Buschauer, A. & Bernhardt, G. A split luciferase-based probe for quantitative proximal determination of $G\alpha_q$ signalling in live cells. *Sci Rep* **8**, 17179, doi:10.1038/s41598-018-35615-w (2018).

37 Hida, N., Awais, M., Takeuchi, M., Ueno, N., Tashiro, M., Takagi, C., Singh, T., Hayashi, M., Ohmiya, Y. & Ozawa, T. High-sensitivity real-time imaging of dual protein-protein interactions in living subjects using multicolor luciferases. *PLoS One* **4**, e5868, doi:10.1371/journal.pone.0005868 (2009).

38 Hall, M. P., Unch, J., Binkowski, B. F., Valley, M. P., Butler, B. L., Wood, M. G., Otto, P., Zimmerman, K., Vidugiris, G., Machleidt, T., Robers, M. B., Benink, H. A., Eggers, C. T., Slater, M. R., Meisenheimer, P. L., Klaubert, D. H., Fan, F., Encell, L. P. & Wood, K. V. Engineered luciferase reporter from a deep sea shrimp utilizing a novel imidazopyrazinone substrate. *ACS Chem Biol* **7**, 1848-1857, doi:10.1021/cb3002478 (2012).

39 Cheng, Y. & Prusoff, W. H. Relationship between the inhibition constant (K_1) and the concentration of inhibitor which causes 50 per cent inhibition (I_{50}) of an enzymatic reaction. *Biochem Pharmacol* **22**, 3099-3108 (1973).

40 Oakley, R. H., Laporte, S. A., Holt, J. A., Caron, M. G. & Barak, L. S. Differential affinities of visual arrestin, β-arrestin1, and β-arrestin2 for G protein-coupled receptors delineate two major classes of receptors. *J Biol Chem* **275**, 17201-17210, doi:10.1074/jbc.M910348199 (2000).

41 Kendall, R. T. & Luttrell, L. M. Diversity in arrestin function. *Cell Mol Life Sci* **66**, 2953-2973, doi:10.1007/s00018-009-0088-1 (2009).

42 Seifert, R. Functional selectivity of G-protein-coupled receptors: from recombinant systems to native human cells. *Biochem Pharmacol* **86**, 853-861, doi:10.1016/j.bcp.2013.07.029 (2013).

43 Ferguson, S. S. Evolving concepts in G protein-coupled receptor endocytosis: the role in receptor desensitization and signaling. *Pharmacol Rev* **53**, 1-24 (2001).

44 Kim, J. H., Lee, S. R., Li, L. H., Park, H. J., Park, J. H., Lee, K. Y., Kim, M. K., Shin, B. A. & Choi, S. Y. High cleavage efficiency of a 2A peptide derived from porcine teschovirus-1 in human cell lines, zebrafish and mice. *PLoS One* **6**, e18556, doi:10.1371/journal.pone.0018556 (2011).

45 Dixon, A. S., Schwinn, M. K., Hall, M. P., Zimmerman, K., Otto, P., Lubben, T. H., Butler, B. L., Binkowski, B. F., Machleidt, T., Kirkland, T. A., Wood, M. G., Eggers, C. T., Encell, L. P. & Wood, K. V. NanoLuc Complementation Reporter Optimized for Accurate Measurement of Protein Interactions in Cells. *ACS Chem Biol* **11**, 400-408, doi:10.1021/acschembio.5b00753 (2016).

46 White, C. W., Vanyai, H. K., See, H. B., Johnstone, E. K. M. & Pfleger, K. D. G. Using nanoBRET and CRISPR/Cas9 to monitor proximity to a genome-edited protein in real-time. *Sci Rep* **7**, 3187, doi:10.1038/s41598-017-03486-2 (2017).

7. Summary

In G protein-coupled receptor (GPCR) research, there is an increasing interest in the development of biased agonists as pharmacological tools and ultimately also as drugs, since adverse effects of certain pharmaceuticals are supposed to be associated with the activation of unfavourable signalling pathways. Additionally, for several receptors, bias of endogenous agonists has been discovered. Currently, the most common approach to determine biased agonism implies the application of two separate assays for detecting G protein-dependent and β-arrestin-dependent signalling, respectively. Apart from the additional time needed to perform two assays instead of one, major shortcomings are associated with this approach. On one hand, the receptor sources in the employed assays can substantially differ in the extent of receptor and effector expression. On the other hand, the influence of signal amplification on the readouts of the two assays can vary tremendously. Taken together, this can lead to misinterpretations with respect to the signalling profile of the analysed agonist.

Therefore, the aim of this thesis was the development of two techniques, applicable to live cells with high throughput. Firstly, for the proximal determination of $G\alpha_q$ protein activation and secondly, for assessing β-arrestin recruitment. The two probes were designed to be potentially compatible with a multiparametric assay format, affording information on both signalling pathways at the same time. Both probes were engineered at a similar, proximal level within each signalling cascade, to receive information unaltered by signal amplification. Methodologically, this was achieved by split luciferase complementation (SLC) using two luciferases emitting light spectra with substantially different emission maxima.

The first assay was developed by applying SLC, using a red light-emitting luciferase, to probe the interaction of $G\alpha_q$ with phospholipase C-β3 (PLC-β3) proteins. By being independent on genetical receptor modifications and with its excellent Z' value of 0.7, the sensor was proven to be very suitable for ligand characterization, which was shown for five different GPCRs. Furthermore, the sensor proved to be useful for imaging, as shown by live cell bioluminescence microscopy. Beyond these applications, the sensor might become a valuable tool for de-orphanisation and subsequent determination of signalling pathways of orphan GPCRs, the analysis of $G\alpha_q$ activation in cells endogenously expressing $G\alpha_q$ protein-coupled receptors and imaging in laboratory animals.

Attempts to translate this assay principle to $G\alpha_s$ and $G\alpha_i$ proteins, interacting with adenylyl cyclases (AC), in a reproducible manner, failed. The most probable reason for this is poor membrane trafficking of the modified ACs, which could be improved by using artificial signalling sequences or generating a synthetic and soluble AC surrogate.

For measuring β-arrestin2 recruitment, a blue light-emitting luciferase was used. During assay development it became apparent that solely focusing on signal-to-background (S/B) ratios in the initial phase, as often practiced, can be inappropriate. In fact, the development must also take the functional behaviour of the proteins into account, because otherwise, the resulting assays do not reflect the physiological

behaviour of the analysed proteins anymore. For this reason, two different approaches to measure β-arrestin2 recruitment by SLC were compared: on one hand with respect to their impact on the recruitment process and, on the other hand, with respect to their influence on second messenger formation. Despite lower S/B ratios, the assay based on GPCR-NLucC/NLucN-β-arrestin2 was proven to be useful for determining ligand potencies and efficacies, and it was sensitive enough to identify iperoxo as a putative superagonist at the muscarinic acetylcholine receptors hM_1R and hM_5R with respect to β-arrestin2 recruitment. It was further demonstrated that temporal analyses of the receptor/β-arrestin2 interaction can be performed to e.g. discriminate between receptors that only transiently interact with arrestins after activation, presumably because they recycle to the plasma membrane very fast (class A), and those that show sustained interaction (class B). Furthermore, this assay principle should be broadly applicable to other GPCRs.

Finally, both probes were expressed in combination in a single HEK293T cell population. This approach was applied successfully to the hM_1R, the hM_5R and to the neurotensin receptor $hNTS_1R$, and to a lesser extent also to the histamine receptor hH_1R, allowing the construction of concentration-response-curves of agonists and the determination of antagonistic activities for both, $G\alpha_q$ activation and β-arrestin2 recruitment at the same time. Results from the former three receptors suggest that both sensors do not interfere with each other when co-expressed. However, the results obtained at the hH_1R implicate that the expression levels of the sensors need to be optimised, ideally by restricting them to the endogenous expression level of their native counterparts.

8. Appendix

8.1 Appendix 1

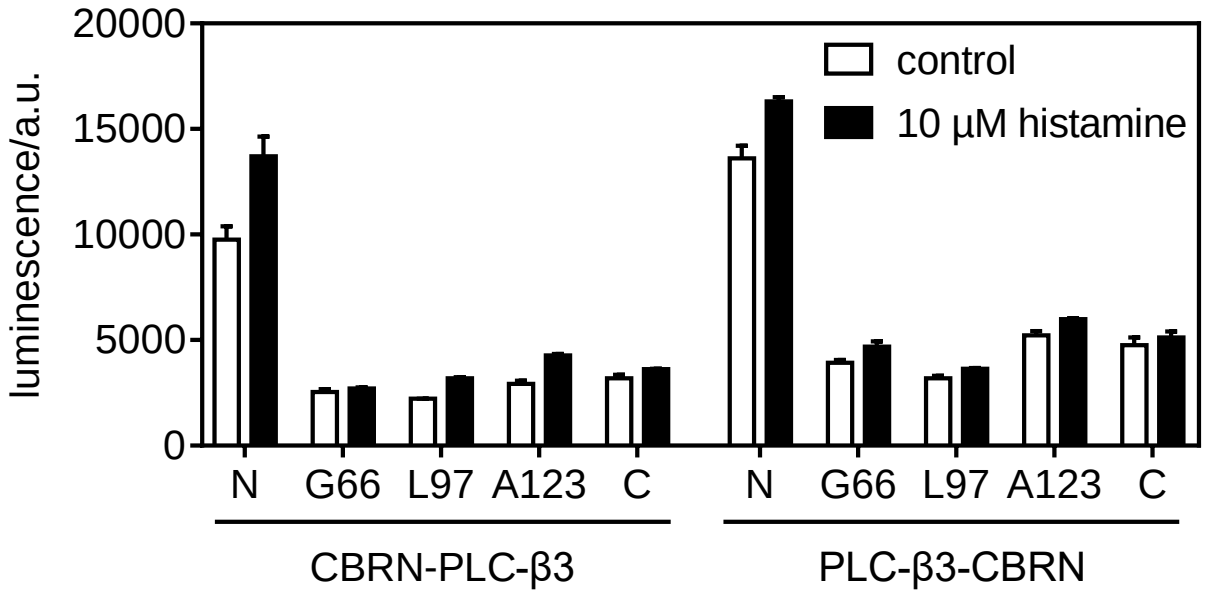

Fig. A1: Raw luminescence intensities of all investigated fusion protein combinations. HEK293T cells were transfected with the different combinations of fusion proteins and the hH_1R. Subsequently, the cells were stimulated with histamine, or with a solvent control for 25 min, before the cells were lysed and the substrate was added. Data (means ± SEM) are shown from one of three experiments, each performed in triplicate.

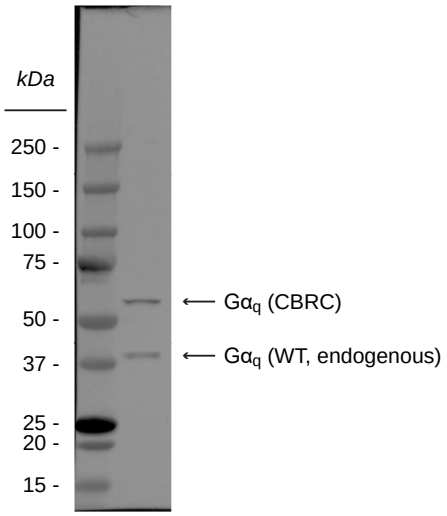

Fig. A2: Anti-Gα_q immunoblot of a lysate from HEK293T cells stably expressing the developed sensor. To confirm reliable cleavage of the 2A autoproteolysis site separating CBRN-PLC-β3 and Gα_q(123) an immunoblot with an anti-Gα_q antibody was performed. The detection revealed two distinct bands originating from endogenous Gα_q (≈ 42 kDa) and most probably from the Gα_q CBRC fusion protein (≈ 59 kDa). No higher molecular weight protein was stained, indicating complete cleavage of the autoproteolysis site. It can also be seen that expression of the modified Gα_q was comparable with endogenous Gα_q. Blotting was performed as follows: HEK293T cells with the pIRESpuro3 CBRN-PLC-β3-2A-Gα_q(123) vector stably integrated in their genome were lysed using a RIPA lysis buffer (50 mM Tris, 0.1% sodium dodecyl sulfate, 0.5% sodium deoxycholate, 1% Triton X 100, 150 mM NaCl) supplemented with a SIGMAFAST protease inhibitor cocktail (Sigma, Germany). Of this lysate, 20 µg were separated on an 8-16% Novex Tris-Glycine polyacrylamide gel (Thermo Scientific, Germany). The proteins were blotted on a nitrocellulose membrane at 0.13 A for 1 h, and unspecific binding sites were blocked using skim milk powder (5%) in phosphate-buffered saline (137 mM NaCl, 2.7 mM KCl, 10 mM Na_2HPO_4, 1.8 mM KH_2PO_4), supplemented with Tween 20 (0.05%) (PBS-T), for 1 h. The polyclonal primary antibody against Gα_q, produced in rabbit (Cat. 371754, Merck Millipore, Germany), was used at a dilution of 1:500 in PBS-T with milk powder (5%) to incubate the blot at 4 °C overnight. On the next day, the blot was washed three times using PBS-T and a HRP-conjugated secondary antibody against rabbit IgG, produced in donkey (sc-2313, Santa Cruz, TX, USA), was added at a dilution of 1:10000 in PBS-T devoid of milk powder. The blot was incubated with the secondary antibody for 1 h before being developed using an ECL reagent (Bio-Rad, Germany). Luminescence emitted by the stained bands was quantified using a ChemiDoc MP imaging system (Bio-Rad, Germany) with an exposure time of 2 min. Shown is a superposition of the chemiluminescent blot with a colorimetric image showing the molecular weight marker Precision Plus Dual Color (Bio-Rad).

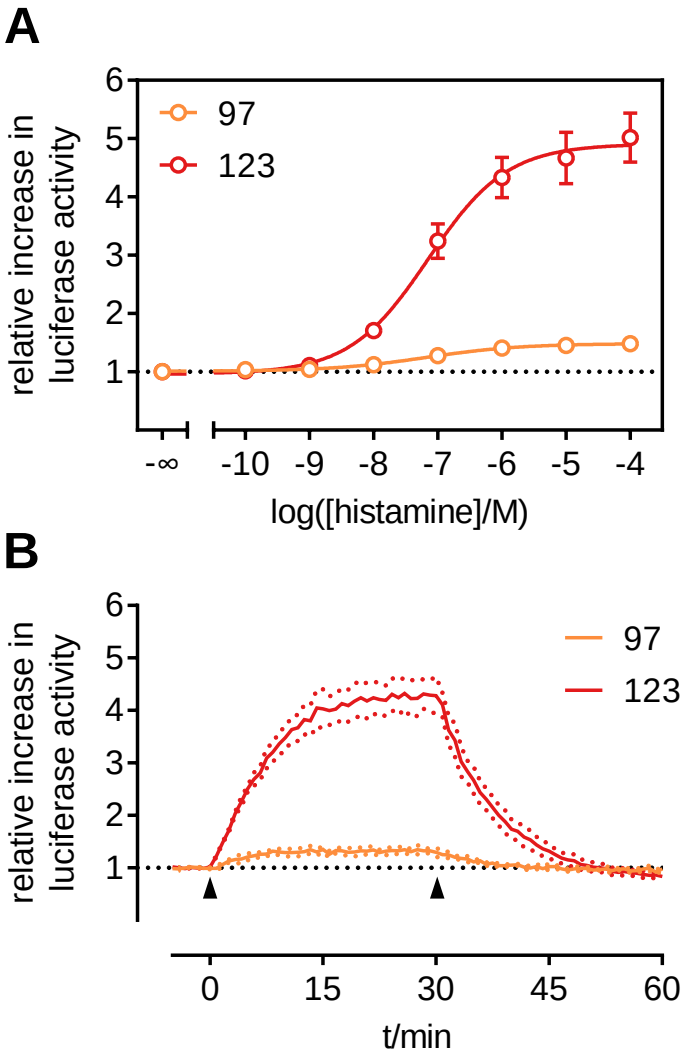

Fig. A3: Characterisation of the $G\alpha_q$(97) and $G\alpha_q$(123) variants in live cells co-expressing the hH_1R. HEK293T cells, stably transfected either with the pIRESpuro3 CBRN-PLC-β3-2A-$G\alpha_q$(97) or the pIRESpuro3 CBRN-PLC-β3-2A-$G\alpha_q$(123) together with the hH_1R, were generated. **A**: The cells were analysed with respect to their response to increasing concentrations of histamine, yielding a large difference in S/B ratio ($G\alpha_q$(97): 1.49 ± 0.08, $G\alpha_q$(123): 5.02 ± 0.42), but similar pEC_{50} values for histamine ($G\alpha_q$(97): 7.18 ± 0.22, $G\alpha_q$(123): 7.15 ± 0.16). **B**: The cells were stimulated with 300 nM histamine (first arrow) before mepyramine to a final concentration of 1 µM was added (second arrow). Again, the $G\alpha_q$(97) variant shows a lower S/B ratio, but the interaction of both sensor protein pairs is fully reversible. Data represent means ± SEM from three independent experiments, performed in triplicate.

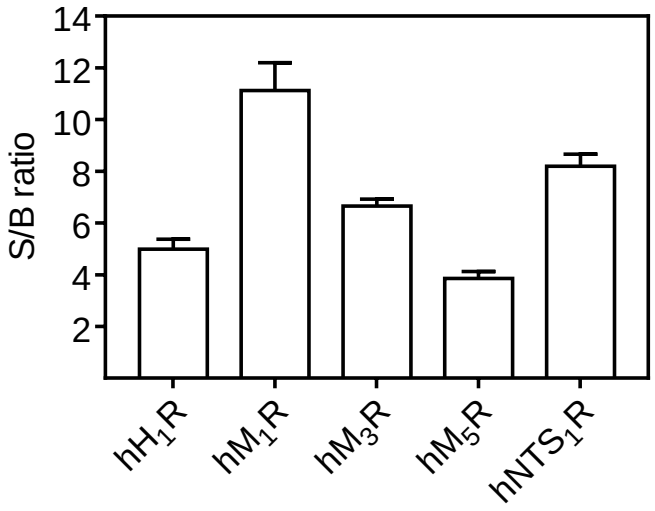

Fig. A4: S/B ratios of the sensor when activated by different GPCRs. HEK293T cells, expressing the developed sensor were stimulated via the given receptor. Luminescence intensities obtained from maximally stimulated cells were divided by those obtained from unstimulated cells. Data represent means ± SEM of at least three independent experiments, each performed in triplicate.

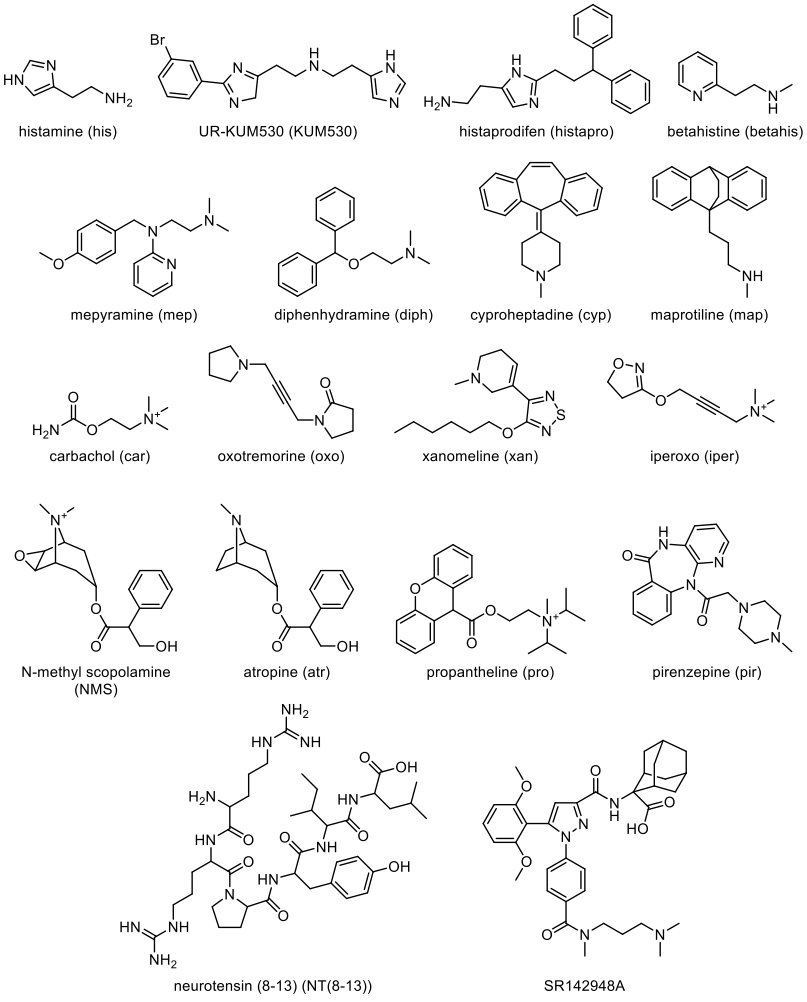

Fig. A5: Structures of the compounds analysed in chapter 3.

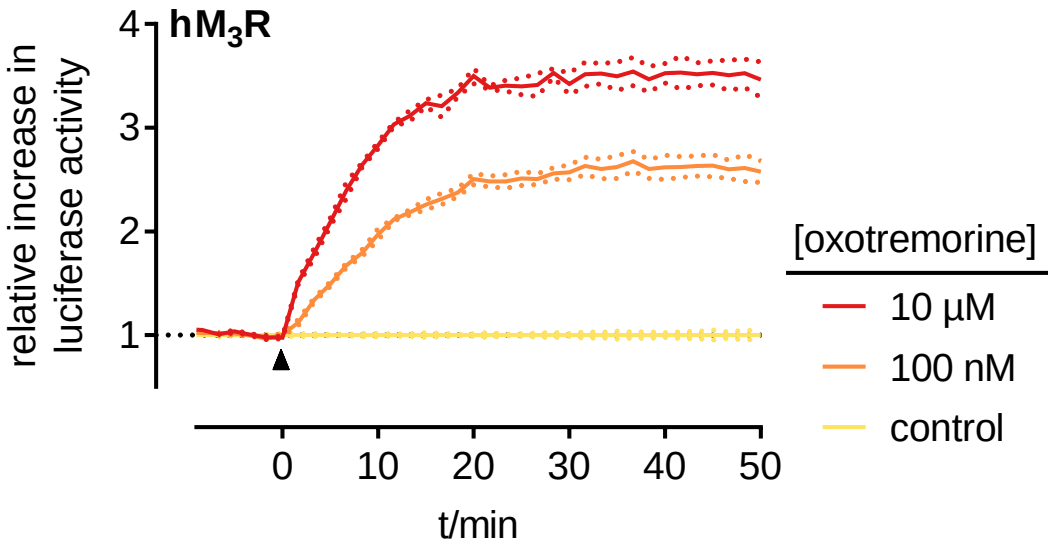

Fig. A6: Effect of the oxotremorine concentration on the onset kinetics of the hM_3R-mediated luminescence signal. The cells were stimulated with a concentration at E_{max} (10 µM) in comparison to the concentration used in the imaging experiments (100 nM, approx. EC_{60}). Data are given as means ± SEM and are a representative of eight independent experiments, each performed in triplicate

Table A8.1: Determined potencies and efficacies of standard agonists at $M_{1,3,5}R$ using the developed probe, in comparison to values reported in literature. Live HEK293T cells, expressing the developed sensor and the indicated receptor, were investigated with respect to their response to standard agonists. Data are given as means ± SEM. *N* denotes the number of biological replicates, each determined in triplicate. Except for [17] were ex vivo (rabbit and guinea pig) pharmacology results are reported, all other references contain in vitro data obtained at human receptors.

					Competition binding	Proximal readout assays (e.g. [^{35}S]-GTPγS)		Second messenger assays (e.g. IP_x, $[Ca^{2+}]_i$)		Distal readout assays (e.g. gene transcription, ex vivo)	
	cpd	**pEC_{50}**	**$\%E_{max}$**	***N***	**pK_i**	**pEC_{50}**	**$\%E_{max}$**	**pEC_{50}**	**$\%E_{max}$**	**pEC_{50}**	**$\%E_{max}$**
hM_1R	car	6.12 ± 0.08	100	4	3.17 – 4.46[1-3]	4.67 – 6.08[4-6]	93 – 100[4-6]	4.73 – 6.96[6-12]	99.6 – 103[6-12]	5.19 – 5.82[3,7,13,14]	93.6 – 100[3,7,13,14]
	xan	7.19 ± 0.17	80.6 ± 3.2	3	6.68 ± 0.02[3]	5.98 – 8.15[4,15]	40 – 127[4,15]	6.96 – 7.78[7,9,10,16]	29.8 – 117[7,9,10,16]	6.82 – 8.34[3,7]	41.7 – 105[3,7]
	oxo	7.32 ± 0.05	83.6 ± 1.8	3	5.48 – 5.86[1,2]	6.64 ± 0.21[6]	62 ± 4[6]	5.70 – 6.70[6,12]	51 – 56[6,12]	6.41 – 7.72[13,17]	75 – 100[13,17]
	iper	9.42 ± 0.05	99.8 ± 2.3	4		< 7[18]	100[18]	7.97 ± 0.09[16]	101 ± 3.3[16]	8.69 – 9.87[17,19]	100 – 102[17,19]
hM_3R	oxo	7.09 ± 0.09	100	8	5.28 – 5.71[1,2]			6.39 – 7.33[10,12]	48 – 100[10,12]	6.68 – 7.98[13,17]	66 – 100[13,17]
	xan	6.51 ± 0.11	87.2 ± 6.0	5	7.21 ± 0.06[3]			7.10 ± 0.10[10]	≈ 106[10]	6.16 – 6.82[3,14]	97.5 – 100[3,14]
	car	6.65 ± 0.06	101 ± 4.9	5	3.61 – 4.42[1-3]	5.83 – 6.3[5,20]	100[5,20]	5.33 – 7.40[10-12,20,21]	84 – 131[10-12,20,21]	5.85 – 6.96[3,13]	91 – 100[3,13]
	iper	9.24 ± 0.10	96.4 ± 1.3	4						9.78 ± 0.10[17]	100[17]
hM_5R	car	6.78 ± 0.06	100	5	4.51 – 4.92[1,3]			5.72 – 6.9[10,12,21-24]	100[10,12,21-24]	5.89 – 7.22[13,14,25]	100[13,14,25]
	xan	5.88 ± 0.14	73.3 ± 2.8	4	7.09 ± 0.19[3]			6.52 – 7.63[10,21,22,24]	25 – 80[10,21,22,24]		
	oxo	7.19 ± 0.06	101.4 ± 4.3	4	6.05 ± 0.04[1]			6.24 – 7.29[10,12]	58 – 88[10,12]	7.26[13]	74 ± 2[13]
	iper	9.80 ± 0.07	101.4 ± 1.1	4							

8.2 Appendix 2

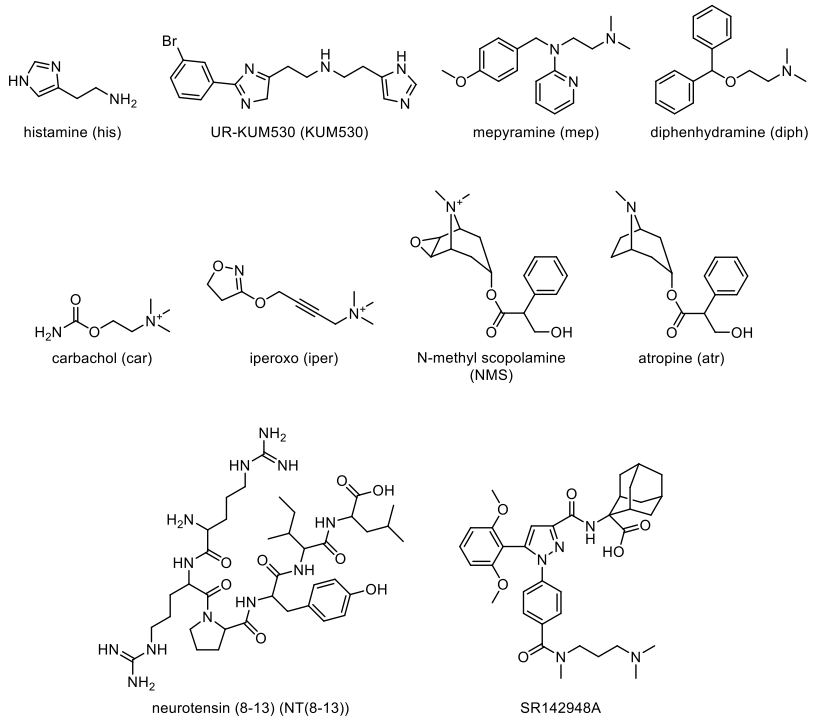

Fig. A7: Structures of the compounds analysed in chapter 5.

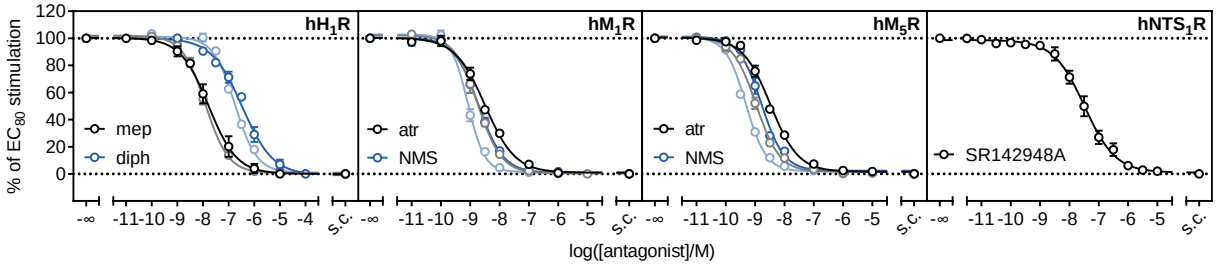

Fig. A8: Activities of selected reference antagonists at the analysed receptors. HEK293T cells, co-expressing the indicated GPCR and either NLucC (dark colours), or NLucN (light colours) fused to its C-terminus, as well as the complementary-tagged β-arrestin2 were analysed with respect to β-arrestin2 recruitment in the antagonist mode. The indicated antagonist was pre-incubated for 15 min before the agonist (hH_1R: histamine, $hM_{1,5}R$: carbachol, $hNTS_1R$: NT(8-13)) was added at a concentration corresponding to the respective EC_{80}. Data are presented as means ± SEM from at least three independent experiments, each performed in triplicate.

8.3 References

1 Dong, G. Z., Kameyama, K., Rinken, A. & Haga, T. Ligand binding properties of muscarinic acetylcholine receptor subtypes (m1-m5) expressed in baculovirus-infected insect cells. *J Pharmacol Exp Ther* **274**, 378-384 (1995).

2 Jakubík, J., Bačáková, L., El-Fakahany, E. E. & Tuček, S. Positive cooperativity of acetylcholine and other agonists with allosteric ligands on muscarinic acetylcholine receptors. *Mol Pharmacol* **52**, 172-179 (1997).

3 Wood, M. D., Murkitt, K. L., Ho, M., Watson, J. M., Brown, F., Hunter, A. J. & Middlemiss, D. N. Functional comparison of muscarinic partial agonists at muscarinic receptor subtypes hM_1, hM_2, hM_3, hM_4 and hM_5 using microphysiometry. *Br J Pharmacol* **126**, 1620-1624, doi:10.1038/sj.bjp.0702463 (1999).

4 Jakubík, J., El-Fakahany, E. E. & Doležal, V. Differences in kinetics of xanomeline binding and selectivity of activation of G proteins at M_1 and M_2 muscarinic acetylcholine receptors. *Mol Pharmacol* **70**, 656-666, doi:10.1124/mol.106.023762 (2006).

5 Jakubík, J., Janíčková, H., Randáková, A., El-Fakahany, E. E. & Doležal, V. Subtype differences in pre-coupling of muscarinic acetylcholine receptors. *PLoS One* **6**, e27732, doi:10.1371/journal.pone.0027732 (2011).

6 Waelbroeck, M. Activation of guanosine 5'-[γ-^{35}S]thio-triphosphate binding through M_1 muscarinic receptors in transfected Chinese Hamster ovary cell membranes: 2. Testing the "two-states" model of receptor activation. *Mol Pharmacol* **59**, 886-893 (2001).

7 Christopoulos, A., Pierce, T. L., Sorman, J. L. & El-Fakahany, E. E. On the unique binding and activating properties of xanomeline at the M_1 muscarinic acetylcholine receptor. *Mol Pharmacol* **53**, 1120-1130 (1998).

8 Digby, G. J., Noetzel, M. J., Bubser, M., Utley, T. J., Walker, A. G., Byun, N. E., Lebois, E. P., Xiang, Z., Sheffler, D. J., Cho, H. P., Davis, A. A., Nemirovsky, N. E., Mennenga, S. E., Camp, B. W., Bimonte-Nelson, H. A., Bode, J., Italiano, K., Morrison, R., Daniels, J. S., Niswender, C. M., Olive, M. F., Lindsley, C. W., Jones, C. K. & Conn, P. J. Novel allosteric agonists of M_1 muscarinic acetylcholine receptors induce brain region-specific responses that correspond with behavioral effects in animal models. *J Neurosci* **32**, 8532-8544, doi:10.1523/JNEUROSCI.0337-12.2012 (2012).

9 Randáková, A., Dolejší, E., Rudajev, V., Zimčík, P., Doležal, V., El-Fakahany, E. E. & Jakubík, J. Classical and atypical agonists activate M_1 muscarinic acetylcholine receptors through common mechanisms. *Pharmacol Res* **97**, 27-39, doi:10.1016/j.phrs.2015.04.002 (2015).

10 Šantrůčková, E., Doležal, V., El-Fakahany, E. E. & Jakubík, J. Long-term activation upon brief exposure to xanomleline is unique to M_1 and M_4 subtypes of muscarinic acetylcholine receptors. *PLoS One* **9**, e88910, doi:10.1371/journal.pone.0088910 (2014).

11 Pronin, A. N., Wang, Q. & Slepak, V. Z. Teaching an Old Drug New Tricks: Agonism, Antagonism, and Biased Signaling of Pilocarpine through M_3 Muscarinic Acetylcholine Receptor. *Mol Pharmacol* **92**, 601-612, doi:10.1124/mol.117.109678 (2017).

12 Kukkonen, J. P., Nasman, J., Ojala, P., Oker-Blom, C. & Akerman, K. E. Functional properties of muscarinic receptor subtypes Hm1, Hm3 and Hm5 expressed in Sf9 cells using the baculovirus expression system. *J Pharmacol Exp Ther* **279**, 593-601 (1996).

13 Bräuner-Osborne, H. & Brann, M. R. Pharmacology of muscarinic acetylcholine receptor subtypes (m1-m5): high throughput assays in mammalian cells. *Eur J Pharmacol* **295**, 93-102 (1996).

14 Burstein, E. S., Spalding, T. A. & Brann, M. R. Pharmacology of muscarinic receptor subtypes constitutively activated by G proteins. *Mol Pharmacol* **51**, 312-319 (1997).

15 Salah-Uddin, H., Thomas, D. R., Davies, C. H., Hagan, J. J., Wood, M. D., Watson, J. M. & Challiss, R. A. Pharmacological assessment of M_1 muscarinic acetylcholine receptor-$G_{q/11}$ protein coupling in membranes prepared from postmortem human brain tissue. *J Pharmacol Exp Ther* **325**, 869-874, doi:10.1124/jpet.108.137968 (2008).

16 van der Westhuizen, E. T., Spathis, A., Khajehali, E., Jörg, M., Mistry, S. N., Capuano, B., Tobin, A. B., Sexton, P. M., Scammells, P. J., Valant, C. & Christopoulos, A. Assessment of the Molecular Mechanisms of Action of Novel 4-Phenylpyridine-2-One and 6-Phenylpyrimidin-4-One Allosteric Modulators at the M_1 Muscarinic Acetylcholine Receptors. *Mol Pharmacol* **94**, 770-783, doi:10.1124/mol.118.111633 (2018).

17 Dallanoce, C., Conti, P., De Amici, M., De Micheli, C., Barocelli, E., Chiavarini, M., Ballabeni, V., Bertoni, S. & Impicciatore, M. Synthesis and functional characterization of novel derivatives related to oxotremorine and oxotremorine-M. *Bioorg Med Chem* **7**, 1539-1547 (1999).

18 Messerer, R., Kauk, M., Volpato, D., Alonso Canizal, M. C., Klockner, J., Zabel, U., Nuber, S., Hoffmann, C. & Holzgrabe, U. FRET Studies of Quinolone-Based Bitopic Ligands and Their Structural Analogues at the Muscarinic M_1 Receptor. *ACS Chem Biol* **12**, 833-843, doi:10.1021/acschembio.6b00828 (2017).

19 Chen, X., Klöckner, J., Holze, J., Zimmermann, C., Seemann, W. K., Schrage, R., Bock, A., Mohr, K., Tränkle, C., Holzgrabe, U. & Decker, M. Rational design of partial agonists for the muscarinic M_1 acetylcholine receptor. *J Med Chem* **58**, 560-576, doi:10.1021/jm500860w (2015).

20 Noetzel, M. J., Grant, M. K. & El-Fakahany, E. E. Mechanisms of M3 muscarinic receptor regulation by wash-resistant xanomeline binding. *Pharmacology* **83**, 301-317, doi:10.1159/000214843 (2009).

21 Randáková, A., Rudajev, V., Doležal, V., Boulos, J. & Jakubík, J. Novel long-acting antagonists of muscarinic ACh receptors. *Br J Pharmacol* **175**, 1731-1743, doi:10.1111/bph.14187 (2018).

22 Randáková, A., Dolejší, E., Rudajev, V., Zimčík, P., Doležal, V., El-Fakahany, E. E. & Jakubík, J. Role of membrane cholesterol in differential sensitivity of muscarinic receptor subtypes to persistently bound xanomeline. *Neuropharmacology* **133**, 129-144, doi:10.1016/j.neuropharm.2018.01.027 (2018).

23 Berizzi, A. E., Gentry, P. R., Rueda, P., Den Hoedt, S., Sexton, P. M., Langmead, C. J. & Christopoulos, A. Molecular Mechanisms of Action of M_5 Muscarinic Acetylcholine Receptor Allosteric Modulators. *Mol Pharmacol* **90**, 427-436, doi:10.1124/mol.116.104182 (2016).

24 Grant, M. K. & El-Fakahany, E. E. Persistent binding and functional antagonism by xanomeline at the muscarinic M_5 receptor. *J Pharmacol Exp Ther* **315**, 313-319, doi:10.1124/jpet.105.090134 (2005).

25 Bräuner-Osborne, H., Ebert, B., Brann, M. R., Falch, E. & Krogsgaard-Larsen, P. Functional partial agonism at cloned human muscarinic acetylcholine receptors. *Eur J Pharmacol* **313**, 145-150 (1996).

8.4 List of Abbreviations

460/50 BP	460/50 band-pass filter
610 LP	610 nm long-pass filter
AC	adenylyl cyclase
ATP	adenosine-5'-phosphate
atr	atropine
betahis	betahistin
BRET	bioluminescence resonance energy transfer
cAMP	3'-5'-cyclic adenosine monophosphate
car	carbachol
CBR	engineered click-beetle luciferase emitting red light
CBRC	C-terminal fragment of CBR (amino acids 395-542)
CBRN	N-terminal fragment of CBR (amino acids 1-416)
CRC	concentration-response-curve
cyp	cyproheptadine
DAG	diacyl glycerol
diph	diphenhydramine
DMEM	Dulbecco's modified Eagle's medium
EM	electron microscopy
E_{max}	maximal response of a given compound
ER	endoplasmic reticulum
ERK1/2	extracellularly-regulated kinase 1 and 2
FCS	fetal calf serum
FRET	Förster resonance energy transfer
G418	geneticin

GFP	green-fluorescent protein
GPCR	G protein-coupled receptor
GRK	G protein-coupled receptor kinase
GTP	guanosine-5'-phosphate
$G\alpha_q(123)$	$G\alpha_q$ fusion protein in which CBRC was introduced after amino acid 123
$G\alpha_q(97)$	$G\alpha_q$ fusion protein in which CBRC was introduced after amino acid 97
HBSS	Hank's balanced salt solution
hH_1R	human histamine H_1 receptor
hH_2R	human histamine H_2 receptor
hH_3R	human histamine H_3 receptor
hH_4R	human histamine H_4 receptor
his	histamine
histapro	histaprodifen
hM_1R	human muscarinic acetylcholine M_1 receptor
hM_2R	human muscarinic acetylcholine M_2 receptor
hM_3R	human muscarinic acetylcholine M_3 receptor
hM_5R	human muscarinic acetylcholine M_5 receptor
$hNTS_1R$	human neurotensin NTS1 receptor
IP_3	inositol trisphosphate
iper	iperoxo
KUM530	UR-KUM530
L-15	Leibovitz' L-15 medium
MAP	mitogen-activated protein
map	maprotiline
mep	mepyramine

NLuc	NanoLuc
NLucC	C-terminal, smaller NLuc fragment
NLucN	N-terminal, larger NLuc fragment
NMS	N'-methylscopolamine
NT(8-13)	neurotensin (8-13)
oxo	oxotremorine
PBS	phosphate-buffered saline
PCR	polymerase chain reaction
pEC_{50}	negative logarithm of the concentration at half-maximal response
PIP_2	phosphatidylinositol 4-phosphate
pir	pirenzepine
pK_b	negative logarithm of the equilibrium dissociation constant of the antagonist-receptor complex, according to Cheng et al., *Biochem Pharmacol* **22**, 3099-3108 (1973).
PLC-β	phospholipase C-β
PPI	protein/protein interaction
prop	propantheline
RET	resonance energy transfer
Rluc	luciferase from *Renilla reniformis*
S/B	signal-to-background
SLC	split luciferase complementation
SRP	signal-recognition particle
xan	xanomeline

Ich erkläre hiermit an Eides statt, dass ich die vorliegende Arbeit ohne unzulässige Hilfe Dritter und ohne Benutzung anderer als der angegebenen Hilfsmittel angefertigt habe; die aus anderen Quellen direkt oder indirekt übernommenen Daten und Konzepte sind unter Angabe des Literaturzitats gekennzeichnet.

Einige der experimentellen Arbeiten wurden in Zusammenarbeit mit anderen Institutionen und Personen durchgeführt. Vermerke zu den Beiträgen der betreffenden Personen finden sich in den jeweiligen Kapiteln.

Weitere Personen waren an der inhaltlich-materiellen Herstellung der vorliegenden Arbeit nicht beteiligt. Insbesondere habe ich hierfür nicht die entgeltliche Hilfe eines Promotionsberaters oder anderer Personen in Anspruch genommen. Niemand hat von mir weder unmittelbar noch mittelbar geldwerte Leistungen für Arbeiten erhalten, die im Zusammenhang mit dem Inhalt der vorgelegten Dissertation stehen.

Die Arbeit wurde bisher weder im In- noch im Ausland in gleicher oder ähnlicher Form einer anderen Prüfungsbehörde vorgelegt

Regensburg, den 14.12.2018 _____

Timo Littmann